Wind Energy; Turkey's chance for energy independence and a technical look for Horizontal Axis Wind Turbines

Kamer DOGAN

IHU ID: 3302120020

SCHOOL OF SCIENCE & TECHNOLOGY

A thesis submitted for the degree of

Master of Science (MSc) in Energy Systems

OCTOBER 2013

THESSALONIKI – GREECE

INTERNATIONAL HELLENIC UNIVERSITY

Wind Energy; Turkey's chance for energy independence and a technical look for Horizontal Axis Wind Turbines

Kamer DOGAN

IHU ID: 3302120020

Supervisor:

Supervising Committee Members: Assoc. Prof. Name Surname

Assist. Prof. Name Surname

SCHOOL OF SCIENCE & TECHNOLOGY

A thesis submitted for the degree of

Master of Science (MSc) in Energy Systems

OCTOBER 2013

THESSALONIKI – GREECE

Abstract

This dissertation was written as a part of the MSc in Energy Systems at the International Hellenic University. The focus of the dissertation is the wind energy as a renewable source. To illuminate the necessity of clean wind energy the study starts with a chapter where the global energy outlook is described and discussed. Later the technical study begins with fundamental concepts of fluid dynamics and continues with more specific issues concerning wind energy.

Wind energy harvesting is not new and has a background dating back to thousands of years. In the era we are living, it may play an utmost role to secure our energy needs without harming the environment with CO_2 emissions.

In this dissertation, an aerodynamic investigation of horizontal axis wind turbines is presented. Special attention is given to the wind speed of 7.25 m/s as available wind energy at this average speed (more precisely, the sites where wind speed is between 7m/s and 7.5m/s) constitutes 60% of all the economically viable wind energy potential in Turkey. The programs Qblade and ANSYS CFX used for this dissertation thesis with the concept of Blade Element Momentum Theory and numerical Navier-Stokes solution respectively.

Kamer DOGAN

October 2013

Acknowledgement

Thanks to the friends who let me feel like home… Special thanks to the Jean Monnet Committee of Turkey and IHU who gave me the chance to conduct this master program. I would like to thank Dr. Georgios Martinopoulos for his guidance and help during the academic year and dissertation period.

Kamer DOGAN

October 2013

Contents

Chapter 1: INTRODUCTION

Energy is deemed to be the main reason for wars. But history has shown that it can be an instrument for peace also. This dualistic relation exists for almost everything and energy is not an exception. Founded on a basis of energy resources' share and partnership, EU is a good example for that (40). Despite being one of the main reasons for the First and Second World Wars which broke out in Europe, energy played the dominant role for the process which ended up with the unification of Europe. This peerless peace project started at first in minds of some great men and had the motto: "make war not only unthinkable but materially impossible". As the French Foreign Minister Robert Schuman declared the aim of European Coal and Steel Community, another French politician Jean Monnet was already dreaming of the united Europe. Under those circumstances the Treaty of Paris was signed by West (Federal) Germany, France, Italy and three Benelux countries in 1951(40). That was the first step towards the European Union. From then on, coal (at that time the major energy source) was no longer a reason for war but peace.

Energy is now again in the stage, this time for even a bigger project: sustainable world. Since 1970s we have realized that the way we are developing is not sustainable, that is, we cannot go on like this for ever. Sustainability discussions started in an era when world faced first oil shocks and CO_2 concentration in the atmosphere broke the 330 ppmv (particulates per million by volume) barrier alarming for global warming (41). Until then energy was cheap and people used to think in such a way that world had infinite resources. But the increase in energy prices forced people to think of other energy resources also. Although large scale renewable energy production did not start immediately, that was a milestone. While fossil fuel prices kept increasing, the green ways like wind energy became more and more competitive with the traditional coal, naturel gas etc. At the same time the discussion for sustainable energy production expanded to many other industries and now it is a concept applicable to every process taking place on planet earth.

In the second chapter of this study a short and comprehensive energy outlook will be shown not only in global scale but particularly for Turkey. The global energy trends will be discussed. In the final part of the study, some ideas concerning EU-Turkey relations, particularly energy relations will be discussed. Also Turkey's future energy strategy and its connection with renewables, particularly wind energy, will be another issue for which information will be provided. I hope to be able take the general true picture as simple as possible. Because the aim here is not to make any political and/or economic analysis but just to understand what we are facing globally and as a country (Turkey) in energy concerns the study is kept short.

In the consequent chapter after defining the general energy outlook, beginning from the third one, a technical discussion starts. The aim is to understand a Horizontal Axis Wind Turbine, the energy extraction process from wind and trying to design an effective turbine blade. In this chapter, it was found useful to start from the very basics of fluid dynamics. But while doing so,

many times the given information was related to this master study. The main assumptions were set and the necessary nomenclature was formed. Types of flows, concepts of fluid motion, milestone experiments in the area and some other relevant fundamental knowledge was summarized. The chapter then continues with the literature review of aerodynamic models for wind turbines. The theories and models include the Betz theory as well as other important contributions to the Blade Element Momentum Theory. Afterwards comes another part which is very necessary to understand the 4th chapter of this study, the numerical methods. Numerical methods in general and specific to the aerodynamics are vital to understand as almost all solutions in technology are numerical rather than exact.

In the 4th chapter a generated blade will be examined in different scales by different computer programs. QBlade and ANSYS CFX will be the main programs used. The first one uses a Blade Element Momentum theory while the latter makes use of complex turbulence models to solve the Navier-Stokes equations numerically. Results of the simulations will be discussed and detailed visualization by using post-process tools of the programs is presented.

The last chapter is devoted to the conclusion part and results of the simulations are summarized and discussed here. Possible future study path is introduced with closing comments.

Chapter 2: TURKEY'S CHANCE FOR ENERGY INDEPENDENCE, TOWARDS A GREEN FUTURE

2.1 WORLD ENERGY OUTLOOK

Energy demand is a close function of population and economic growth. Those phenomenons are in close relation. As population increases, so does economic growth and energy demand. According to most trustable projections like BP Energy Outlook (1), the world economy will almost double by 2030. The question arising here is whether or not this growth is sustainable. There are many different perspectives on the issue. But they share the common point that if the energy efficiency and savings increase, the answer could be positive. Keeping the trend, it is projected by the aforementioned source that by 2030 we will be almost 30% more efficient. In other words, the energy demand will rise slower than economic growth which will help the sustainability of the growth. Renewables will keep growing at an average of 8% annually and remain the fastest growing fuel group. This growth will result in a 6% global renewable energy use by 2030. Shale oil production will change the energy import-export patterns because the world's giant energy consumer North America will lead tight oil production followed by Russia and China. North America will produce 73% of the shale gas. These resources will turn North America's energy deficit into a surplus. Because fossil fuels will continue to dominate at 81%, greenhouse gases will continue increasing in the atmosphere. CO_2 concentration will be about 500 ppmv which is a quarter more than today.

As mentioned above population-economic growth-energy demand cannot be separated from each other. So it is important to start with population. As can be seen in Figure2.1, the world population will jump from about 7 billion to approximately to 8.3 billion. The population growth will be important in Non-OECD countries. The OECD countries will have only a slight increase. This extra 1.3 billion will be an important reason for the energy demand expectation seen in Figure 2.2. Like the situation in population, OECD countries will undergo only a slight increase in primary energy consumption. On the contrary Non-OECD countries will see a big demand for energy. This increase will be more than the population increase suggesting some other reasons behind this huge demand increase. This reason is that energy consumption per capita will also increase in Non-OECD countries partly because the better living standards but mainly due to the economic growth.

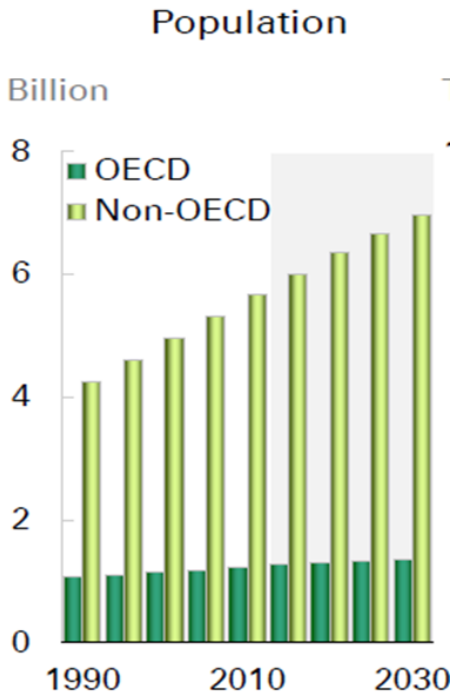

Figure 2.1 World Population (1)

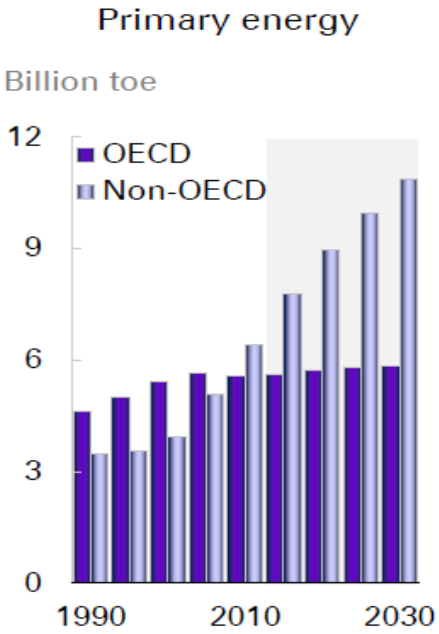

Figure 2.2 World Primary Energy Consumption (1)

Economic growth rate can be chased by looking at the GDP graph (Figure 2.3). It was traditionally the rule that the GDP of OECD countries had higher GDP values than Non-OECD countries. But this situation is under dramatic change and in the near future the GDP, that is also economic growth, will be more in Non-OECD countries (1).

Shortly, we see that as Non-OECD countries industrialize and urbanize they cause most of the new energy demand. Below some important aspects of energy outlook are highlighted:

1) The global energy map is changing. This will certainly have far-reaching consequences for energy markets and trade.

2) Despite all new developments and policies, the world is still failing to put the global energy system onto a more sustainable path.

3) Energy efficiency is widely thought as a key option to decrease energy demand but current efforts are not enough.

4) Recent studies have shown that the climate goal of limiting warming to 2 °C is becoming more difficult and more costly year by year.

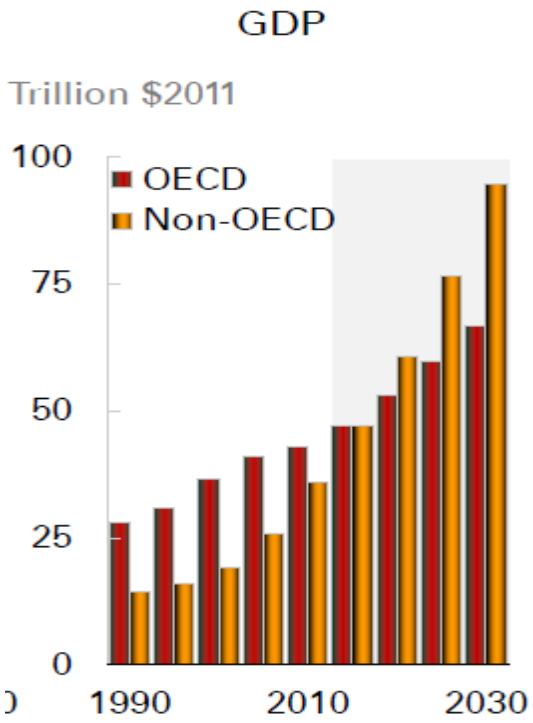

Figure 2.3 GDP of OECD and Non-OECD Countries (1)

2.2 EU ENERGY CONCERNS

EU is a net energy importer and because of this fact security of supply (*The concept of security of supply encompasses reduction of external dependence, enforcement of transport infrastructure and gas storage facilities and diversification of supply of gas and electricity (2)*) has always been the most important aspect of energy concerns for the EU. Another important aspect of its strategy is environmental protection and combating global warming. This stems mainly from public awareness and environmentalists pressure on governments.

In order to have success in its energy policy, EU has set the ambitious target (3) of 20-20-20 (20% increase in energy efficiency, 20% reduction of CO_2 emissions, and 20% renewables by 2020). Shortly describing, EU wants to achieve security of supply with a sustainable, environmental friendly policy. At this point it is useful to give the definition of sustainability. "Sustainable development is development that meets the needs of the present without compromising the ability of future generations to meet their own needs."(4)

In fact to name this as "energy policy" only would be a mistake. EU combines energy and climate/environment objectives and acts accordingly. In fact, the logic behind EU strategy is simple and makes sense. In order to be more energy independent, first of all, it is important to

increase efficiency and savings. After that, finding new sources of non-imported energy is vital. If this new source is a clean source, combined with efficiency and savings, combatting climate change will be easier. Putting in a different way, EU is dependent on imported fossil fuels which lead to greenhouse gases. If ;

a) Energy demand is decreased by efficiency and savings measures

b) The need is covered more and more by clean and domestic sources

it is possible to achieve security of supply while protecting environment and combatting climate change.

Although EU has a great effort, it is difficult to say everything is going well so far. The share of renewables is still far less than 20% as seen in Figure 2.4. Especially due to the global economic recession, it is now harder to achieve those ambitious targets. This is mainly because those targets need regulation and subsidies in order to come to effect. But in times of economic shrinkage, strategies need revising. People's and governments' willingness to pay more for clean and domestic energy is abating. Global investment in renewable energy fell 22% in the first quarter of 2013 compared to a year ago, according to a report released by Bloomberg New Energy Finance (5). $40.6 billion was invested in the first three months of the year 2013 and this corresponds to the lowest investment as of 2009, when the global financial crisis was in full strength. Investment dropped 54% in the US and 25% in Europe in the first quarter of year 2013. And despite China's ambitious renewable energy targets for 2013, investment there also fell 15% to $8.8 billion.

To be more concrete, it is useful to have a look at the up-to-date "European Semester" (6), which evaluates the progress of each Member State towards meeting the 20-20-20 targets every spring as part of the annual Europe 2020 policy coordination exercise.

1) While projections suggest that the 2020 GHG emissions target – a 20% reduction compared to 1990 levels – will be reached by the EU as a whole, currently only 11 Member States are expected to reach their national target with existing measures. The other 16 Member States will not reach their target without significant extra efforts. Luxembourg, Malta, Ireland, Lithuania, Belgium, Greece and Slovakia are furthest from meeting their 2020 targets.

2) On renewable energy, all Member States are expected to meet their national targets for 2020 on the basis of the commitments given in their National Renewable Energy Action Plans under the Renewable Energy Directive. Overall the EU aims to raise the share of renewable energy consumption produced from renewable resources to 20% in 2020.

Here it is of importance to open an extra parenthesis. Although EU seems to be more or less successful with its 20-20-20 targets, there are many points to discuss. First, EU has carried much of its energy intensive industry outside of EU. That means in global sense, there is not really much decrease in greenhouse gas emissions but only the place the gas is emitted. Second, 1st generation biofuels, which contribute to renewables' share, do not really have any positive effect on greenhouse gas emissions (42). This is because they need quite a lot of energy to be processed and transported. But more than that, the fuel corns are raised in areas where it used to be rainforests in Latin America.

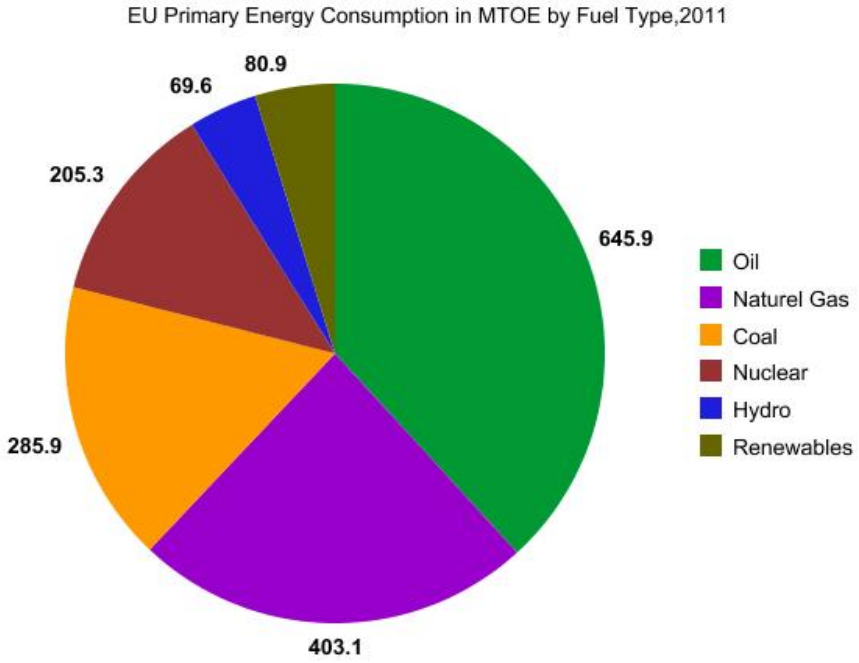

Figure 2.4 Energy Consumption in EU by Fuel Type in MTOE (3)

2.3 ENERGY AND TURKEY

After describing the world energy outlook and EU Energy policy, we can now proceed with Turkey. First major energy figures will be depicted. As in the Figure 2.8 seen, Turkey's primary energy consumption increases steadily. So it becomes more and more difficult to have security of supply because Turkey is a net energy importer like EU. The fact making the situation even worse is that Turkey is highly dependent on Russia in natural gas and Iraq on oil (7). That means Turkey lacks diversification of import counties and this is a threat to security of supply.

Like EU 20-20-20 targets, Turkey has a 2023 energy targets. This year corresponds to the 100th year of foundation of modern Turkey. Shortly describing below (10);

- Turkey expects that the electricity need will double compared to today and become about 500 billion kWh. In order to meet this demand, Turkey has to increase the installed power capacity and reach 100,000 MW
- The energy investment amounting to $ 5 billion each year has to be implemented accordingly.
- Share of the private sector in energy production will be 75% by privatization and other measures.
- Only 37% of coal resources in Turkey is used today and this percent will reach 100% by 2023.
- In Turkey, the hydro-electricity potential and corresponding installed capacity is about 140 billion kWh and is 36,000 MW, respectively. Accordingly, Turkey targets to construct another 20,000 MW hydro-power plants by means of private sector.
- Turkey's targets as installed capacity in wind, solar, and geothermal are 20,000 MW, 3000 MW and 600 MW respectively.
- Turkey plans to have 10,000 MW installed nuclear power by 2023.
- At 2023, the electricity production fuel mix will constitute 30% renewables including hydros, 30% coal, 30% natural gas and 10% nuclear.
- Turkey wants to be an energy hub in his region. As the map (7) below shows, it will not only guarantee security of supply but also strengthen country's position in its region.

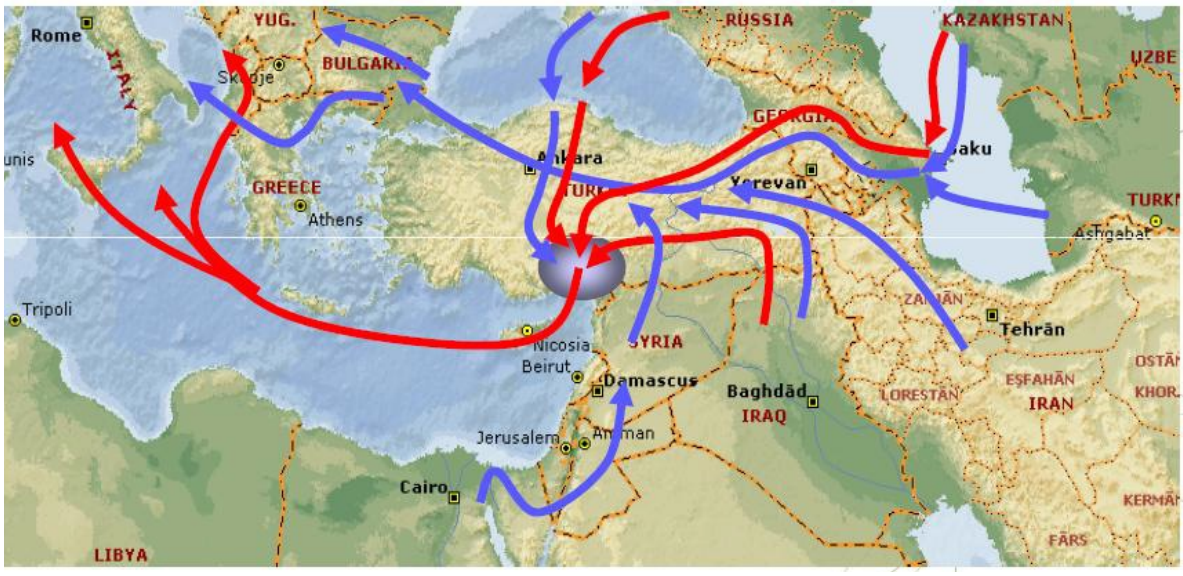

Figure 2.5 Existing and Planned Transit Energy Pipelines (Red=Oil, Blue=Naturel Gas) (7)

2.3.1 Wind Energy Potential in Turkey

Turkey has quite a good amount of wind potential. Out of approximately 48,000 MW wind power potential (8) only a tiny fraction corresponding to 2312 MW is in operation (9). As discussed earlier, Turkey aims to have 20,000 MW of wind power installed which corresponds to wind sites with average wind speed more than 7.5 m/s.

Wind Speed (m/s)	Wind Power Density (W/m2)	Usable Area (km²)	Techno-economical Potential (MW)
7.0 – 7.5	400 – 500	5,852	29,259
7.5 – 8.0	500 – 600	2,599	12,994
8.0 – 9.0	600 – 800	1,080	5,400
> 9.0	> 800	39	196
Total	9,570	47,849	

Table 2.1 Wind Energy Potential in Turkey (8)

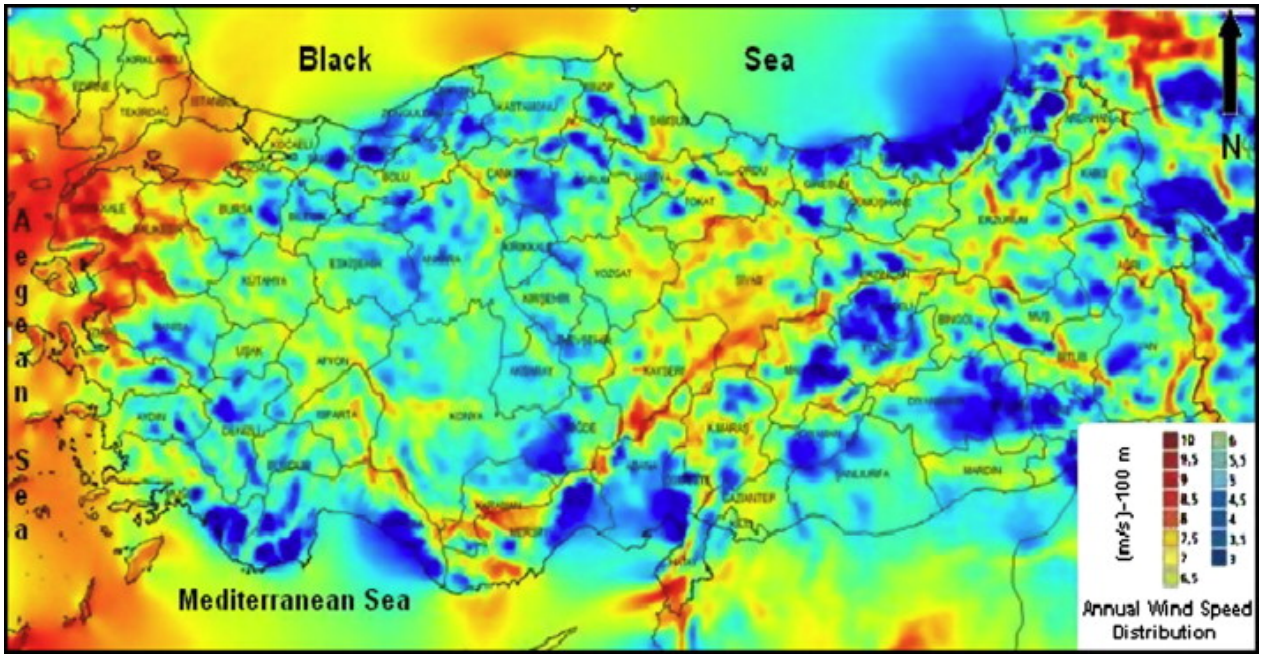

Figure 2.6 Annual Wind Speed Distribution in Turkey (8)

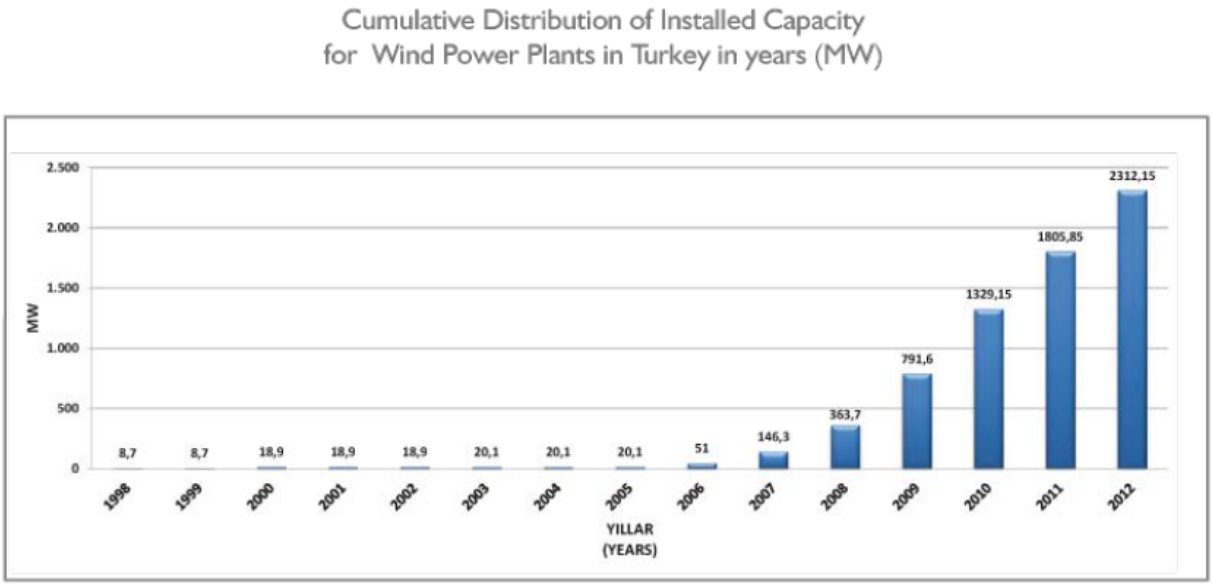

Figure 2.7 Cumulative Distribution of Installed Wind Power Capacity (8)

2.3.2 Some Final Remarks

Turkey's energy demand increases mainly due to growing population, urbanization and industrialization. In order to support industrialization, energy prices in Turkey need to be low as otherwise it will be difficult for Turkish companies to compete in the international market.

According to a 2010 report of the World Energy Council Turkey imports about 80% of its primary energy consumption. That means Turkey lacks security of supply. There are some additional points making the situation worse. These are; Turkey depends heavily on natural gas and lacks supplier diversification. Turkey buys natural gas mainly from Russia and Iran (55% and 21% of the total imported natural gas respectively). Crude oil imports are from Iran, Iraq and Russia mainly with 51%, 17% and 12% respectively (10). That means Turkey needs not only resource but also supplier diversification.

Knowing that Turkey is heavily dependent on imported fossil fuels has high wind potential and renewables have strong environmental benefits a significant alteration towards the renewable energy production and of course including wind energy in particular, is a strong probability.

Factors affecting this evolution are; Turkey's energy policy, legislative framework, support mechanisms, supply/demand balance, environment policy, grid ability and available fund.

As seen in Figure 2.8 with 118.8 million tons of oil equivalent primary energy consumption (2011), Turkey constitutes 1% of all world primary energy demand. This is in agreement with its 75 million population which is slightly more than 1% of the global population.

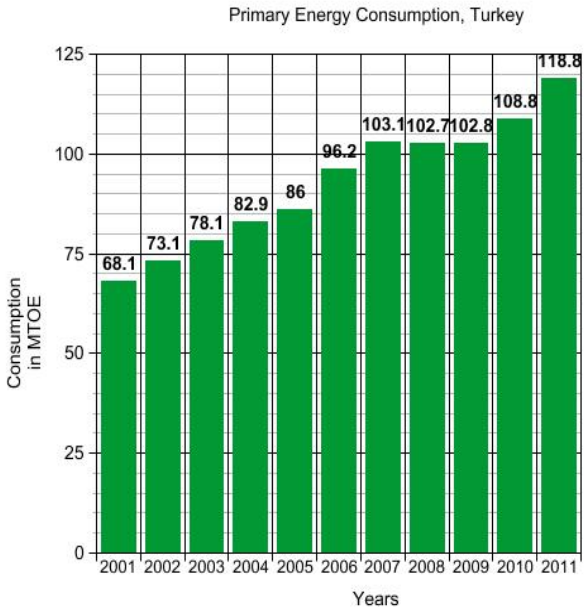

Figure 2.8 Primary Energy Consumption of Turkey (10)

The pie graph in Figure 2.9 shows that Turkey is highly dependent on fossil fuels with 89%. This value for EU is about 83%.

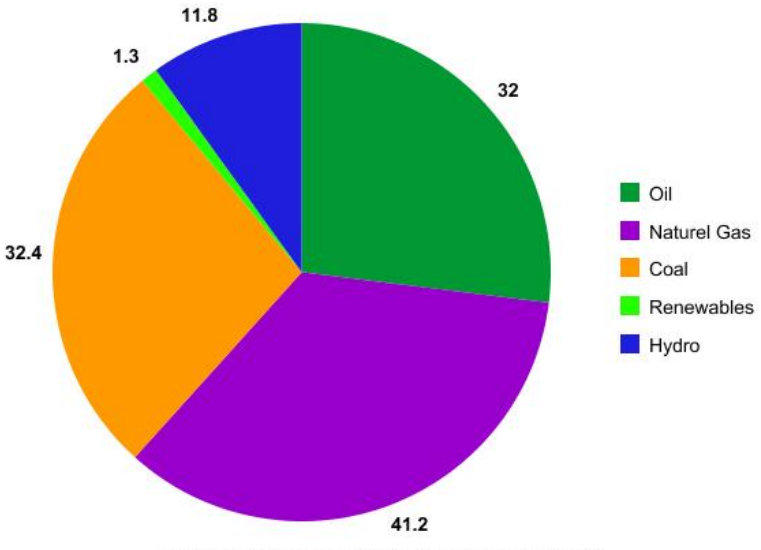

Figure 2.9 Turkey Primary Energy Consumption by Fuel Type in MTOE (10)

The graph in Figure 2.10 shows the fuel mix of electricity generation in Turkey for 2012. Turkey produced 239.1 billion kWh of electricity in the same year corresponding to an increase of 4.2%. The production in 2011 and 2010 was 229.4 and 211.2 respectively.

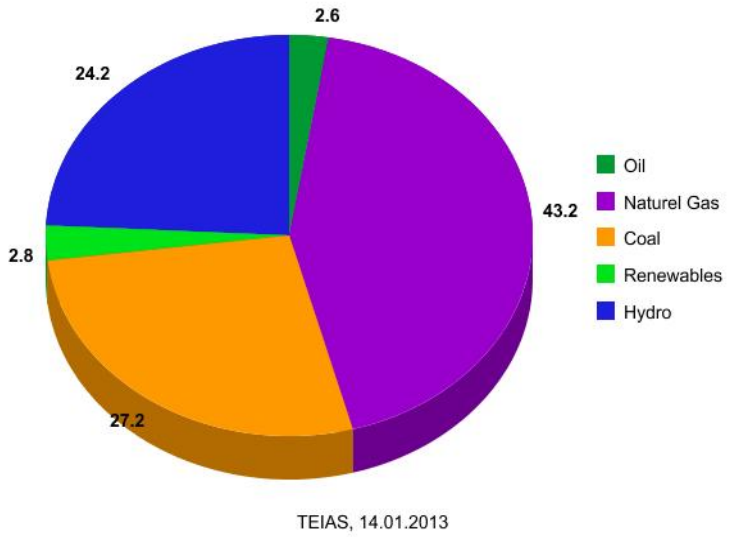

Figure 2.10 Electricity Production in Turkey by Fuel Types (10)

2.4 TURKEY-EU RELATIONS IN LIGHT OF ENERGY

Energy is a topic of key interest in EU-Turkey relations. Both Turkey and the EU will benefit if Turkey's role in being an energy bridge and potential energy hub increases. In view of their geographic proximity, a further market integration would be in the interest of both sides. Turkey and the EU furthermore have many challenges in common in their endeavors to secure sustainable energy supplies and to ensure competitive energy markets.

Turkey and the EU are important energy partners, both sharing common challenges and objectives. There is great scope for cooperation on issues which are in the interest of both sides. These are:

1) Long term perspectives on energy scenarios and energy mix
2) Market integration and development of infrastructures of common interest (gas, electricity, oil)
3) Global and regional energy cooperation
4) Promotion of renewable energy, energy efficiency and clean energy technologies

5) Nuclear safety and radiation protection(Positive Agenda, Stuttgart)

This cooperation will contribute to a positive agenda for EU-Turkey relations in general, and it will facilitate the eventual integration of EU and Turkey energy markets. Such integration will not only increase security of energy supply in Europe and Turkey, it will also create important business opportunities.

It is useful to have a look at the Turkey Progress Reports in order to understand the situation better. Every year European Commission prepares a report concerning the EU-Turkey acquisition progress. Below is the latest report's conclusion for Energy chapter.

Some progress can be reported in the energy sector, especially as regards renewable energy and energy efficiency. Further efforts are needed in the areas of natural gas, nuclear safety and radiation protection, including responsible and safe management of spent fuel and radioactive waste. Competition remains limited in the gas sector. The functioning of the cost-based pricing mechanism in the electricity market needs to be improved whereas it remains to be established in the gas markets. The independence and institutional capacity of the regulatory authority need strengthening. Overall, in the area of energy, Turkey is at a moderately advanced stage of alignment. (11)

As a last note it is important to name the main focuses of EU legislation in the context of energy chapter:

1. Internal energy market (electricity and natural gas markets),
2. Energy efficiency,
3. Promotion of renewable energy resources,
4. Nuclear safety and radiation protection and
5. Security of supply.

2.5 WIND ENERGY CONVERSION

2.5.1 History and Trends

Windmills go back almost 3,000 years; they were used mainly for grinding or water pumping and remained important for the society until the emerge of fossil fuels and electrification. From then on wind power lost most of its attraction due to the cheap and abundant fossil driven energy.

It was only at the beginning of the twentieth century when electricity came into use and windmills gradually became wind turbines as the rotor was connected to an electric generator. Because first electrical grids consisted of low-voltage DC cables with high losses in the past, electricity had to be generated close to the site of use to overcome the problem. Gradually, however, diesel engines and steam turbines took over the production of electricity. Only during the two world wars, due to the scarcity of fuel supply, could wind power flourish again. Luckily after the World War II, the study and development efforts for wind turbines continued in big European counties like Germany, France, the UK and Denmark and also in the US.

The boom of the wind turbines started about 20 years ago and is closely related to sustainability and security of energy issues, particularly in EU. Because with subsidies wind energy can compete with fossil driven technologies, there is further expectation for the more and more penetration of wind generated electricity in the fuel mix.

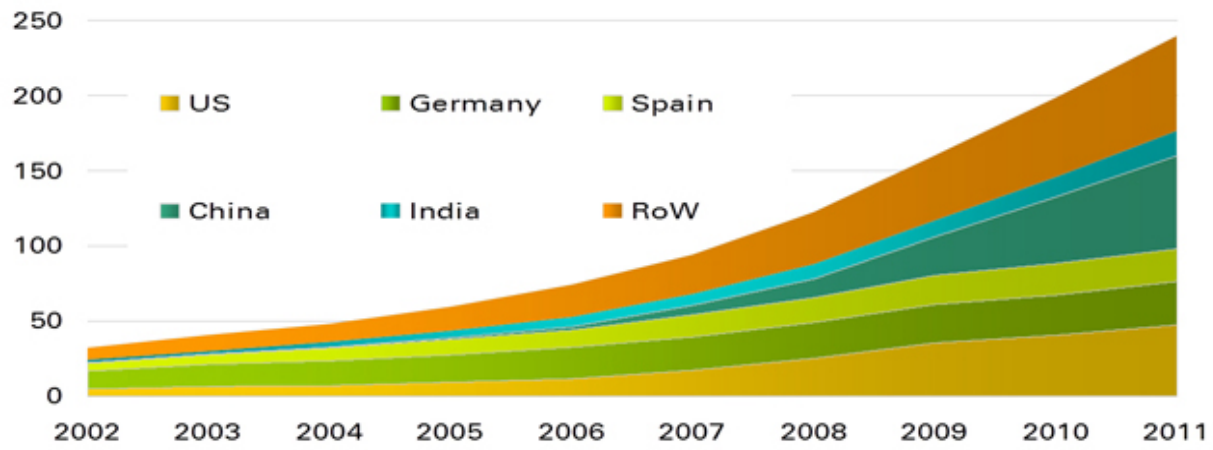

Figure 2.11 World Wind Energy Installed Power (1)

Wind power generating capacity grew by 20.5% in 2011, with capacity increasing by a record 40.8 GW to reach 239 GW by the end of 2011. The trend rate of capacity growth over the past 10 years is just over 25% pa, which implies a doubling of capacity every three years. Wind power now generates 437 TWh of electricity, around 2% of total electricity generation.

China remains the largest market for wind power; both in terms of capacity added (17.6 GW) and in terms of cumulative installed capacity (62.4 GW). The second largest market, the US, added 6.8 GW in 2011 to reach 47.1 GW installed capacity.

Led by Germany and Spain, Europe remains the largest regional market for wind power in terms of total installed capacity (96.8 GW, or 44% of the world total). The fastest growing region over the past five years has been Asia-Pacific, led by China and India. Asia-Pacific's share of installed wind capacity has doubled since 2007, reaching 36% by the end of 2011 (12).

The illustration in Figure 2.12 by Steve Connors from MIT shows representative size, height, and diameter of wind turbines. It is expected in the near future to have higher towers and larger rotor diameters to decrease the cost of energy produced. But as the wind industry grows so rapid, it is essential to collect necessary site date for many years before proceeding to avoid any dramatic accidents or safety risks.

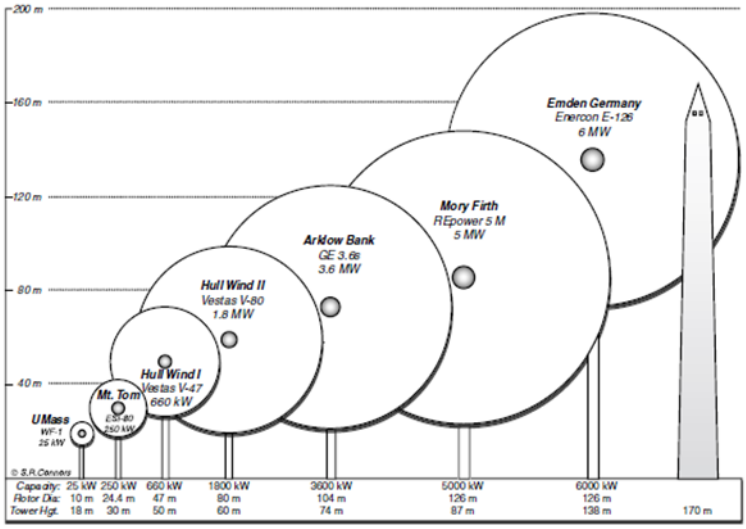

Figure 2.12 Wind Turbine Size-Capacity (39)

But before we continue with other aspects of wind energy usage, it is necessary to distinguish between different ways we follow to exploit the wind power.

2.5.2 Classification

First differentiation is done for the target energy type; a windmill is the device which extracts wind energy and converts it to mechanical shaft power for direct use. If the shaft is connected to a generator by any means in order to produce electricity the wind energy converter device is called a wind turbine.

Another differentiation is done for the principle made use of in order to exploit the wind energy. That is, a wind turbine or a windmill is either lift or drag driven.

Depending on the rotor orientation relative to the wind, the turbine is either upwind or downwind machine.

Another classification is the number of the blades.

The illustration seen below by Schilling (13) clearly reveals the different types of wind machines.

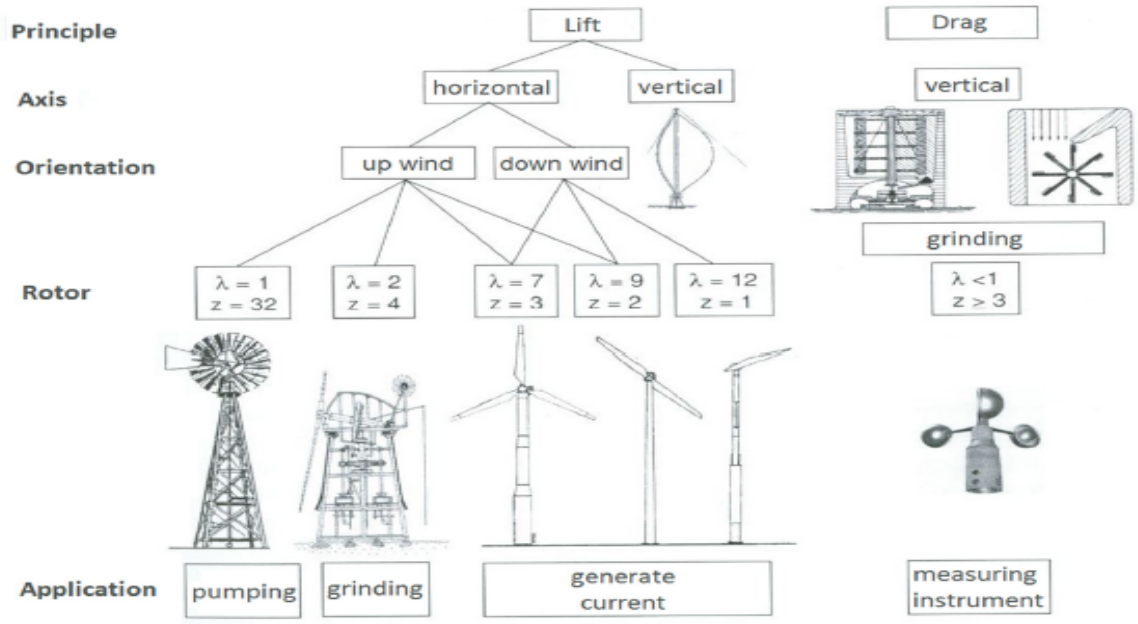

Figure 2.13 Wind Conversion Classification (13)

2.5.3 The Parts of a Horizontal Axis Wind Turbine

The Figure 2.14 describes the main parts of a wind turbine (43) schematically. Please note that this is just a shematic representation and some parts shown here may not exist in some commercial wind turbines and vice versa.

The Rotor

The hub and blades together form the rotor of the wind turbine. Taking into account both performance and overall cost blades and the hub are the turbine's most important components.

Most turbines today are upwind rotors with three blades. Modern wind turbine blades use lift principle to exploit the wind's energy. Due to the blade's special shape, the wind creates a pressure difference as it passes over the blade. This pressure field forces the blade to rotate. The blades spin at a slow rate of about 20 rpm. Some small-to-intermediate-sized turbines use stall control. But most manufacturers use pitch control, and this trend is dominant especially in larger machines. The reason is that pitch control gives 2-3% more annual energy output. This extra gain is not important for small sized turbines but quite important for big ones. Also pitch control provides better structural performance. From a materials point of view, the blades are made of composites, especially fiberglass or carbon fiber reinforced plastics(26).

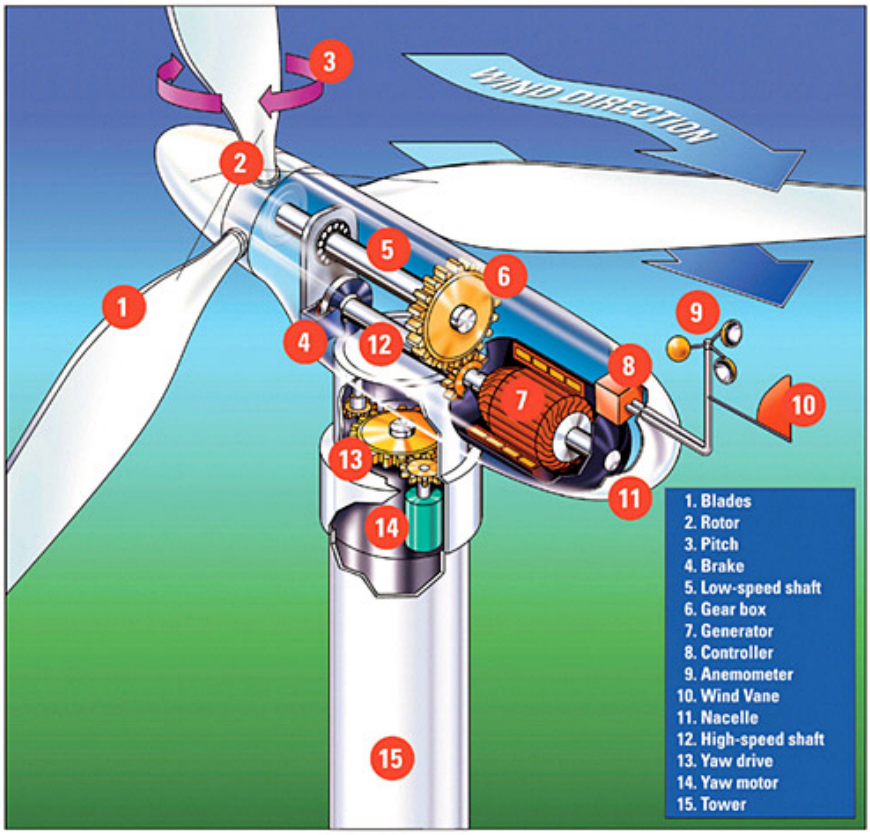

Figure 2.14 Wind Turbine Parts (43)

The Drive Train

The drive train consists of the rotating parts of the wind turbine other than the rotor. These typically consist of a low-speed shaft connected to the shaft, a gearbox and a high-speed shaft

connected to the generator. The bearings, couplings and a brake consist the rest of the drive train. The gearbox serves to speed up the rate of rotation of the rotor from a low value like 20-30 rpm to a rate suitable for driving a generator, generally hundreds of rpm. Parallel shaft or planetary type gearboxes are used in wind turbines. For machines over approximately 500 kW, planetary gearboxes are generally in use because the weight and size advantages become more pronounced for this range. While most of the time wind turbine designs use multiple generators and are coupled to a gearbox with more than one output shaft, occasuanally use of specially designed low-speed generators which require no gearbox can be seen. The design of wind turbine drive train components usually follows conventional mechanical engineering machine design practice.But the unique loading of wind turbine drive trains requires special consideration. Unsteady nature of winds and the dynamics of large rotating rotors impose significant fluctiated loads on drive train components.

The Generator

Induction or synchronous generators are the generator types used in wind turbines. These designs necessitate a more or less constant rotational speed if the generator is directly connected to a utility network without making use of any power electronics. But if the generator is used with power electronic converters however, the turbine may operate at variable rotational speed. Many wind turbines installed in grid connected applications use squirrel cage induction generators which operate within a narrow range of speeds slightly higher than its synchronous. The main advantage of this induction generator is that it is firm, cheap, and easy mountable to an electrical network. An increasingly popular option today is the doubly fed induction generator which is often used in variable-speed applications. There are a number of advantages which such a configuration allows; the reduction of wear and tear on the wind turbine and potential operation of the wind turbine at maximum efficiency over a wide range of wind speeds. This in turn results increased energy capture.

The Nacelle and Yaw System

This category consists of the wind turbine housing, the machine bedplate, and the yaw system. The main frame provides for the mounting and proper alignment of the drive train components. The nacelle cover protects the contents from the weather. A yaw orientation system is required to keep the rotor shaft properly aligned with the wind. Its primary component is a large bearing that connects the main frame to the tower. An active yaw drive, always used with upwind wind turbines and sometimes with downwind turbines, contains one or more yawmotors, each of which drives a pinion gear against a bull gear attached to the yaw bearing. This mechanism is controlled by an automatic yaw control system with its wind direction sensor usually mounted on the nacelle of the wind turbine. Sometimes yaw brakes are used with this type of design to hold the nacelle in position, when not yawing. Free yaw systems (meaning that they can self-align with the wind) are often used on downwind wind machines.

The Tower and Foundation

This category includes the tower itself and the supporting foundation. The principal types of tower design currently in use are the free-standing type using steel tubes, lattice (or truss) towers, and concrete towers. For smaller turbines, guyed towers are also used. Tower height is typically 1 to 1.5 times the rotor diameter, but in any case is normally at least 20 m. It is a known fact that as the tower height increases, the energy output also goes up. The underlying reason is that, the wind speed is higher at high alltitutes due to the decrease of friction effect of the ground. Tower selection is greatly influenced by the characteristics of the site. The stiffness of the tower is a major factor in wind turbine system dynamics because of the possibility of coupled vibrations between the rotor and tower. For turbines with downwind rotors, the effect of tower shadow(the wake created by air flow around a tower) on turbine dynamics, power fluctuations, and noise generation must be considered. For example, because of the tower shadow, downwind turbines are typically noisier than their upwind counterparts (26).

The Controls

The control system of a wind turbine has two important aspects, machine operation and power production. The control system includes the following components:

- Sensors: A turbine control system has many sensors to get the date of position, temperature, current, voltage, etc.;
- Controllers
- Actuators: Motors, pistons, magnets etc. give the needed moves.
- Intelligence: Computers, microprocessors, special software help the system stay at the best efficiency point.

CHAPTER 3: A TECHNICAL LOOK FOR HORIZONTAL AXIS WIND TURBINES

This chapter includes the basics of fluid dynamics, a review of aerodynamic models and turbulence.

3.1 BASICS OF FLUID DYNAMICS

In this thesis, we are dealing with air flow over a turbine blade. This means we are in the topic of fluid dynamics. That is why it is important to have the basic fundamental idea of fluid dynamics. This part will be an introduction to the topic. The covered issues are directly related to this thesis and this is the reason why this part cannot be considered as a general introduction but a pathway to the core of the thesis.

It is necessary to start with the definition of "fluid". Although it is easy to feel what is fluid and what is not we need a mathematical formulation and a scientific definition for that. In any fluid mechanics textbook we can see the definition as "A fluid is a substance that deforms continuously under the application of a shear (tangential) stress no matter how small the shear stress may be." Putting it in a different way a fluid can not resist any shear stress. A solid resists it with a static deformation but a fluid has no static deformation but a continuous one. That means a fluid at rest has no shear component on the Mohr's circle and the circle itself becomes a point.

Fluids have two distinct types; liquids and gases. But the classification is made with the help of cohesive forces. "A liquid, being composed of relatively close-packed molecules with strong cohesive forces, tends to retain its volume and will form a free surface in a gravitational field if unconfined from above."(14) A gas has very weak cohesive forces and it fills any volume totally without forming a free surface.

3.1.1 Continuum concept

Continuum concept of fluids is very important and must be given special attention. In this study thesis fluid(air) will be considered as continuum and all calculations will be based on differential calculus. But in order to have a sight we must know why and under what conditions differential calculus is valid and when not for studying fluid motion. We know that a fluid cannot resist any shear force and it deforms. This fact stems from that fluid particles are free to move and have no certain lattice position. So the particles move randomly and this freedom of movement has an important result. The fluid density is not certain to detect, rather it has uncertainity. But this effect becomes less and diminishes as the volume considered becomes

more. For a very small volume the number of fluid molecules contained in it may vary a lot as the molecules move freely. But studies show that after reaching a volume of $10^{-9}mm^3$ we can assume the density is constant under the same conditions.

As this thesis deals with dimensions a lot larger than this($10^{-9}mm^3$) value, we can safely say that density is a point function. So all fluid properties vary continually and smoothly in space. There can be no abrupt change for any of them. A fluid behaving like this is called a continuum. The change is smooth enough that differential calculus is valid for analyzing a continuum.

3.1.2 Euler versus Lagrange

In the Eulerian method velocity field v(x, y, z, t) of the flow pattern is computed, not the velocity changes v(t) which a particle undergoes while it moves through the field as it is done in Lagrangian method. Of course the different perspektives are valid for any other properties like pressure or density.

3.1.3 Shear Stress in a Moving Fluid:

If a fluid is at rest the particles do ot move relative to each other under continuum assumptin. If there is no velocity gradient the result is the same, that means again there is no relative motion. If in a fluid there is no relative motion, there can be no distortion of the original shape.And if there is no distortion, we say thay there is no shear stress. But for the case where there is relative motion, the situation changes and we conclude that shear stress develops between succesive layers of the fluid.

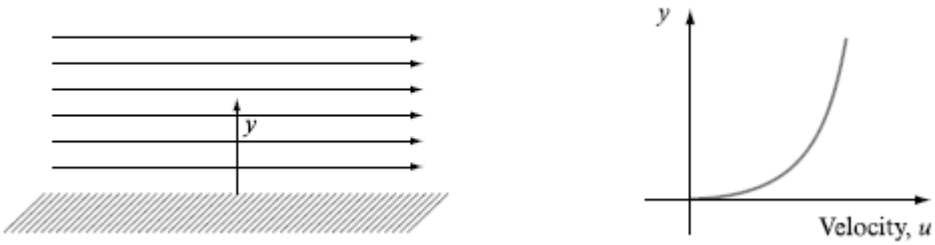

Figure 3.1 Shear Stress in a Moving Fluid (15)

As depicted in the figure(15) above,due to no slip condition(this condition states that the fluid touching to the solid boundry sticts to it and takes its velocity) velocity varies in the flow. It increases from zero just above the boundry to the potential flow velocity in the positive y direction.

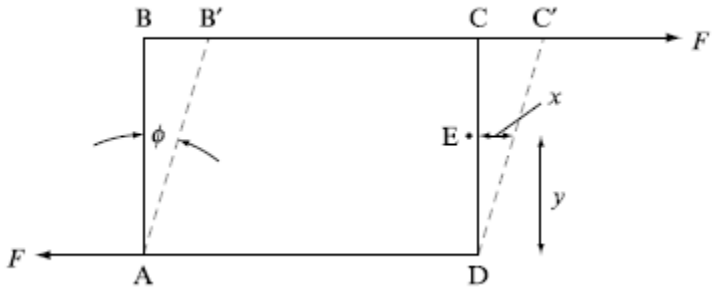

Figure 3.2 Force on Moving Plate (15)

In the figure just above it is shown that a force F acts to the plate BC which has a length "s" perpendicular to the sketch plane. The shear stress is F/A where A=IBCI x s. Now lets suppose that at time t the point E(more preciously the particle at E at time t) moves from its original place a distance equal to x. The shear strain φ is x/y where y is the perpendicular distance of the point E from AD. Of course this is valid only for small angles of φ, otherwise tanφ=x/y. But here we are dealing with very small angles.

Now if shear strain=φ=x/y, rate of shear strain becomes x/yt = (x/t)/y=u/y. Here the u=x/t is the velocity of the particle at E. If shear stress is proportional to shear strain we can conclude that

τ= constant × u/y … [1]

The u/y can be written in differential form as du/dy and indicates the velocity dependence of y distance at any point. The constant of proportionality is called as the dynamic viscosity μ of the fluid. Thus we reach the Newton's law of viscosity.

$$\tau = \mu \frac{du}{dy} \text{ ... [2]}$$

μ is an intensive property and depends on the fluid, temperature etc.

So far we defined the Newton's law of viscosity. But unfortunately not all fluids in nature obey this rule. Because while defining the rule we made an assumption that the shear stress is proportional to shear stress which may not be the case all the time for all fluids. If we look at the sketch just below we can notice that there are different fluid types classified on their behaviour to shear strain-shear stress relation.If a fluid is not Newtonian then it is called non-Newtonian and these are further classified into distinct groups depending on their behaviors.

In this study the only fluid dealt with is air and it is a Newtonian Fluid.

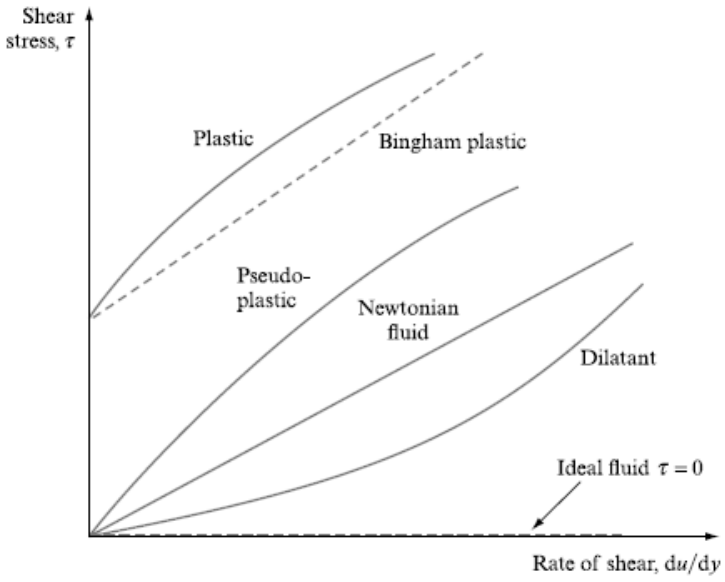

Figure 3.3 Shear stress-Rate of shear (15)

3.1.4 Viscosity

Viscosity is a measure of intermolecular cohesive forces. If the attractive force is large so is the viscosity and vice versa. Thus normally liquids tend to have lower viscosity if the temperature increases. This is because the cohesive forces become less important due to high energy particles. But viscosity is not only due to the cohesive forces but also intermolecular interaction. This is why for gases the temperature increases the viscosity. For gases the main source of the viscosity is not intermolecular cohesive forces but interaction. Thus although

higher temperature decreases further the cohesive forces it increases the intermolecular intaeraction so that the total affect is the increased viscosity with increased temperature.

3.1.5 Flow Types

Conditions in a fluid may vary from one point to another and, at any point, may change from time to time. Flow is uniform if the velocity at a given instant is the same at every point in the fluid. Otherwise flow is described as non-uniform. In practice, when a fluid flows past a solid boundary there will be variations of velocity in the region close to the boundary. However, if the size and shape of the cross-section of the stream of fluid are constant, the flow is considered to be uniform(16).

A steady flow is one in which the velocity, pressure and cross-section of the stream may vary from point to point but do not change with time. If, at a given point, conditions do change with time, the flow is described as unsteady. In practice, there will always be slight variations of velocity and pressure, but, if the average values are constant, the flow is considered to be steady. There are, therefore, four possible types of flow;

1.Steady uniform flow. Conditions do not change with position or time. The velocity and cross-sectional area of the stream of fluid are the same at each cross-section: for example, flow of a liquid through a pipe of uniform bore running completely full at constant velocity.

2.Steady non-uniform flow. Conditions change from point to point but not with time. The velocity and cross-sectional area of the stream may vary from cross-section to cross-section, but, for each cross section, they will not vary with time: for example, flow of a liquid at a constant rate through a tapering pipe running completely full.

3.Unsteady uniform flow. At a given instant of time the velocity at every pointis the same, but this velocity will change with time: for example, accelerating flow of a liquid through a pipe of uniform bore running full, such as would occur when a pump is started up.

4.Unsteady non-uniform flow. The cross-sectional area and velocity vary from point to point and also change with time: for example, a wave travelling along a channel.

In our study, when the blade first sees the air the flow is unsteady and non-uniform. But after enough time the flow might be assumed as steady and non-uniform. But due to complex turbulence it will behave unsteady and non-uniform also.

3.1.6 Comressible or not

In reality fluids are compressible whatever they be. This means their density is pressure dependent. But we know that studying fluid mechanics is hard and we need reasonable assumptions to reach useful results. That is why under steady flow conditions and small density

changes, to simplify the analysis of a problem we assume that the fluid is incompressible and thus has constant density.

Since liquids are already difficult to compress, they are generally treated as if they were incompressible for all cases of steady flow. But, in unsteady flow conditions, pressure differences can be high and the compressibility must be taken into account.

Gases can be compressed without much difficulty. Thus, unless pressure changes and density are very small, the effects of compressibility must be taken into account. In this study air can be assumed to be incompressible due to small pressure differences and Mach number being less than 0.1.

3.1.7 Basic Conservation Equations

Matter is neither created nor destroyed. This is a well known saying. Of course it will be true only if we add that this law does not apply to nuclear reactions.We are also neglecting relativistic effects, where Newton's law must be modified according to Einstein's famous theory.

There are three main conservation equations in fluid mechanics:

1) Conservation of mass
2) Conservation of momentum
3) Conservation of energy

The Navier-Stokes equations are based on those conservation rules. The Computational Fluid Dynamics tries to solve those equations via computer power numerically.

3.1.8 System and Control Volume

A system is defined as an arbitrary quantity of mass. Mechanics has many laws applying to the system. What is not system is surrounding and the boundries seperate the system from its surroundings. The law of mechanics are for determining the interactions and results of such interactions between the system and its surroundings.

The system is a fixed quantity of mass, m. Mathematically expressing it, msyst = const and $\frac{dm}{dt} = 0$ …[3]

For a control volume the situation needs further explanation. In the figures below, the amount of fluid swept through dA in time dt is the volume of the slanted parallelopiped. Mathematically,

$dV = V\,dt\,dA\cos\theta = (\mathbf{V}\cdot\mathbf{n})\,dA\,dt$ ...[4]

Then; $Q = \int_s (\mathbf{V}\cdot\mathbf{n})\ dA = \int_s V_n\,dA$ …[5]

By convention we n is considered to be the outward normal unit vector. Therefore **V . n** means outflow if it is positive and inflow if negative. When volume flow is multiplied by density to obtain the mass flow $\dot{m}$ and as a second condition if density varies over the surface, it must be in the surface integral to give

$\dot{m} = \int_s \rho(\mathbf{V}\cdot\mathbf{n})\,dA = \int_s \rho V_n\,dA$ …[6]

In case the density is constant, the equation simplifies to $\dot{m} = \rho Q$ …[7]

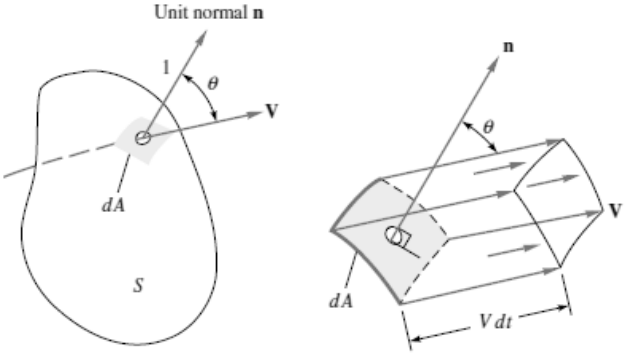

Figure 3.4 Vectors on a Fluid Particle (18)

3.1.9 Turbulence

In this study the core is to understand the flow field around a wind turbine blade. Here the main problem is understanding the turbulence phonemenon. Because the air flow over the blade becomes turbulent after some time and in fact this is desired. Otherwise the seperation of flow

occurs and the pressure drag becomes too high and as a result the lift over drag ratio decreases. This is not desired and if it occurs the blade and of course the turbine efficiency drops.

Thus it is a must in this thesis to have a part explaining the turbulence. Without knowing what it is, any model trying to solve the complex flow field problem will become nonsense. Of course turbulence itself is a main topic of research and it still lacks adaquate info. There are many reasons for that. In this part a sight will be developed.

Observing turbulent flows in our surrounding is common. We see for example smoke going up of a chimy, strong winds and many others like a waterfall. What comes to our mind waching all those events is that it is not predictable. The flow is caotic and not steady. In fact from all observations on turbulent flow we come to a very important conclusion: the velocity field is not regular and varies to a large extent. This in turn brings chaos to all other properties.

As a catogorisation we can divide turbulence into small-scale and large-scale. But this classification needs further explanation for sure. It is highly personel to call something small or large. At high Reynolds range, the large scale motion is affacted by the geometry of the problem such as boundry conditions. Transport and mixing is mainly dominated by flow geometry. In this study we will use mainly large scale motions and the motion will depend heavily on the geometry of the blade. On the other hand for small scale, motion is determined by viscosity and energy exchange.

3.2 A REVIEW OF AERODYNAMIC MODELS

3.2.1 Actuator Disc Model

This model is the first and most simplified explanation of the kinetic energy extraction process of wind turbines which is developed by Betz.(19) Though, it is very important to understand in general what is happening through the use of a wind machine.

As it is mentioned, the wind turbine exploits the kinetic energy of moving air, which is wind. According to conversation of mass principle, slower moving air must expand in order to have the same mass flow rate with the fast moving one. This is illustrated below in the drawing (20). It is seen that as air approaches the turbine its velocity decreases while the cross section increases. In this way, the mass flow rate is constant throughout the whole process.

Before we continue further, we must set our assumptions for this analysis:

1. Homogenous, incompressible, steady state fluid flow
2. There is no friction in the flow and no frictional drag on the disc. Therefore no change in the internal energy of flow from the inlet to the outlet occurs.

3. An infinite number of blades, meaning no air can escape without leaving some of its kinetic energy
4. The wake behind the disc is non–rotating which means this analysis is one-dimensional and the only velocity direction is along the flow axially
5. The static pressure far upstream and far downstream of the rotor is equal to the undisturbed ambient static pressure

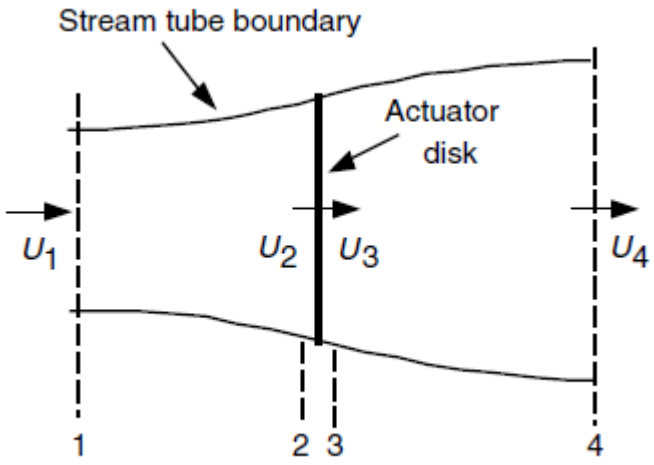

Figure 3.5 Actuator Disk Model (20)

We can define mass flow rate as density times cross sectional area times velocity and it is constant throughout the control volume.

$(\rho AU)_1 = (\rho AU)_4 = \dot{m}$ ... [8]

Here subscript "1" refers to the upwind, putting in a different way the incoming air and "4" refers to the downwind which is the wake behind the turbine.

The air undergoes a change in velocity whist passing through the disc. The rate of change of momentum is the overall change in velocity times the mass flow rate and equals to a force, a thrust force which slows down the wind:

$T = U_1(\rho AU)_1 - U_4(\rho AU)_4$ ... [9]

As in this control volume system we have change of momentum, there must be a force responsible. By definition the stream tube is surrounded by air at atmospheric pressure and

cannot create any force. So the only force is the one stemming from the pressure difference across the disc.

$T = A_2(p_2 - p_3)$ ... [10]

To find the pressure difference we can apply Bernulli equation to either side of the disc but not as a whole from upwind to downwind. This is because there is extraction of energy at the disc which prevents application of Bernoulli equation whole through the tube. But we can apply the equation separately to both sides.

$p_1 + \frac{1}{2}\rho U_1^2 = p_2 + \frac{1}{2}\rho U_2^2$ ... [11] This is for the upwind side.

$p_3 + \frac{1}{2}\rho U_3^2 = p_4 + \frac{1}{2}\rho U_4^2$ ... [12] This is for the downwind, wake side.

Rearranging those two;

$p_2 - p_3 = \frac{1}{2}\rho U_1^2 - \frac{1}{2}\rho U_4^2$ ... [13]

Assumption 5 says that pressure at section 1 and 4 is equal. As seen in the illustration, the cross section changes smoothly and there is no jump in velocity from 1 to 4. So the velocity at section 2 and 3 can safely be considered as equal.

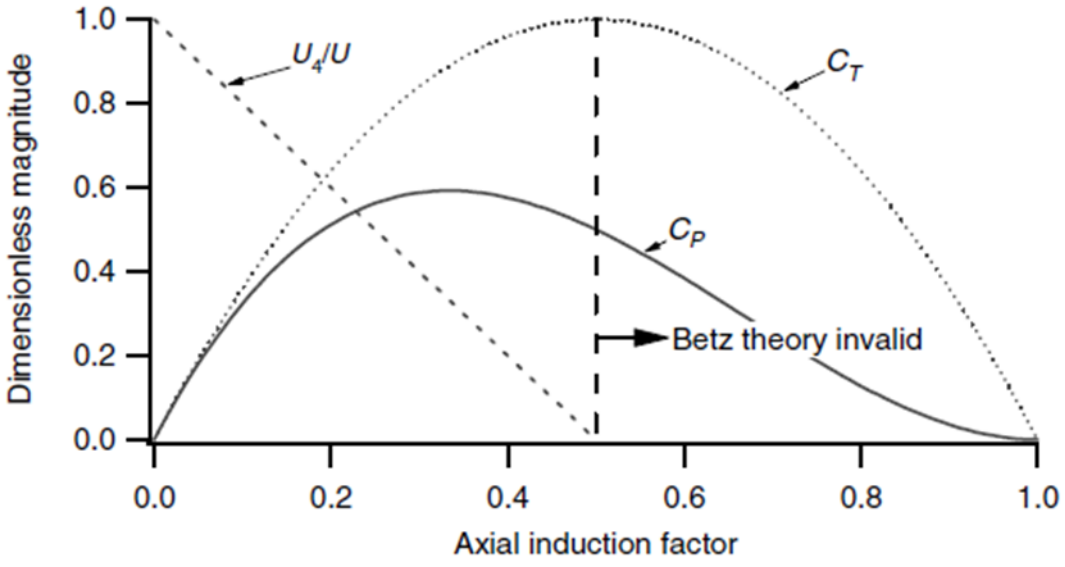

Figure 3.6 Axial Induction Factor (23)

Above is the graph of both power and trust coefficients (20). Obviously this simple theory is not valid for axial induction factor values more than 0.5. Otherwise we have to admit that air velocity becomes negative at wake side of the actuator disc meaning back flow. This phenomenon is out of the initial assumptions of this theory. But the measured thrust coefficient

as a function of the axial induction factor and the corresponding rotor states are to be seen in the illustration below (21) by Eggleston and Stoddard (1987) If we look at what is happening when the Momentum Theory is not valid, that means for axial induction factor "a" values larger than approximately 0.4, the Turbulent Wake State is to be seen. Briefly describing, this state corresponds to one at which momentum is transported from outer flow to the wake. That is; there is momentum added to the stream tube from ambient air. The reason for that is simple. If the "a" value gets larger, the wind velocity of the wake becomes small. This creates a velocity difference between the free stream and if this difference becomes larger than a certain value the free shear layer of the stream tube corresponding to the edge of it losses stability. Eddies are formed. Those eddies are responsible for the momentum transfer from out of the tube to the inside.

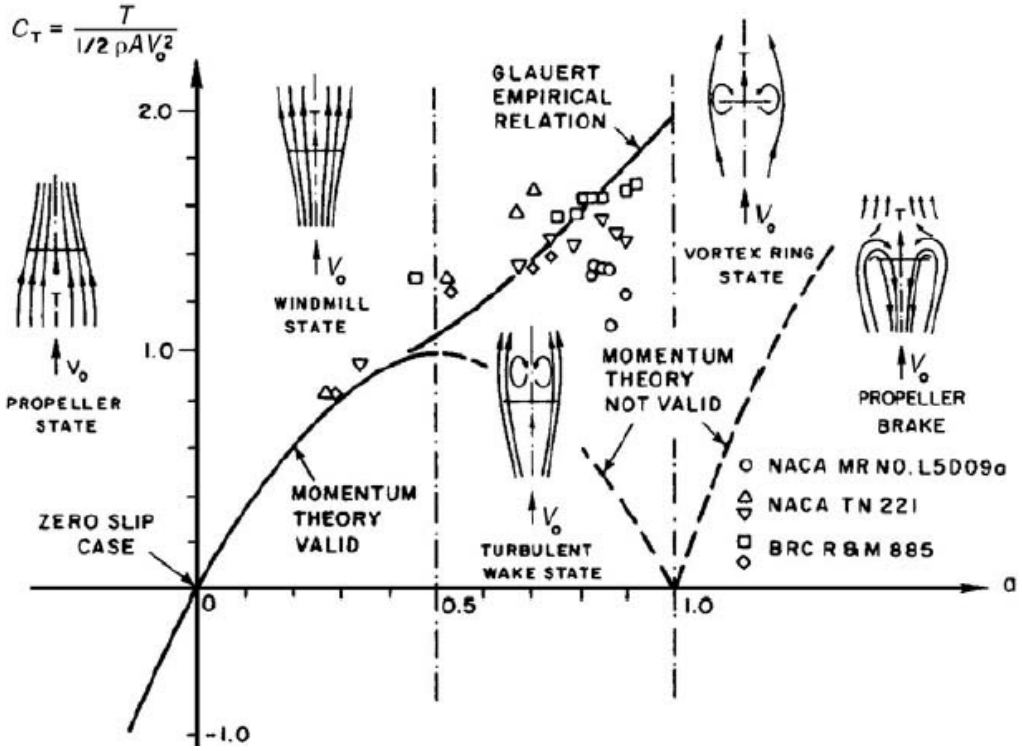

Figure 3.7 Wind States (23)

Now we are in a point to understand basics of wind turbines under certain assumptions. As seen below in the drawing (22) velocity and cross sectional area of the stream tube differs smoothly. As velocity decreases, the area increases to keep the mass flow rate constant. The mass passing through the disc per unit time is less than it could be if there was no disc. That is the main restriction why we cannot have power coefficient more than 0.5926, Betz limit. As air slows down while it approaches the disc, its pressure increases above ambient atmospheric level. This pressure does useful work and drops instantly below atmospheric level on the downwind side

of the disc. But as it continues the air velocity carries on decreasing causing the pressure to increase. In the end air pressure reaches undisturbed level while the cross section of the flow tube has further grown to compensate the further decrease in velocity.

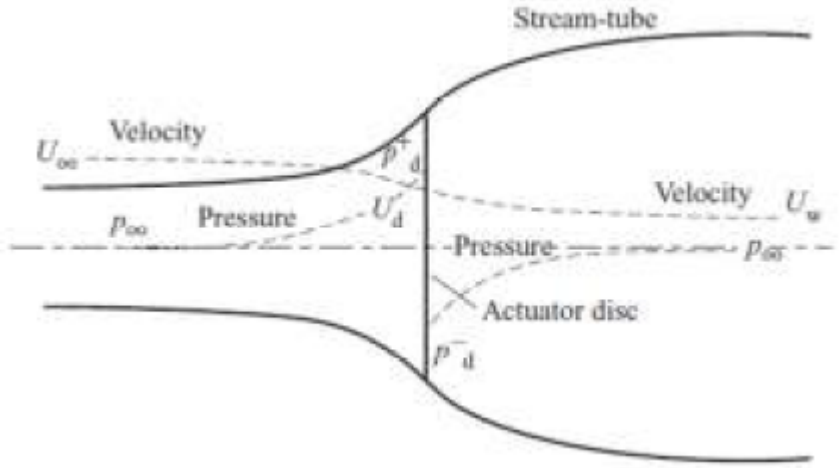

Figure 3.8 Velocity-Pressure Change in Stream Tube (20)

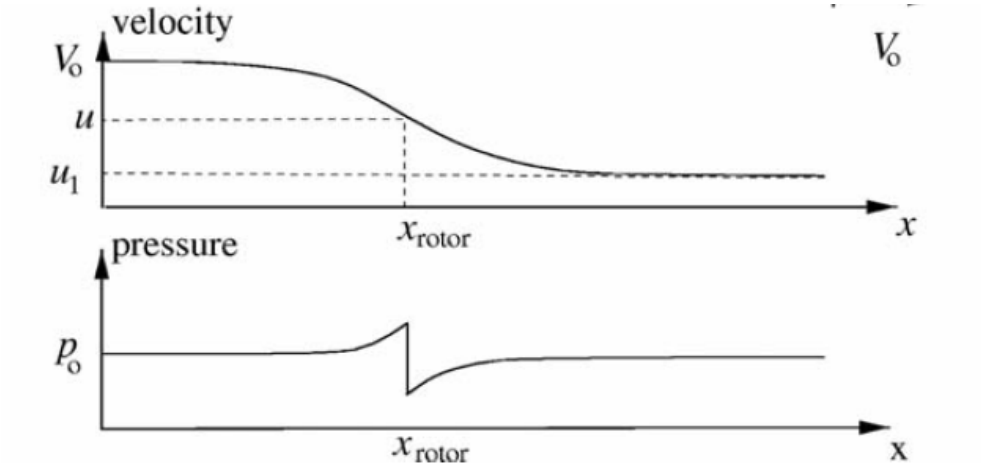

Figure 3.9 Velocity-Pressure Change in Stream Tube (20)

In the illustration just above by Hansen (23) the velocity and pressure along the stream tube is better seen.

3.2.2 Rotation in the Wake and Corresponding Effects

In the actuator disc model, the flow is assumed to be 1-D. But in reality the flow over a turbine blade is of course 3-D. This feature will be discussed later in this study. But for the time being what is aimed is that the actuator disc model is not sufficient for good estimates of a wind turbine performance. If we remember the assumptions made to develop the actuator disc model, we see that one of our main assumptions was the non-rotating wake behind the turbine. In reality the wake after the turbine is rotating. Thus there is another model developed by many scientists among who Glauert was a pioneer (24).

Basically it is easy to predict that the performance of a wind machine will decrease provided the wake rotation is taken into account. The Betz's 1-D model is the ideal wind turbine without wake rotation. It is ideal because it does not include friction and wake rotation. There can be turbines without wake rotation. This can be achieved by a counter rotating two discs or using any other stator. But as this would bring other problems and increase the cost, modern wind turbines let the wake rotate at the expense of efficiency loss. This sub-chapter will deal with ideal rotors with wake rotation. Wake rotation brings a radial induction factor. This rotor allowing wake rotation is still considered to be ideal because the friction is still not included in the calculations.

Generally saying, the extra kinetic energy in the rotating wake will decrease the possible upper limit of kinetic energy extraction of the flow. This will be shown here fallowing the theorem.

As shown in the Figure 3.10 (25) the wake, that is the flow after the rotor, rotates. But the direction is not the same with the rotor blade. It rotates in the opposite direction. This is so because the blade rotates in reaction to the torque which the flow applies to it. This is consistent with the conservation of angular momentum.

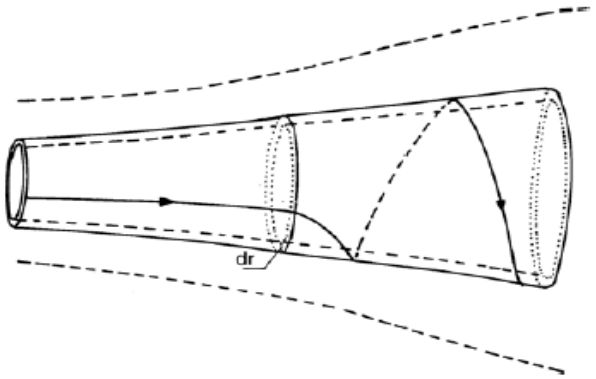

Figure 3.10 Deflection of streamlines (23)

Thus we can foresee a fact: The higher the torque of the rotor, the more the kinetic energy of the wake due to rotation. Thus, the higher the torque, the smaller the efficiency is. We can

conclude that, if the rotor has low torque and high rotational speed, the efficiency will be higher. So instead of a high torque-low speed, a low torque-high speed rotor has better performance.

Below is the result of calculation of ideal rotor performance with wake rotation (26). This result is sometimes attributed to German scientist Schmitz. Here instead of the long calculation procedure, attention is given to the results. As seen easily, the performance of with and without wake rotation ideal rotors deviate a lot for small tip speed ratios. To make it clear, tip speed ratio is the speed ratio of the rotor tip to the upcoming flow. High values of tip speed ratio means high rotational speed. Here it is obvious that increasing the rotational speed increases the efficiency of the rotor as predicted earlier. That is why modern wind turbines operate at tip speed ratios around 8. Due to noise problem, higher rotational speeds are not desired.

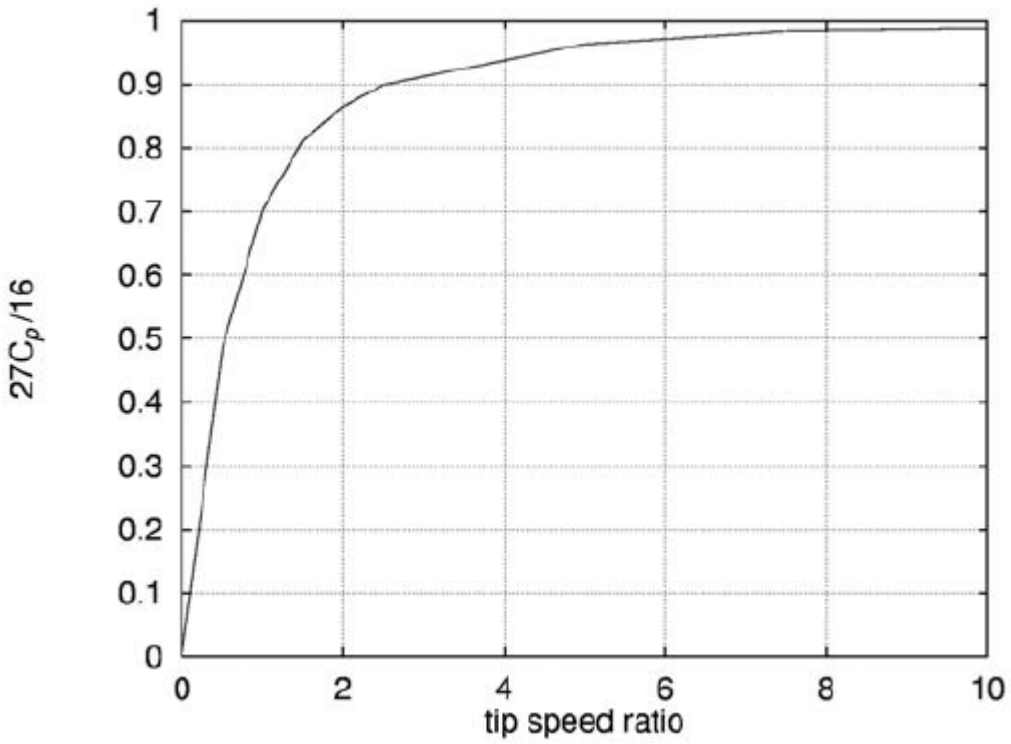

Figure 3.11 Efficiency limit of a Turbine (22)

3.2.3 The Blade Element Momentum Method

The Blade Element Momentum Method was developed first by Glauert in 1935. After him many modifications by many scientists and engineers were done and this method is still in use in wind energy industry widely.

The main reason for its popularity comes from fairly accurate results with very low computational energy and time. Thus, this method is used as a first check for any rotor design. The BEM methodology is for horizontal axis wind turbines.

In reality what happens at the rotor is complex and 3D. But it is difficult to build a 3D model. So, what is needed is to develop a lower order model representing the 3D. In fact the BEM method is a 2D method which is extrapolated into 3D. This means the BEM method makes many assumptions. Those assumptions bring deviation from reality. That is why later a correction factor remedy is brought to the original method.

The basis of the model is discretization of the blade. While doing so the main assumption is made such that all those discretized elements of the blade are not affecting each other. The stream tube used before for the actuator disc model is divided into annular elements as shown in the sketch below. Each annular element has the thickness dr.

The BEM method is an iterative procedure. No need to say this is not an exact solution but only a numerical one.

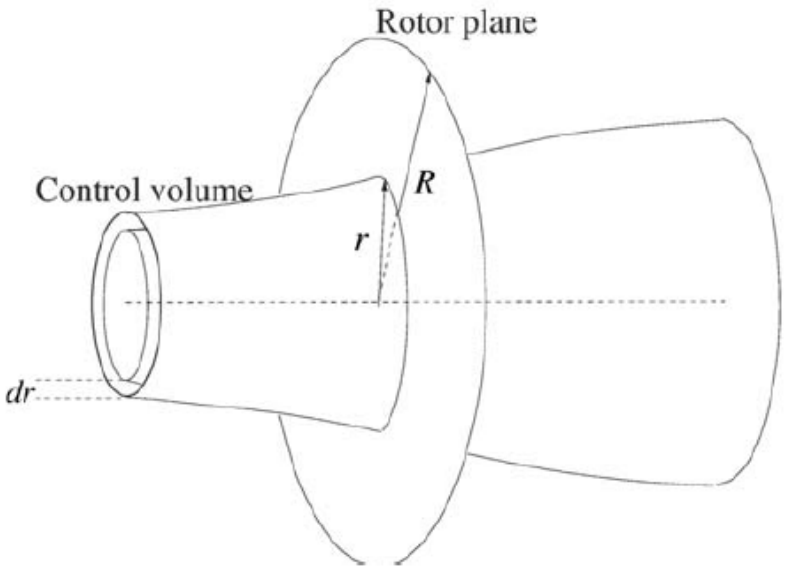

Figure 3.12 Rotor Plane (22)

The velocities at the rotor plane are shown here. The axial induction factor, the radial induction factor and the local pitch angle form such a diagram. Here θ is local pitch and is the sum of pitch and twist angles. The local angle of attack is the difference of geometric angle ϕ and θ.

So; $\alpha = \phi - \theta$ ... [14]

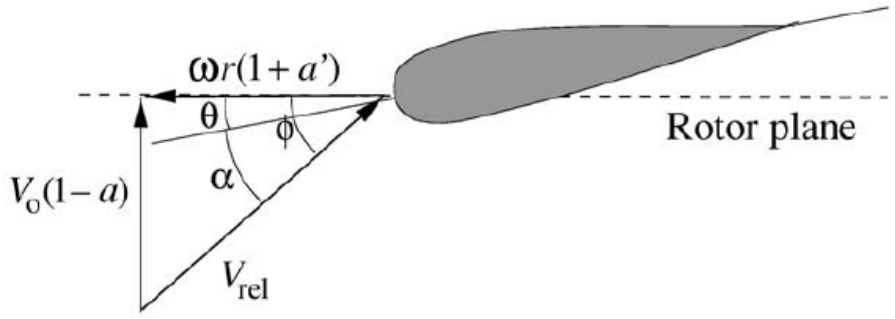

Figure 3.13 Velocity Triangle

The force diagram is also necessary to continue with developing the original method. The method continues with finding the Lift and Drag forces, then further continues by finding the forces normal and tangential to the rotor plane.

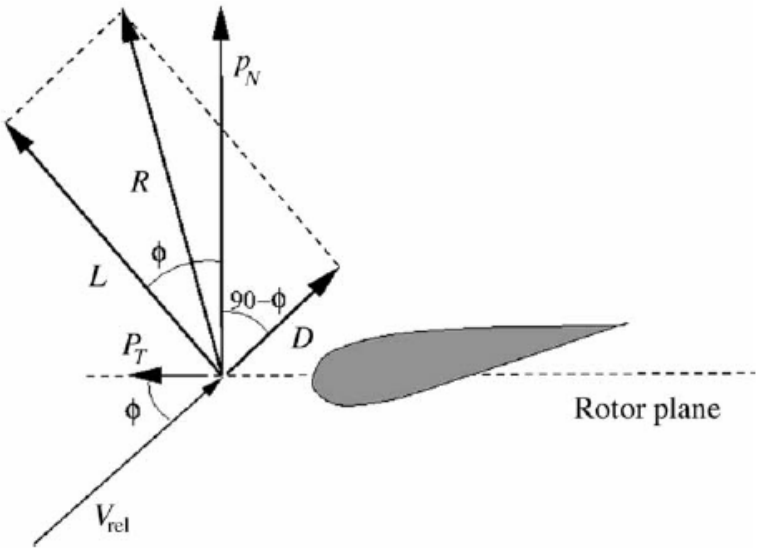

Figure 3.14 Force Triangle

The forces can be calculated by simple relations. From the figure, using trigonometric equations

$P_N = L\cos\phi + D\sin\phi$ and $P_T = L\sin\phi - D\cos\phi$ ... [15]

Dividing both sides of the two equations with $\frac{1}{2}\rho V_{rd}^2 c$ we come to the equations below:

$C_n = C_l\cos\phi + C_d\sin\phi$ and $C_t = C_l\sin\phi - C_d\cos\phi$ ... [16]

This step is done to achieve lift and drag coefficients in the equations. The development of the method carries on by defining the solidity which is the fraction of the annular area covered by blades.

$\sigma(r) = \frac{c(r)B}{2\pi r}$ ... [17]

Here B is the number of blades. C(r) denotes the local chord. From this equation it is seen that solidity is not the same at all discrete sections but a variable of the blade geometry.

The force and torque on each annular area is calculated by the two equations below keeping in mind that *PN* and *PT* are not forces but forces per length.

$dT = Bp_N\,dr$ ... [18]

$dM = rBp_T\,dr$ ... [19]

By means of some algebraic manipulations the two equations just above become

$$dT = \frac{1}{2}\rho B\frac{V_0^2(1-a)^2}{\sin^2\phi}cC_n\,dr \quad \text{... [20]}$$

and

$$dM = \frac{1}{2}\rho B\frac{V_0(1-a)wr(1+\acute{a})}{\sin\phi\cos\phi}cC_t\,rdr \text{ ... [21]}$$

By means of some other manipulations

$$a = \frac{1}{\frac{4\sin^2\phi}{\sigma C_n}+1} \text{ ... [22]}$$

$$a' = \frac{1}{\frac{4\sin\phi\cos\phi}{\sigma C_t}-1} \text{ ... [23]}$$

are achieved. Before writing down the syntax of the BEM method step by step it is of utmost importance to introduce two corrections. These are Prandtl's tip loss factor and Glauert correction. The former serves as a remedy to the assumption of infinite number of blades. The latter is necessary for cases where axial induction factor is more than 0.4. Previously it was

stated that the 1-D momentum theory is valid for axial induction factors less than 0.4. Otherwise turbulent wake state happens. But the BEM method uses 1-D momentum theory. And during iteration process most likely a value greater than 0.4 occurs. So an empirical correction by Glauert is used for those cases.

What is valid for a rotor with finite number of blades is not so with an infinite number of blades. The vortex system in the wake is different for the above mentioned rotors. The BEM assumption is infinite number of blades. An actual turbine has finite number of blades usually 3 for horizontal axis types.

Prandtl changes the induction factors and achieves the ones below:

$$a = \frac{1}{\frac{4F\sin^2\phi}{\sigma C_n}+1} \quad \text{... [24]}$$

$$a' = \frac{1}{\frac{4F\sin\phi\cos\phi}{\sigma C_t}-1} \quad \text{... [25]}$$

where $F = \frac{2}{\pi}\cos^{-1}(e^f)$ ... [26] and $f = \frac{B}{2}\frac{R-r}{r\sin\phi}$ ...[27]

Glauert has found an empirical relation for thrust coefficients for axial induction factors greater than 0.4.

$$C_T = \begin{cases} 4a(1-a)F & a \le \frac{1}{3} \\ 4a\left(1-\frac{1}{4}(5-3a)a\right)F & a > \frac{1}{3} \end{cases} \quad \text{... [27]}$$

Here F is the Prandtl's correction factor for tip losses. Some other empirical relations are as follow

$$a = \frac{1}{\frac{4F\sin^2\phi}{\sigma C_n}+1} \quad \text{... [28]}$$

or $$a = \frac{1}{2}\left[2 + K(1-2a_c) - \sqrt{(K(1-2a_c)+2)^2 + 4(Ka_c^2 - 1)}\right] \quad \text{... [29]}$$

where $K = \frac{4F\sin^2\phi}{\sigma C_n}$ ... [30]

Please note that the described model is the classical model which has been improved a lot afterwards by introducing hub losses etc. Detailed models can be found in AeroDyn Theory Manual by NREL (27).

3.3 NUMERICAL METHODS FOR AERONAUTICS

In aeronautics and in fact almost all other problems which involve fluid flow it is a must to use numerical methods to come to a solution. There are some very simple and rare cases where an exact and analytic solution is possible to reach by making some assumptions and simplifications. But as said right now, these cases are very rare and in engineering problems like air flow over a NACA profile or a 3D blade geometry numerical methods are used.

Numerical methods are defined by many authors like Chapra(28) as " techniques by which mathematical problems are formulated so that they can be solved with arithmetic operations. Although there are many kinds numerical methods, they have one common characteristics: they invariably involve large numbers of tedious arithmetic calculations."

Thanks to the emerged and still fast developing computer technology, it is now possible to solve many fluid dynamics problems accurately. In this thesis a flow problem over different geometries and conditions will be investigated with the help of numerical packages.

When designing a wind turbine, the most important factor is how efficient it is. There are two ways to understand it. Either a prototype is manufactured and tested or the design is computer simulated. The first way is more secure but costly and time consuming. That is why designers prefer the second way. Only after many simulations and comparing different designs, a prototype is constructed depending on the computer results.

A wind turbine design can be enhanced only if the flow around it is well understood. But it is not so simple to predict the flow behaviour. Researchers try to find new techniques to enhance the models that we have.

The flow over an airfoil or a wind turbine blade is not only fully turbulent, but there is a laminar and a transition region also. If the flow is assumed to be only fully turbulent, it is wide experience that a significant deviation from test results occur. Below some widely used methods and their properties are discussed. Some of those methods are also used in the simulations done for this thesis.

In order to understand why we seek a numerical method but not an exact one, some basic properties of turbulence need mentioning. One of the most important information about a flow pattern is the velocity field. This field is in reality 3-dimentional and time-dependent. The random character of turbulence makes it even more difficult. The turbulent motions are very much geometry dependent which has a simple result: the turbulent motions are not universal.

One of the main difficulties in investigating turbulent flow is finding the non-linear convective term which appears in the famous Navier-Stokes equations. Another part which needs a lot of effort is the pressure gradient term. This pressure gradient term is neither linear nor local.

So far many numerical methods and models have evolved to give an answer to the turbulent flow. Unfortunately not all those models are applicable to all types of flows accurately. That is why it is useful to list some important features abut models. Because choosing the right model for a flow problem is very important. The assessment criteria are(29):

i) level of description

ii) completeness

iii) cost and ease of use

iv) range of applicability

v) accuracy

The level of description refers to the complexity of the flow. Shortly saying, a model can be appropriate to a statistically stationary fully developed pipe flow but not to a non-statistically stationary flow in the cylinder of a reciprocating engine. Easy to understand a statistically non-stationary model must have different features than a model which deals with a problem with the other type mentioned.

A model is thought as **complete** under the condition that its constituent equations are free from flow-dependent variables. A flow can be distinguished from another by specification of material properties for example. A distinction can be done also by looking at the boundary conditions and/or initial conditions.

“Incomplete models can be useful for flows within a narrow class (e.g., attached boundary layers on airfoils) for which there is a body of semi-empirical knowledge on the appropriate flow-dependent specifications. However, in general, completeness is clearly desirable.” (29)

Cost and Ease of Use is another factor prescribing whether a model is acceptable. In the end, equations formed in the model are solved numerically by computers. Computer CPU time means cost. The result is of course sought to be as accurate as possible but for a simple problem days of CPU time is not feasible. That means while seeking a solution, models must be assessed not only in terms of accuracy but cost. According to (30) Peterson 200 hours of a supercomputer is the upper limit for research calculations. It seems this limit is still reasonable although many years have passed over the proposal.

There are over one-thousand turbulence models in use and unfortunately for a specific flow type only some of those are **applicable**. To give an example, some mixing-length models have implicit assumptions about the flow geometry. Thus, one can not apply those models to

problems which have a geometry different than the assumed one. Another limitation comes from cost side. More preciously saying, some models need a lot of CPU time and if the computer which runs the simulation is not appropriate and fast enough, the model should not be selected.

Accuracy is perhaps the easiest criteria to understand. As said many times earlier, a flow investigation is a numerical technique rather than an exact solution. An exact solution without simplifying assumptions is the full real solution and does not deviate from real phenomena. But a numerical method is an approximation. Due to lack of analytic solutions of the Navier-Stokes equations, numerical methods must be used. Anyone running a simulation wants the results be as accurate as possible. But most of the time a good thing comes with a disadvantage. In general, if more accurate results are sought, more CPU time and cost must be paid.

As a final remark, modeling and running a simulation imitating a flow problem is an optimization problem at the beginning. How much accuracy is needed in what time and with what cost? All mentioned criteria must be considered at the same time in order to get the best possible results with the least time and cost.

3.3.1 Main Classes of Numerical Methods

In the coming section, some main classes of numerical simulation methods will be discussed.

3.3.1.1 Direct Numerical Simulation

This method is the one which does not make use of any turbulence model, but numerically solves the governing Navier-Stokes equations of the flow. In this method, all temporal and spatial scales of turbulence are resolved. This method needs a lot of CPU time and the number of operations during the solution rise to the cube of Reynolds number. This is the main limitation of the direct numerical method. Owing to this limitation, the flow problems involving high Reynolds numbers are not feasibly solved via this method.

3.3.1.2 Reynolds Averaged Navier Stokes(RANS) Models (32)

The aim of the turbulence models for the RANS equations is to compute the Reynolds stresses. The Reynolds equations are solved for the mean velocity field. In the Reynolds equations, there are terms called Reynolds stresses. Those terms can only be determined by a turbulence model but not analytically. Any turbulence model trying to find the unknown stress terms in the Reynols equations has **either the assumption of turbulent viscosity or it tries to find the stress terms from modeled Reynolds-stress transport equations.**

When a RANS model is based on the first way, that is it tries to find the stress terms via the turbulent–viscosity hypothesis, it has two further assumptions:

1) Assumption one is the intrinsic assumption which says at each point and time the Reynolds-stress anisotropy is found by mean velocity gradients.

2) Assumption two is the specific assumption which says that the relationship between the Reynolds-stress anisotropy is related to the mean rate-of-strain tensor similar to the relation for viscous stress in a Newtonian fluid.

In fact it was found in 1956 in a wind tunnel experiment conducted by Uberio that the turbulent-viscosity assumption is not correct and the Reynolds-stress anisotropies are not determined by the local mean rates of strain. Nevertheless, the models having this assumption are still in use because for simple shear flows, the aforementioned hypothesis is reasonable.

When a RANS model is based on the second way, that is it tries to find the stress terms in the Reynolds equations by modeling and solving Reynolds-stress transport equations, we see that the main deficit of the turbulent-viscosity hypothesis is eliminated.(31) Because in this way, model transport equations are solved for individual Reynolds stresses.

After explaining little bit the theory behind all those models, We come to the question of solving the stress terms in the Reynold equations. This is possible by three main categories of RANS-based turbulence models by making use of the either ways discussed above. Each main category has sub-categories and these will be shortly described as fallows. Please note that any mathematical expression is mostly avoided here. The main reason for that lies in the difficulty of them. Those expressions are mainly tensor equations which is beyond the scope of this thesis dissertation.

Below most common RANS-based turbulence models are named under appropraite catagories. Not all the listed methods will be discussed but the ones which have a wide spread use and also useful for aeronautics.

The Spalart-Allmaras Model

The Spalart-Allmaras model is a more or less simple one-equation model. It solves a modeled transport equation for the kinematic eddy or putting in a different way turbulent viscosity. In this model it is not required to calculate a length scale which is related to the local shear layer thickness. The Spalart-Allmaras model was designed especially for aerospace applications. Wall-bounded flows and boundary layers subjected to adverse pressure gradients are solved to a good accuracy level by this model.

The Spalart-Allmaras model is however still relatively new.That is why it is not tested for all types of complex engineering flows. Besides, one-equation models are questioned for their ability to accommodate changes in length scale. This ability might be necessary when the flow changes suddenly from a free shear flow to a wall-bounded one for example.

k-ε Model

The k-ε model is one of the most common complete turbulence model. Being a complete model, it does not need flow dependent specifications. Many CFD codes make use of it. This model is justified not to perform well in case of significant adverse pressure gradient such that occurring over an airfoil. It is a two equation model. Transport equations are solved for two turbulence quantities. Those quantities may be used to form a lengthscale, a timescale or some others. This allows a two equation model to account for history effects like convection and diffusion of turbulent energy.

(k) refers to the first transported variable, turbulent kinetic energy. (ε) refers to the second transported variable, the turbulent dissipation which is the variable determining the scale of the turbulence. On the other hand, the first variable, k, determines the energy in the turbulence.

There are many different formulations of k-ε model. Jones and Launder have the honor of developing the standard model which was later improved with model constants by Launder and Sharma. The original driving force for the model was to improve the mixing-length model, and also to find another way to solve algebraically prescribing turbulent length scales in moderate to high complex flows.

The k-ε model has shown success for free-shear layer flows with small pressure gradients. That explains why the model gives good results for wall-bounded and internal flows only when the mean pressure gradients are small. Accuracy is proved experimentally to be small for flows which have large adverse pressure gradients. One might come to the conclusion then, that the K-epsilon model is not an appropriate choice for problems like compressors or wind turbine blades.(especially the regions close to the blade surface where adverse pressure gradient is not small)

k-ω Model

The k-ω model is one of the most commonly used turbulence models. It is also a two equation model like k-ε. It also includes two extra transport equations to represent the turbulent properties of the flow. In this way a two equation model can account for history effects like convection and diffusion of turbulent energy.

The first transported variable is turbulent kinetic energy, k. The second transported variable is the specific dissipation, ω . It is the variable that determines the scale of the turbulence. This model is a lot more successful than the k-ε in the near wall region.

SST k-ω

The SST k-ω turbulence model is another two-equation eddy-viscosity model. The shear stress transport formulation combines two different approaches. On one side the use of k-ω code for the boundary layer lets the model be appropriate for direct usage all the way down to the wall

through the viscous sub-layer. Thus the SST k-ω model is used as a turbulence model without any extra damping functions. The SST code switches to a k-ε formulation in the free-stream and by doing so it avoids the common k-ω problem that the model is too sensitive to the inlet free-stream turbulence properties. The SST k-ω model is often praised for its good behavior in adverse pressure gradients and separating flow. Although the SST k-ω model, just like a normal k-ε model, does still produce a bit too large turbulence levels in stagnation regions and regions with strong acceleration, this tendency is much less pronounced.

The shear-stress transport (SST) k-w model was developed by Menter.The aim is to effectively combine the robust and accurate formulation of the k- w model in the viscous near-wall region with the free-stream of the k- ε model in the far field. The SST k- w model is similar to the standard k- w model. However it includes the some refinements:

- There is a blending function designed to be one in the near-wall region to activate the standard k-w model, and zero away from the surface to activate the transformed k-ε model.
- The SST model contains a damped cross-diffusion derivative term in the w equation.
- The definition of the turbulent viscosity is changed in order to render the transport of the turbulent shear stress.
- The modeling constants are altered.

These modifications and specialties make the SST k-w model more accurate and reliable for a wider class of flows like adverse pressure gradient flows than the standard k-w model. Other modifications are done to provide that the model equations behave appropriately not only in the near-wall but also in far-field zones.

The Transition model mathematics by Menter:

The flow over an airfoil has all three (laminar,transition,turbulent) areas at the same time. The transition point moves toward the leading edge if the angle of attack is increased. But, the result of analysis by applying only the fully turbulence model to the whole area has a shortcoming: Flow separation in the laminar boundary layer is faster than that in the turbulent boundary layer, and this phenomenon is an important reason that causes difference between analysis results using a fully turbulent model without considering laminar-transition effects and actual experiment results. In particular, it can have a significant effect on the estimation of the performance of wind turbine blades made of airfoil bundles. Accordingly, in order to get more accurate aerodynamic characteristic analysis results, we need to consider the application of a sophisticated turbulence model that can accurately estimate laminar separation bubble and turbulent reattachment phenomenon.

Remarks: Many turbulence models are not successful to predict the coefficients of an airfoil. The standart k-epsilon medel is reported to overestimate lift force for example. Main reason is that the seperation points are not accurately found. Especially the post-stall behaviour is weekly demonstrated. The underlying reason for this is the wrong prediction of the boundry layer seperation in the viscous sub-layer. SST model(Shear Stress Transfort) model calculates the transport term of the shear stress. It estimates the vortex size well.

3.3.2 Comparison of Turbulence Models

Turbulence models are plenty. But for each application, the selected turbulence model makes a difference. A model giving very good results in agreement with experiments for example may be disastrous for another. Of course the selection of correct turbulence model needs expertise and there is good knowledge in the literature. In this dissertation project, the flow around airfoils and blades is investigated. According to many studies, SST model which is specially developed for aeronautics performs better. In a paper by E. Lutum and F. Cottier "Aerothermal predictions on a highly loaded turbine blade including effects of flow separation" (33) it is shown that SST is the most appropriate model to use in aeronautics. There are plenty of similar papers. In a paper (38) by Robert Maier-Staude, "Wind Turbine Modeling using ANSYS", it is demonstrated that the SST Transition Model predicts the most accurate results. The success of the SST model is for its combining both near wall conditions and far away conditions. **Thus, in this dissertation, the final results will be achieved by SST Turbulence model.** But to show how much the result is dependent on the selected model, some simulations have been conducted. The summary is given in a table. Please note that some models may even not converge after many iterations. Table 3.1 shows Lift/Drag values at different angle of attacks with various turbulence models. The simulations are conducted in CFX and they are 2D. A NACA 0012 profile with a chord length of 1 m is used. Chosen wind speed is 7.25 m/s.

AoA(deg)	0^0	5^0	10^0	15^0
k-Epsilon Model(L/D)	No-convergence	38.5	51	46
k-Omega Model(L/D)	0	34	46	No-convergence
SST Model(L/D)	0	45	45	29

Table 3.1 Comparison of Turbulence Models

As said previously, the selected turbulence model does make a difference. This is proven by the simulation results tabulated in Table 3.1. Especially for higher angle of attacks, the difference gets more absolute. But before all, not all models produce even a result at all. As seen, the k-Epsilon model at AoA 0 degree and k-Omega at AoA 15 degrees gives no result. While the results of different models may be considered to be close to each other at 5 and 10 degrees, they diverse a lot for AoA 15 degrees. Shortly saying, it is one of the vital points to choose the correct turbulence model for the simulation to get a reasonable result. Another issue to note is that the number of iterations, thus CPU time, is dependent on the chosen model.

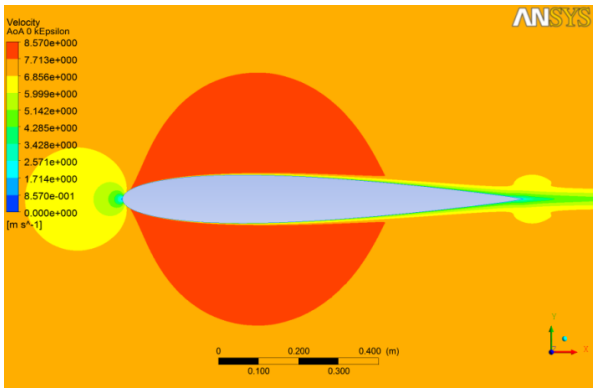

Figure 3.16 k-epsilon, AoA= 0^0, Velocity

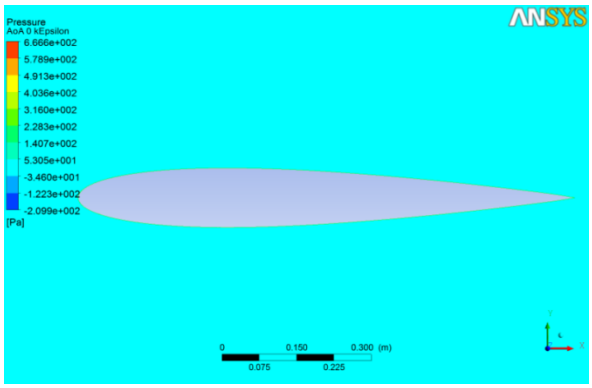

Figure 3.17 k-epsilon, AoA= 0^0, Pressure

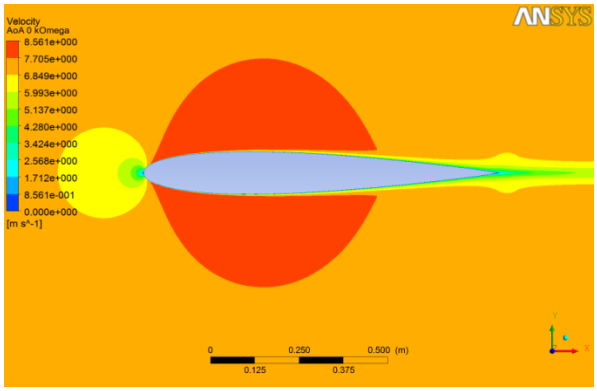

Figure 3.18 k-Omega, AoA= 0^0, Velocity

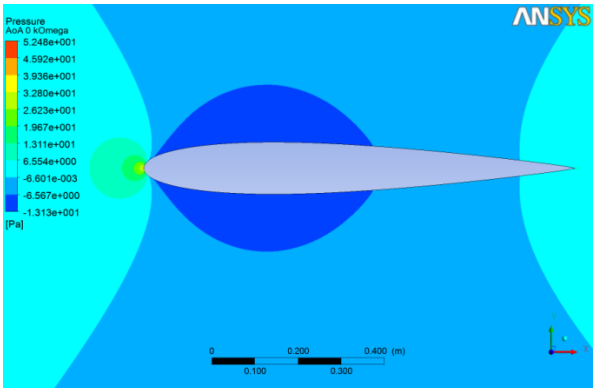

Figure 3.19 k-Omega, AoA= 0^0, Pressure

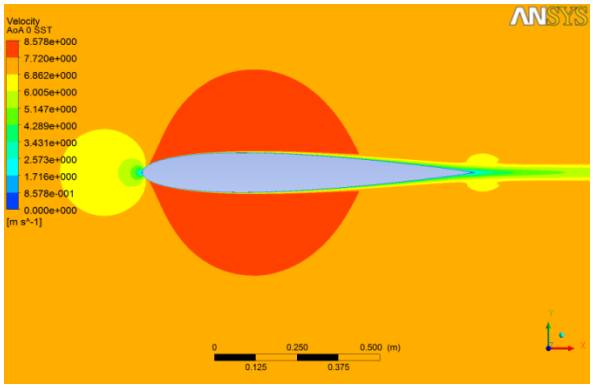

Figure 3.20 SST, AoA= 0^0, Velocity

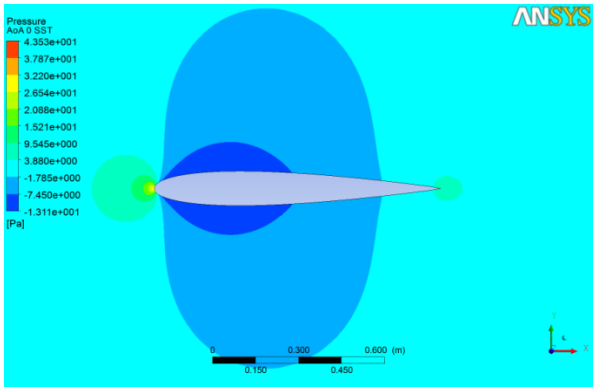

Figure 3.21 SST, AoA= 0^0, Pressure

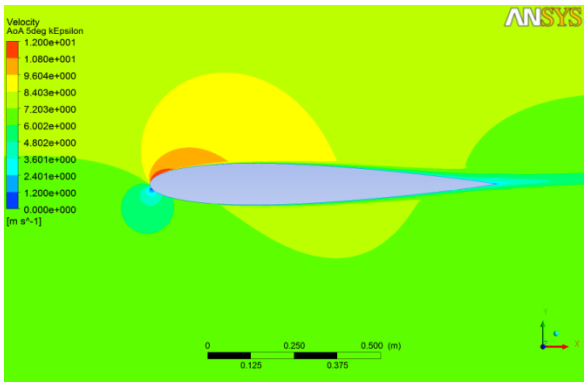

Figure 3.22 k-epsilon, AoA= 5^0, Velocity

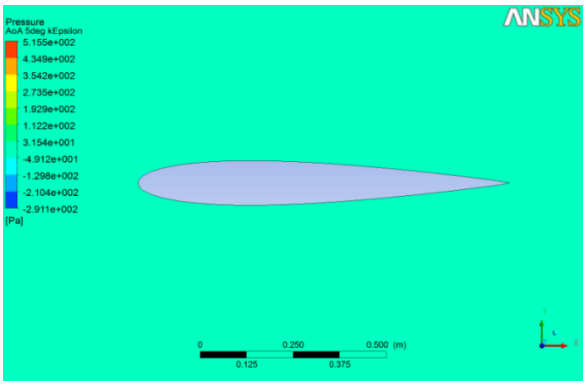

Figure 3.23 k-epsilon, AoA= 5^0, Pressure

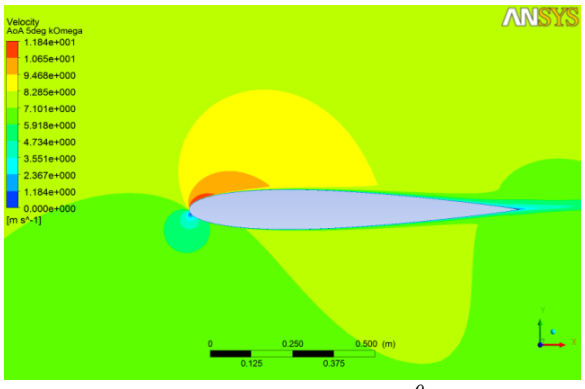

Figure 3.24 k-Omega, AoA= 5^0, Velocity

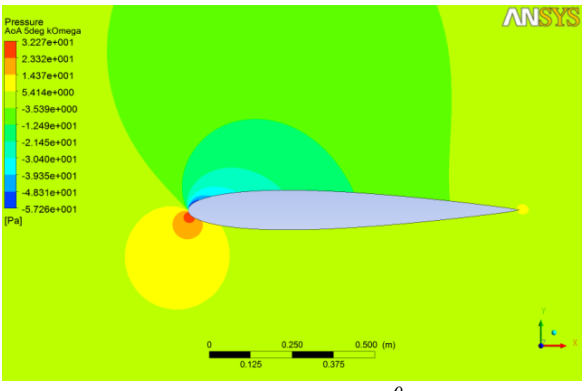

Figure 3.25 k-Omega, AoA= 5^0, Pressure

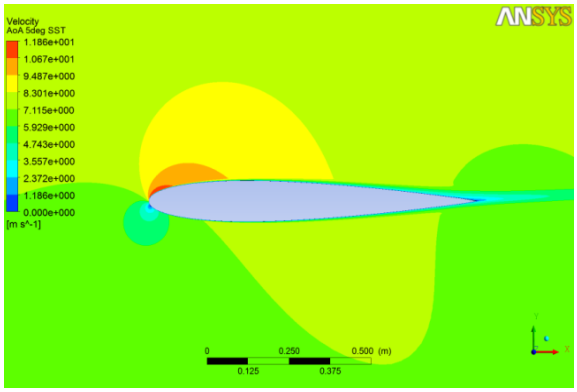

Figure 3.26 SST, AoA= 5^0, Velocity

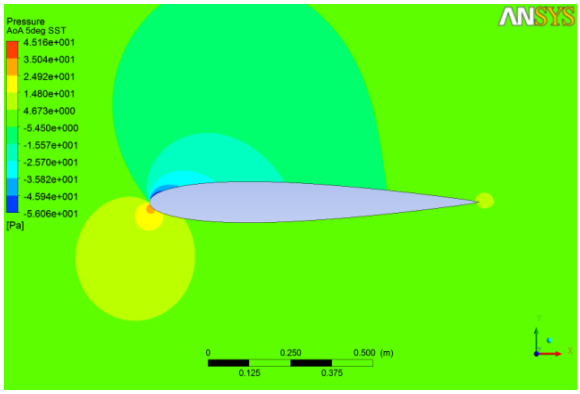

Figure 3.27 SST, AoA= 5^0, Pressure

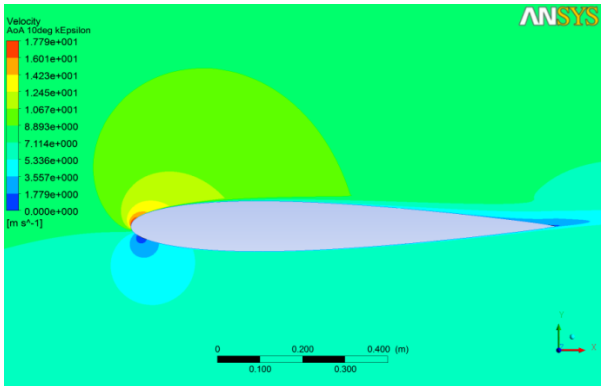

Figure 3.28 *k-epsilon, AoA= 10^0, Velocity*

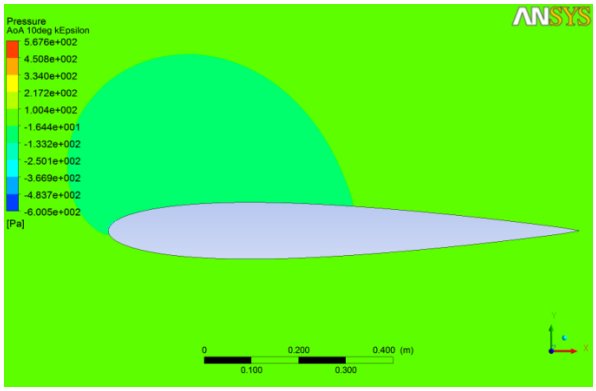

Figure 3.29 *k-epsilon, AoA= 10^0, Pressure*

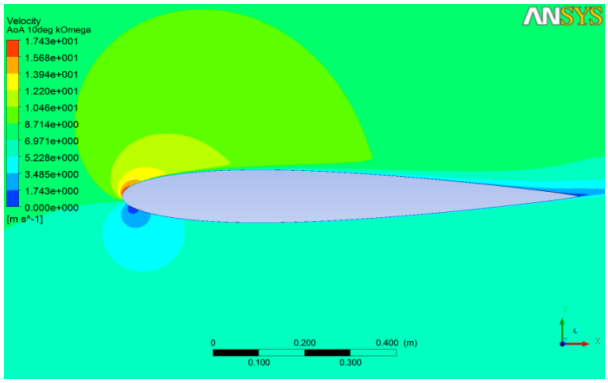

Figure 3.30 k-Omega, AoA= 10^0, Velocity

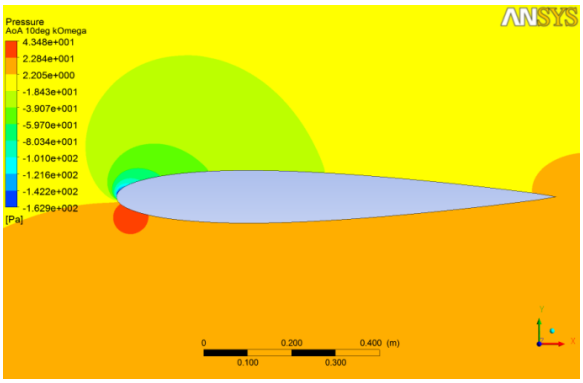

Figure 3.31 k-Omega, AoA= 10^0, Pressure

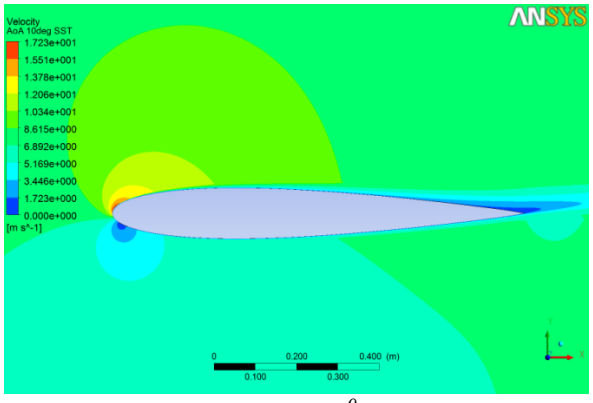

Figure 3.32 SST, AoA= 10^0, Velocity

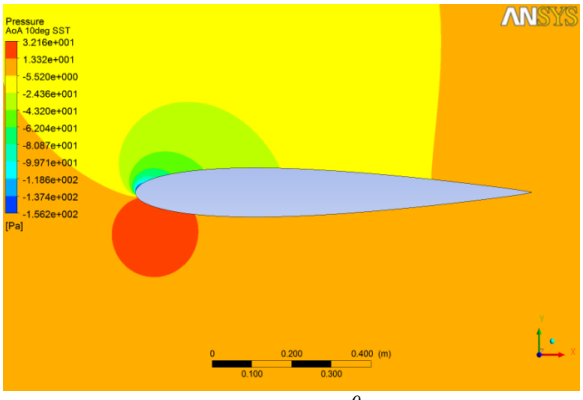

Figure 3.33 SST, AoA= 10^0, Pressure

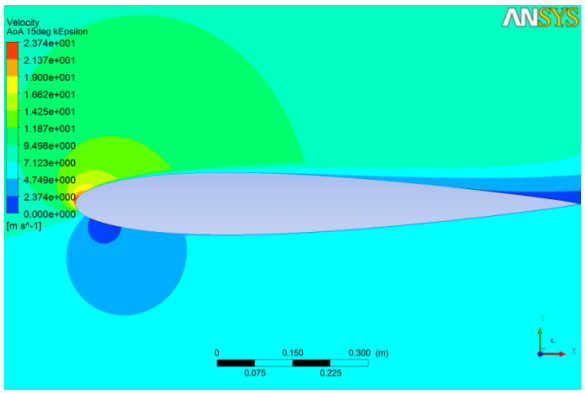

Figure 3.34 k-epsilon, AoA= 15^0, Velocity

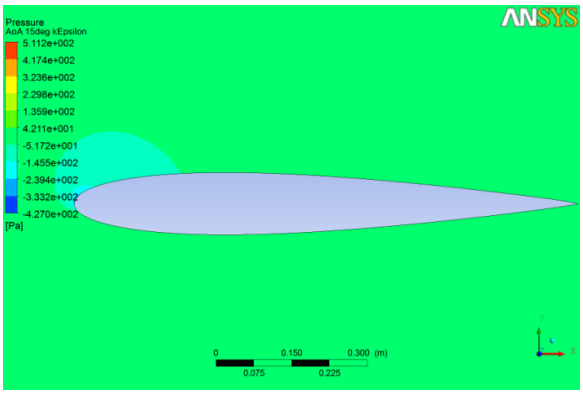

Figure 3.35 k-epsilon, AoA= 15^0, Pressure

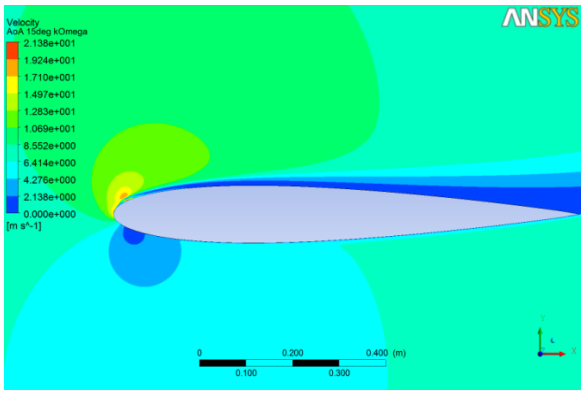

Figure 3.36 k-Omega, AoA= 15^0, Velocity

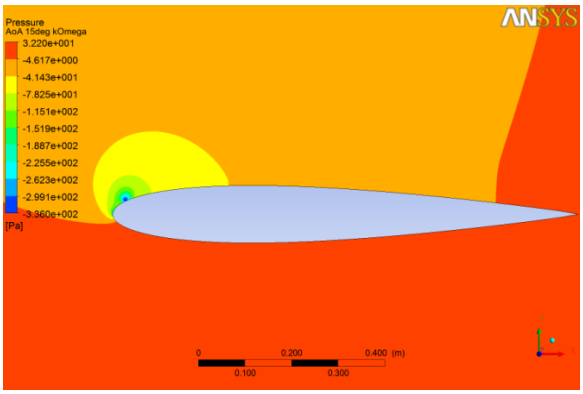

Figure 3.37 k-Omega, AoA= 15^0, Pressure

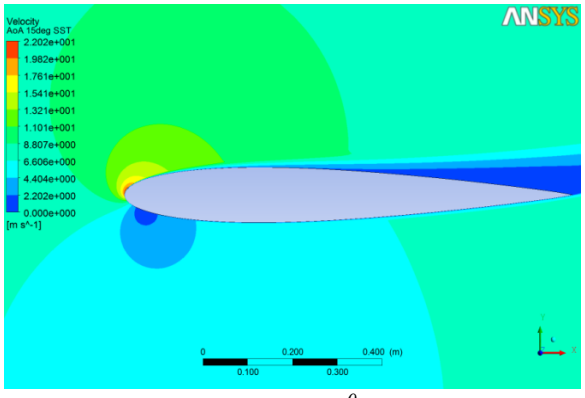

Figure 3.38 SST, AoA= 15^0, Velocity

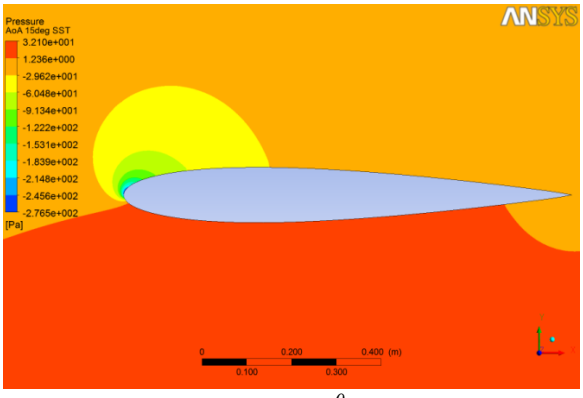

Figure 3.39 SST, AoA= 15^0, Pressure

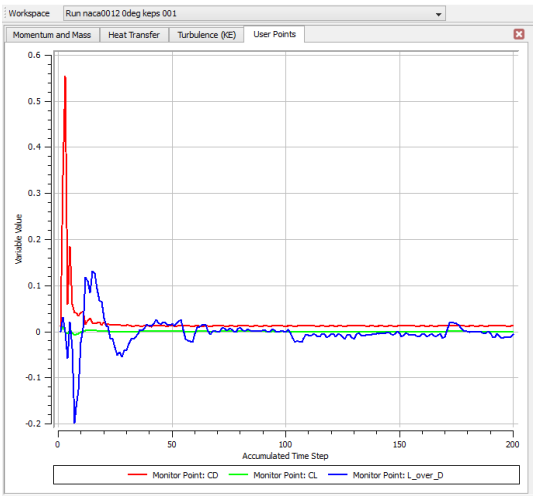

Figure 3.40 Monitor Points 0^0 k-epsilon

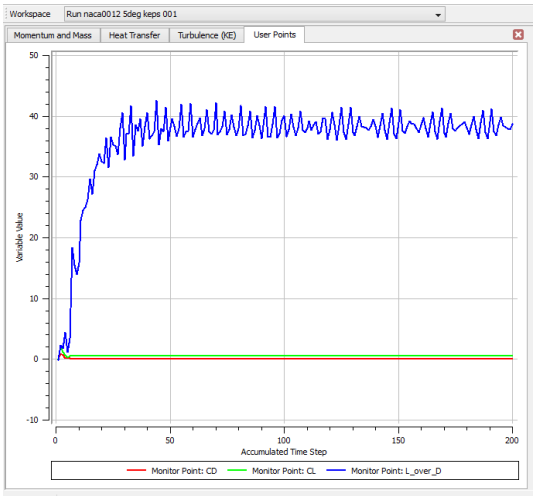

Figure 3.41 Monitor Points 5^0 k-epsilon

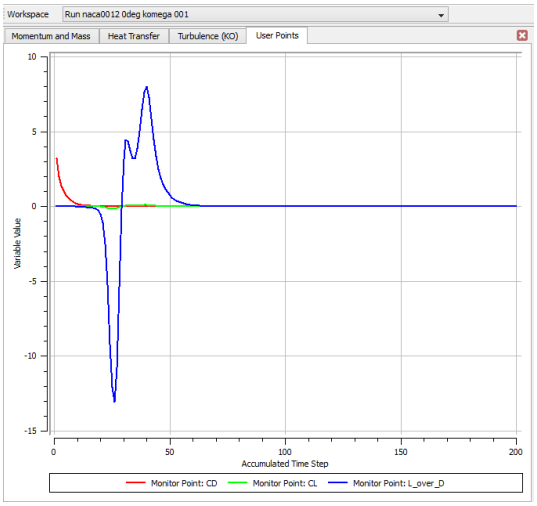

Figure 3.42 Monitor Points 0^0 k-Omega

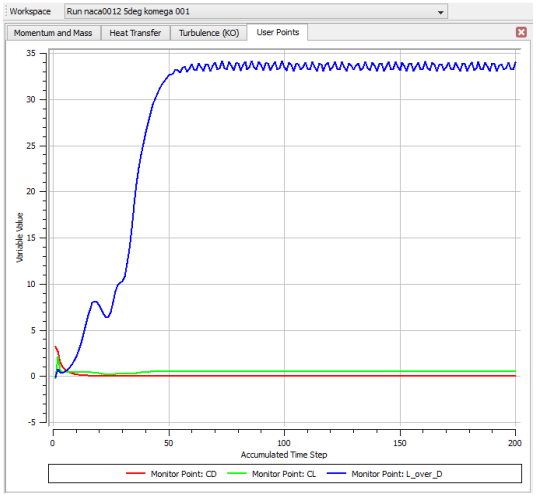

Figure 3.43 Monitor Points 5^0 k-Omega

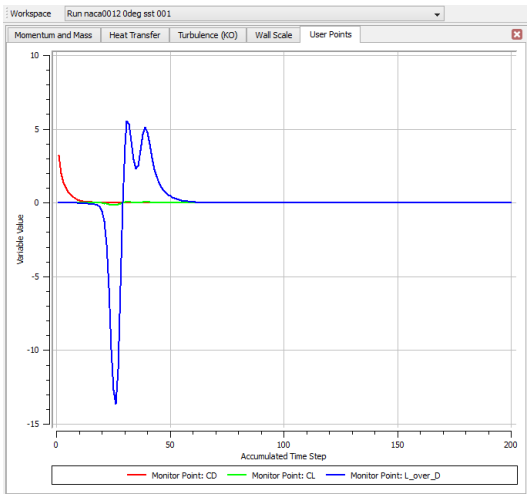

Figure 3.44 Monitor Points 0^0 SST

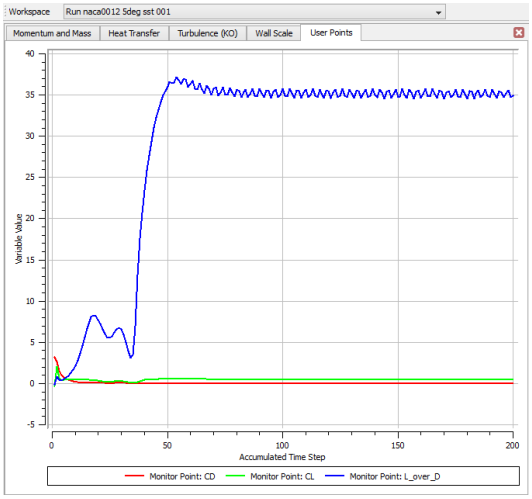

Figure 3.45 Monitor Points 5^0 SST

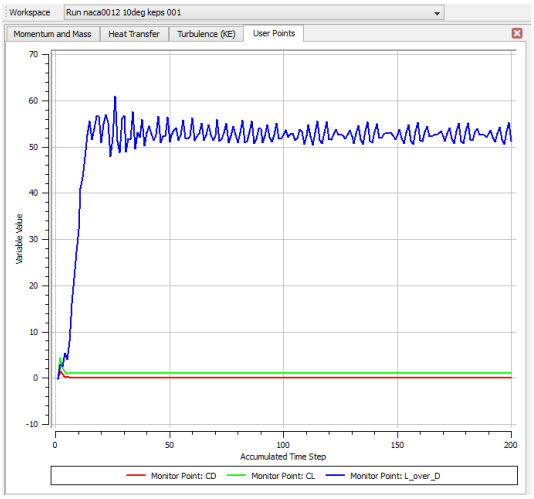

Figure 3.46 Monitor Points 10^0 k-epsilon

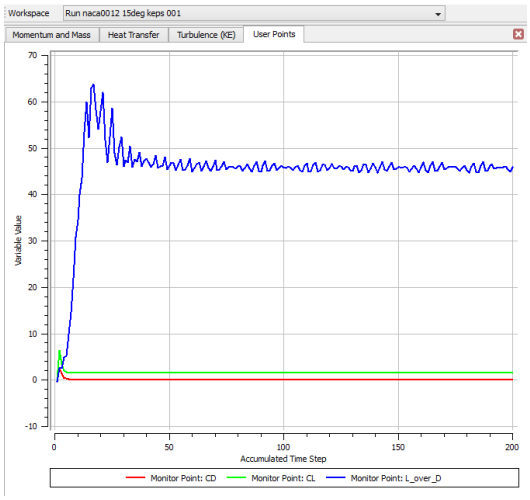

Figure 3.47 Monitor Points 15^0 k-epsilon

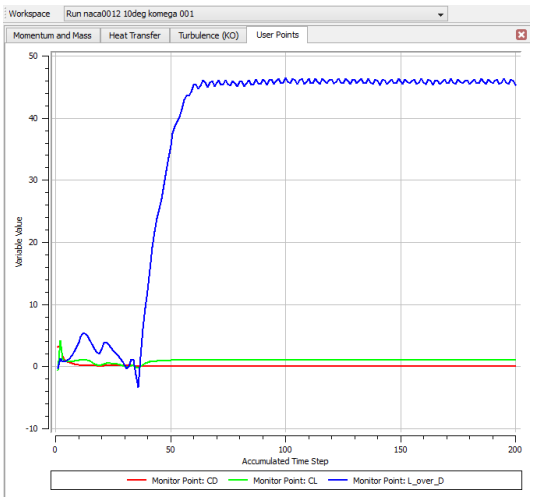

Figure 3.48 Monitor Points 10^0 k-Omega

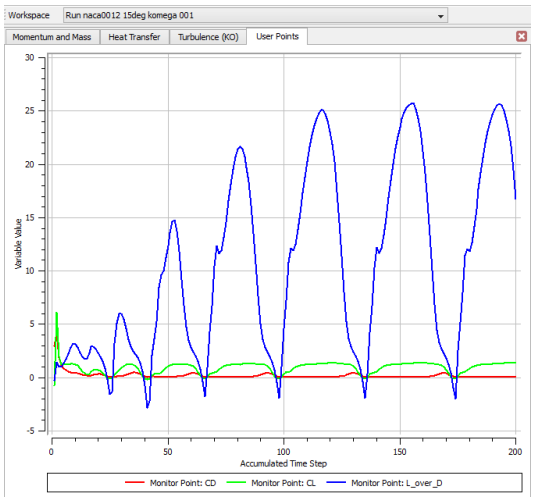

Figure 3.49 Monitor Points 15^0 k-Omega

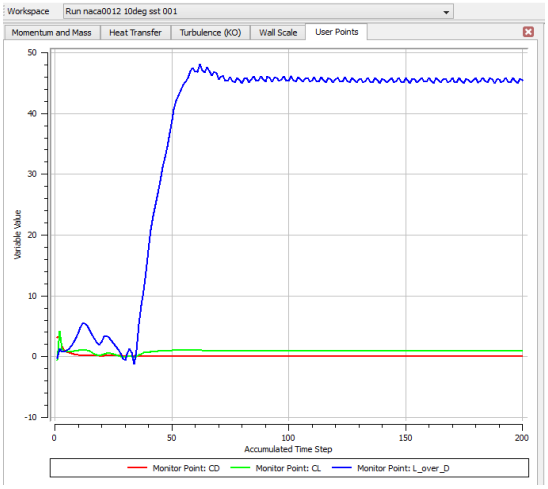

Figure 3.50 Monitor Points 10^0 SST

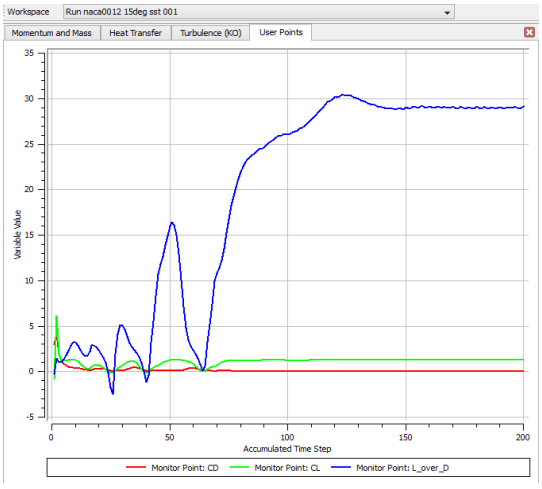

Figure 3.51 Monitor Points 15^0 SST

Looking at figures from 3.16 to 3.51 it is obvious that chosen turbulence model changes the results not only in means of pressure and velocity distribution, but also the time needed. In some cases it determines even whether a result will be achieved or not.

3.3.3 Transition or Fully Turbulent Model

The study of this dissertation tries to model the behavior of wind turbine blades. But the results are highly dependent on the selected model. In reality a uniform wind without any turbulence flowing over a blade does not create a turbulent flow regime just at the contact point, but it

undergoes three successive regimes which are laminar, transition and turbulent. The air around the nose, of course depends also on the roughness, angle of attack etc, is in laminar region and as it goes downside transition starts and in the end after a point it becomes turbulent. No need to say, laminar and turbulent air flows create different effects. A laminar region would be preferred to have high Lift/Drag coefficients provided that the flow is attached to the airfoil. In order to delay stall, turbulence is preferred because compared to laminar flow, it is more resistive to adverse pressure gradients and stays attached longer.

3.3.3.1 Estimating When the Transition Model Should Be Used

The ANSYS CFX has developed a relation whether or not the transition model is necessary (34). This model needs more CPU. Thus, it is important to know what we gain by spending more CPU power. The relation gives Reynolds numbers ratio. If the ratio is high, it means using transitional model is needed.

$$\frac{Re_{xt}}{Re_x} = \frac{380000.(100.Tu)^{-\frac{5}{4}}}{(\frac{\rho}{\mu}.V.L_{Device})}$$

Re_{xt}= Transition Reynolds Number

Re_x= Device Reynolds Number

Tu= Free stream turbulence intensity and is calculated as fallows where “k” is turbulent kinetic energy.

$$Tu = \frac{(2k/3)^{0.5}}{V}$$

For a NACA0012 airfoil for example;

Tu= 1.6 if we take k=687

Here k value is determined from post-processing results of many simulations.

Then putting it in the above formula, we get a result saying that Re_{xt}/Re_x is less than 1%.

Note that the device Re was chosen to be 6 million for the simulation from which k value is extracted.

So, for a result like this: It is not difficult to conclude that avoiding the use of transition model does not affect the accuracy of the simulation a lot. The same simulation models with the only difference being the use of transition model show that the conclusion was correct. (The Lift/Drag values differ less than 2 per cent)

3.3.3.2 Transition Onset Condition for the Simulations

Once the simulation model is selected to be SST Transition, it is a must to describe the program how to decide to shift from laminar to turbulent model. As given some examples below, choosing the right criteria is utmost importance.

When we look at the some selected simulations with every other things being the same but only transition onset criteria different, we see that the result deviates a lot from one model to another. In the first simulation the onset criteria is automatically defined by the CFX when we select the Gamma Theta. This Langtry Menter code gives a bad result. The Lift /Drag ratio is around 48. From experiments conducted at NASA, the result is only 27.

Another criteria is defined by Gamma code with expression 460.0 * (1.0 + x / (1.0 [m])) This timethe result is somewhat better with L/D to be 33.

When the expression is modified by user to be 260.0 * (1.0 + x / (1.0 [m])) this time the result is rather acceptable and equals to 29.

Finally when the expression is further modified to be 180.0 * (1.0 + x / (1.0 [m])) we achieve a fairly good result to be 28.

The examples can easily be reproduced. But what is important and must be taken into consideration when modeling a simulation with transitional turbulence, the transition criteria is very much important and can easily change the results being “acceptable” to “highly errorous”.

It is not difficult to guess that when we further decrease the onset criteria, it is possible to reach even more to the experimental result.

Criteria	Result	Deviation from Experiment(%)
Langtry Menter	48	105.2
460.0 * (1.0 + x / (1.0 [m]))	33	22.2
260.0 * (1.0 + x / (1.0 [m]))	29	7.4
180.0 * (1.0 + x / (1.0 [m]))	28	3.7

Table 3.2

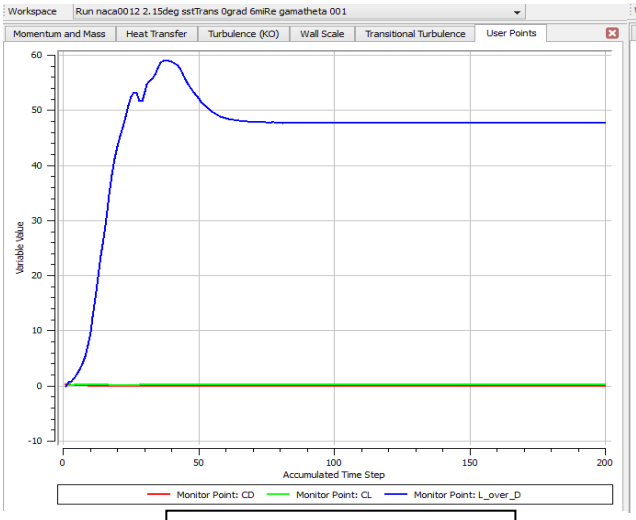

Figure 3.52 SST Transitional Model with Option Gamma Theta (Option: Langtry Menter)

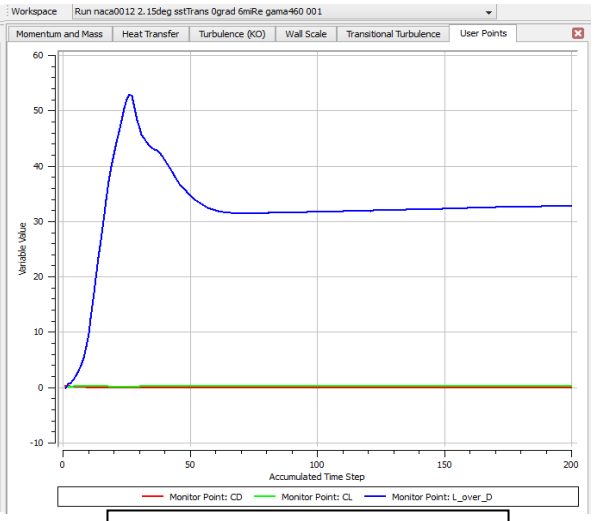

Figure 3.53 SST Transitional with Option Gamma (Transition Onset Reynolds Number = 460.0 * (1.0 + x / (1.0 [m])))

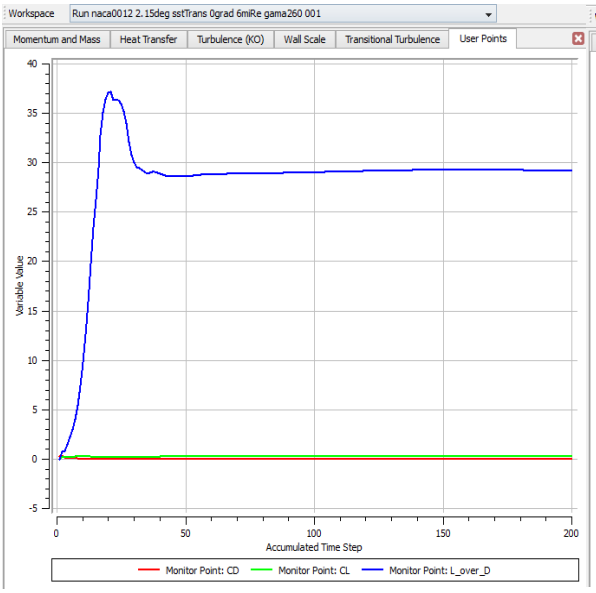

Figure 3.54 SST Transitional with Option Gamma (Transition Onset Reynolds Number = 260.0 * (1.0 + x / (1.0 [m])))

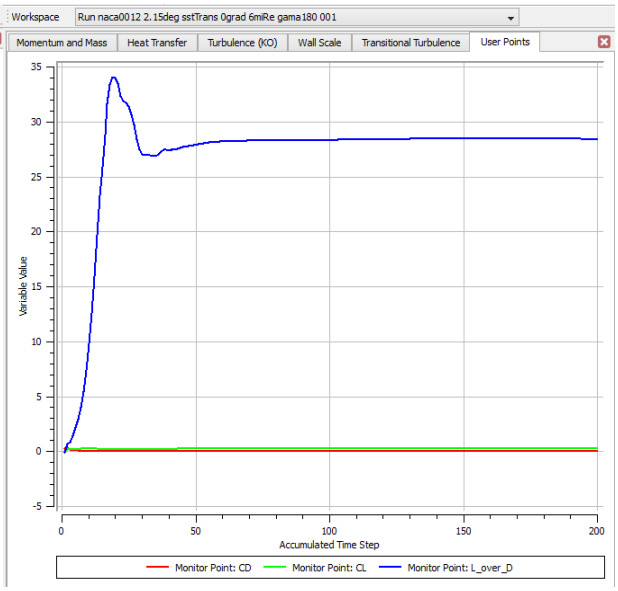

Figure 3.55 SST Transitional with Option Gamma (Transition Onset Reynolds Number = 460.0 * (1.0 + x / (1.0 [m])))

3.3.4 Compressible or Incompressible Model

Two simulations done one after another show that in this range of Reynolds numbers (around 500,000) the flow can be thought as incompressible due to the low Ma numbers.

When conducting a simulation in ANSYS CFX environment, it is possible to take into account the compressibility. It is done under Heat Transfer option. When this option is set to “Thermal

Energy"; the flow is not thought as compressible. In order to take compressibility effects, the Heat Transfer option must be set to "Total Energy" (35).

Here an example is demonstrated. Provided all other parameters being the same, two simulation results which are set to Thermal and Total Energy options differ from each other only slightly. Compressibility effect of air is not really pronounced if the Ma number does not exceed 0.3. In our case, as we are in low Re range, our velocities are also small.

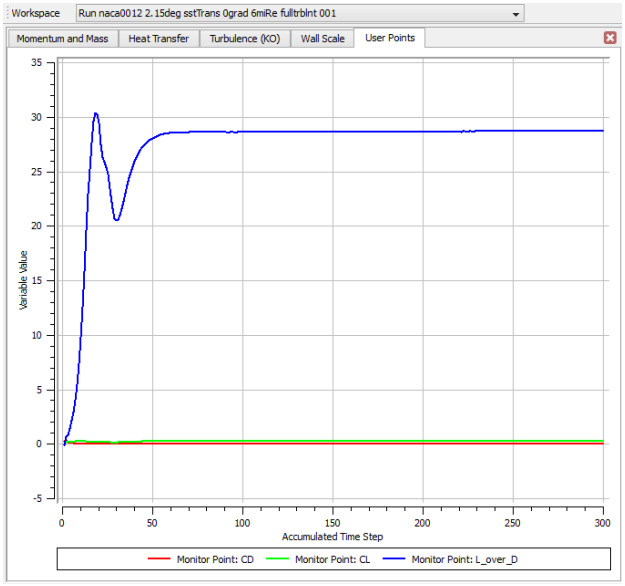

Figure 3.56 Converged simulation

3.3.5 Convergence Criteria

The numerical method used in CFX is an iterative process. That means after each iteration a solution is reached. The question here is to what extend the iteration should be done. We must set a criteria to stop iteration and accept the result of the last iteration as the solution. In order to avoid big mistakes and deviations from reality, there has emerged a method which is called convergence criteria. To converge means to achieve, get closer as a word meaning. It is the same meaning in numerical methods. Getting closer in numerical methods means approaching the reality, the solution.

Generally speaking, the more the iterations the closer the solution to the exact one. So, should be keep iterating for ever? Of course, this is not possible and also not desired. What we desire is to get a result close enough to the exact one. This "close enough" depends heavily on the needs. In an application which needs very accurate results, one needs to be close to the exact solution in the orders of 1/1000000. But for a rough estimate a 1/100 may be enough. Of course the exact esult is not known. Thus, we set a rule, convergence criteria, that results of the

successive iterations should not deviate from each other more than a certain value. If the value is set too low, the number of iteration and the time needed for solution is increased for the sake of better results representing the exact solution.

In the plots below from simulations conducted in CFX environment show clearly what is meant above. Let's think that we are after Lift/Drag coefficient of a NACA 0012 profile under specific flow conditions. We start conducting the simulation. If we stop after 10,20,30,40,50,100,150 and 200 iterations, the results we obtain as a solution will be -0.12514, -0.57001, -0.059303, -0.13511, -0.077297, -0.0088179, -0.0038539, -0.000055417 respectively. We know that the exact result for a symmetrical airfoil at AoA= 0 degree is "0.00"

As can be seen after some oscillations the result converges to the exact solution. Here the decision of whether to stop the simulation after 50 or 200 iterations is a question of both time and needs of accuracy.

During all simulations in this dissertation, special attention is given to the convergence problem and results obtained are accurate enough for wind turbine blade design.

Please note that if enough iteration is not done, the result may even not converge which means the results can not be used at all.

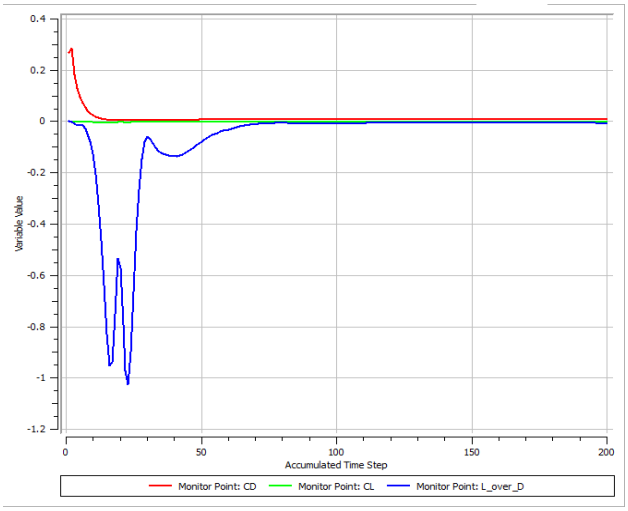

Figure 3.57 (A converged simulation after 200 iterations)

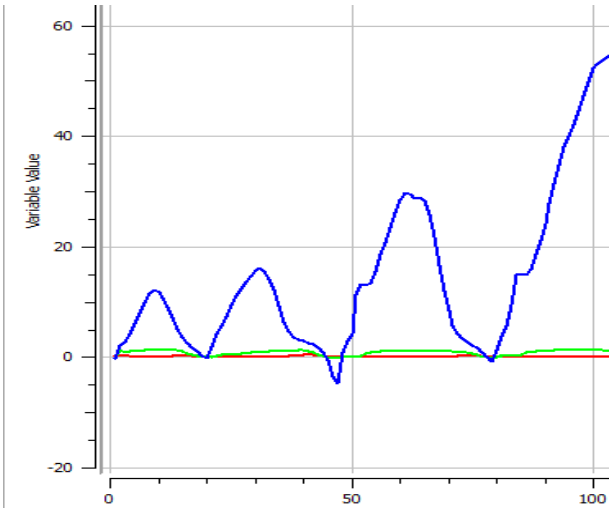

Figure 3.58 (An unconverged simulation after 100 iterations)

Chapter 4: SIMULATIONS IN COMPUTER PROGRAMS

This chapter may be thought as the core of the study as it is the part where the blade geometry is generated and simulated. It starts with the program QBlade which is a BEM solver and finishes with a Navier-Stokes solver ANSYS CFX.

4.1 THE PROGRAM QBLADE AND CONDUCTED SIMULATIOUNS

4.1.1 An Overview of the Program

The program Qblade is a free license wind turbine analysis software which makes use of the Beam Element Momentum Theory. Basically the numerical method it uses depends on the BEM algorithm, but during time many contributions has been done. Thus, the program now is capable of accounting for many loss factors and has correction steps.

This software project is first evoked being a part of the wind energy group at the Berlin Technical University. Prof. Dr. Christian Oliver Paschereit from Department of Experimental Fluid Mechanics was the leader of the group who aimed with this project to provide an open source turbine calculation software. As a basis for the software the group used XFOIL which is another free license software. The XFOIL was first developed at MIT by Mark Drela. It is an airfoil calculation program and is validated by many studies.

Shortly, the Qblade has another integrated software, which creates the polar of a desired airfoil and sends it to BEM part of the program so that the BEM procedure can be established and turbine blade data can be created which is then used for the rotor performance.

In the guidelines of the Qblade (36) the steps and functions of the program are described as follows:

1) -extrapolation of XFOIL generated or imported polar data to 360 AoA

2) -advanced blade design and optimization, including 3D visualization, using XFOIL generated or imported profiles

3) -wind turbine definition (rotor blade, turbine control, generator type, losses)

4) -computation of rotor performance over l range

5) -computation of wind turbine performance over windspeed range

6) -annual yield computation with WEIBULL distribution

7) -manual selection of BEM and DMS correction algorithms

8) -manual selection of all relevant simulation parameters

9) -data browsing and visualization as post processing

10) -export functionality for all created simulation data

11) -blade geometry export in .stl format

12) -storing of projects, rotors, turbines and simulations in a runtime database

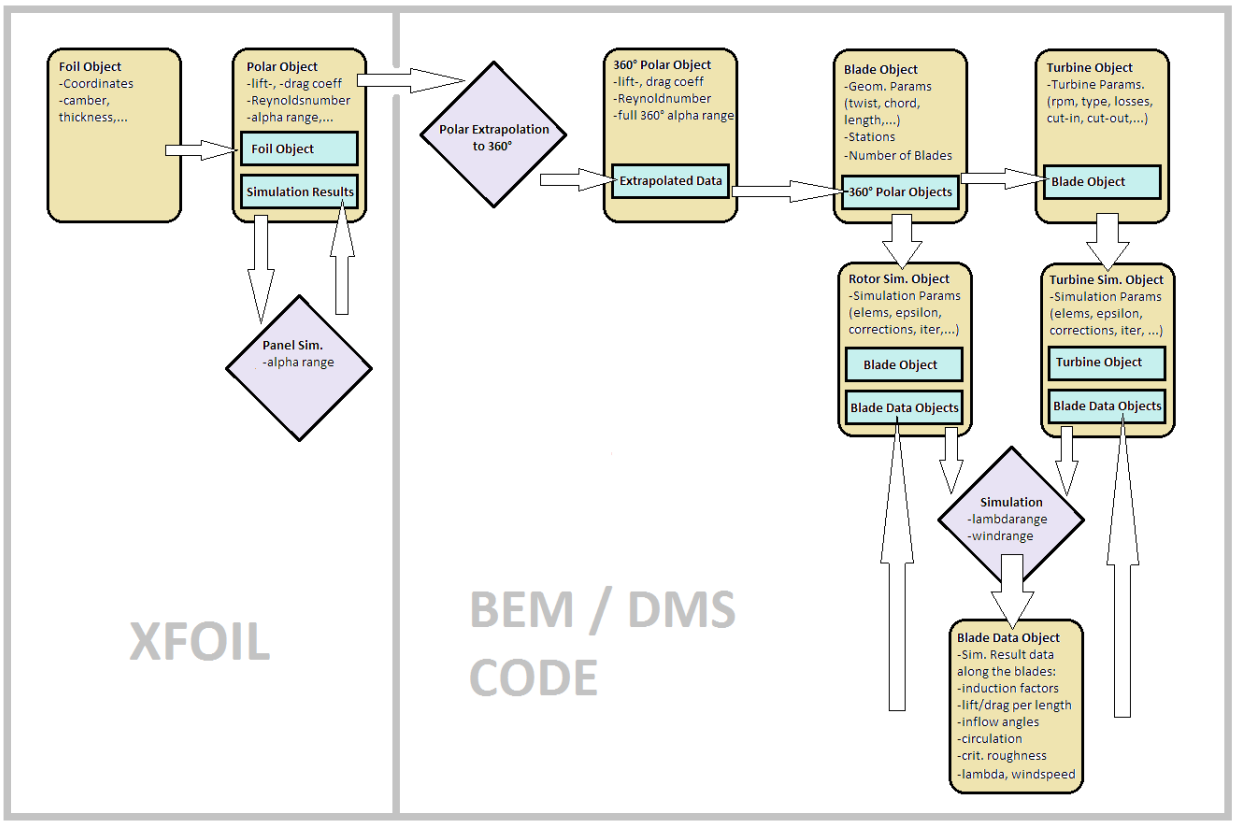

Figure 4.1 (The code tructure diagram from the aforamentioned guidelines)

4.1.2 The Studies conducted in Qblade

In this dissertation, a pair of blade and rotor simulations is done. The main aim is to find out the power output of the designs when the wind speed is 7.25 m/s. This wind speed is chosen consciously and the reason lies here. Turkey has an overall economic viable wind power capacity of 50,000 MW. Of this capacity, unfortunately 30,000 MW is between wind speeds 7.0 to 7.5 m/s. Although now the focus is on the first 20,000 MW for which the average wind

speed is over 8m/s, after implementation of this portion, time will come for the areas where the wind speed average is 7.25 m/s.

The study starts with designing a blade with NACA4412 profile. Afterwards the rotor is created. As a beginning a blade length of 1m is created. Then it is scaled up to 2,4,8,16,32 and 64 meters. The Qblade design optimization tool is available to create and optimize the blade geometry.

Here are the results as tabulated.

Rotor Radius (m)	Peak Power (W)	Torque (N.m)	Rotational Speed(1/min)	Power Coefficient
1.00	394	5.5	680	0.566
2.01	1,654	50	313	0.574
4.10	6,857	418	157	0.570
8.06	26,209	3,100	81	0.573
15.92	104,580	26,100	38	0.590
31.84	438,243	209,250	20	0.590
63.68	1,766,700	1,687,100	10	0.590

Table 4.1

- Please note that the peak power is the maximum power for wind speed of 7.25 m/s. It does not mean the power at the cut-off speed. Rather depending on the tip speed ratios the power changes and the written values are the best values under different rotational speeds.

In the figures from 4.2 to 4.15 Qblade results of the created rotors are given. The same blade and rotor geometry is scaled from 1m radius to 64m radius with small differences. For each rotor simulation Qblade gives C_p(coefficient of power) and C_t(coefficient of torque) values at different TSRs(tip speed ratio). Comparing the results with Figure 3.6, we see that the results are at the best limit with almost C_p= 0.6 and C_t= 0.8. This is because the blade geometry is optimized with the advanced tools of the program.The program shows also the local angle of attacks at different sections of the blade.

Qblade has the capability to show power output for different wind speeds. But as the design is optimized for 7.25m/s, only power output for this speed is given. But the TSR is set free so that the optimum point can be seen. In the result graphs, one can see the torque and power output at different TSRs. Power vs 1/TSR is also given which is useful for the wind turbine industry.

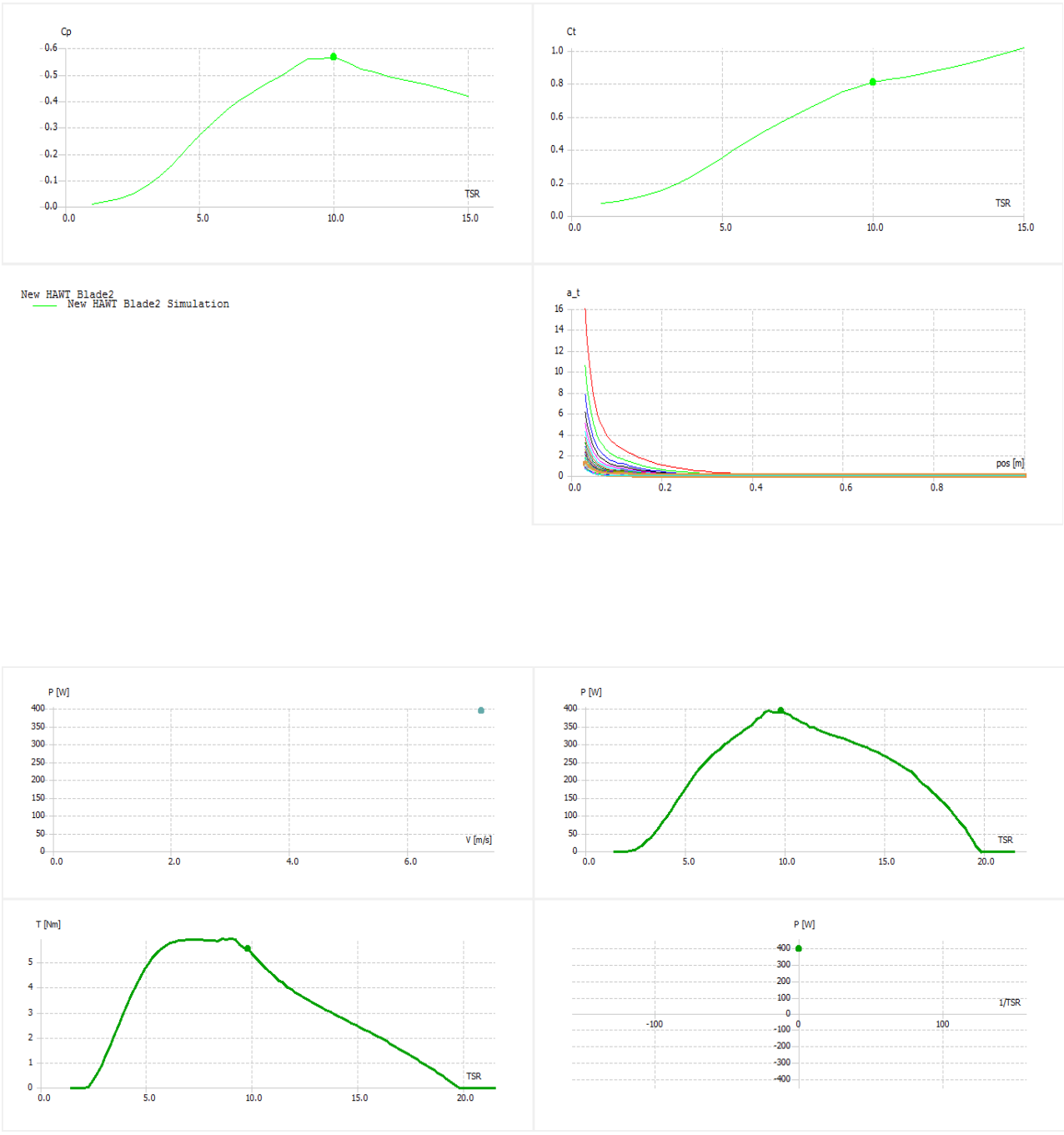

(Figure 4.2-4.3) Rotor Radius of 1m_Plots

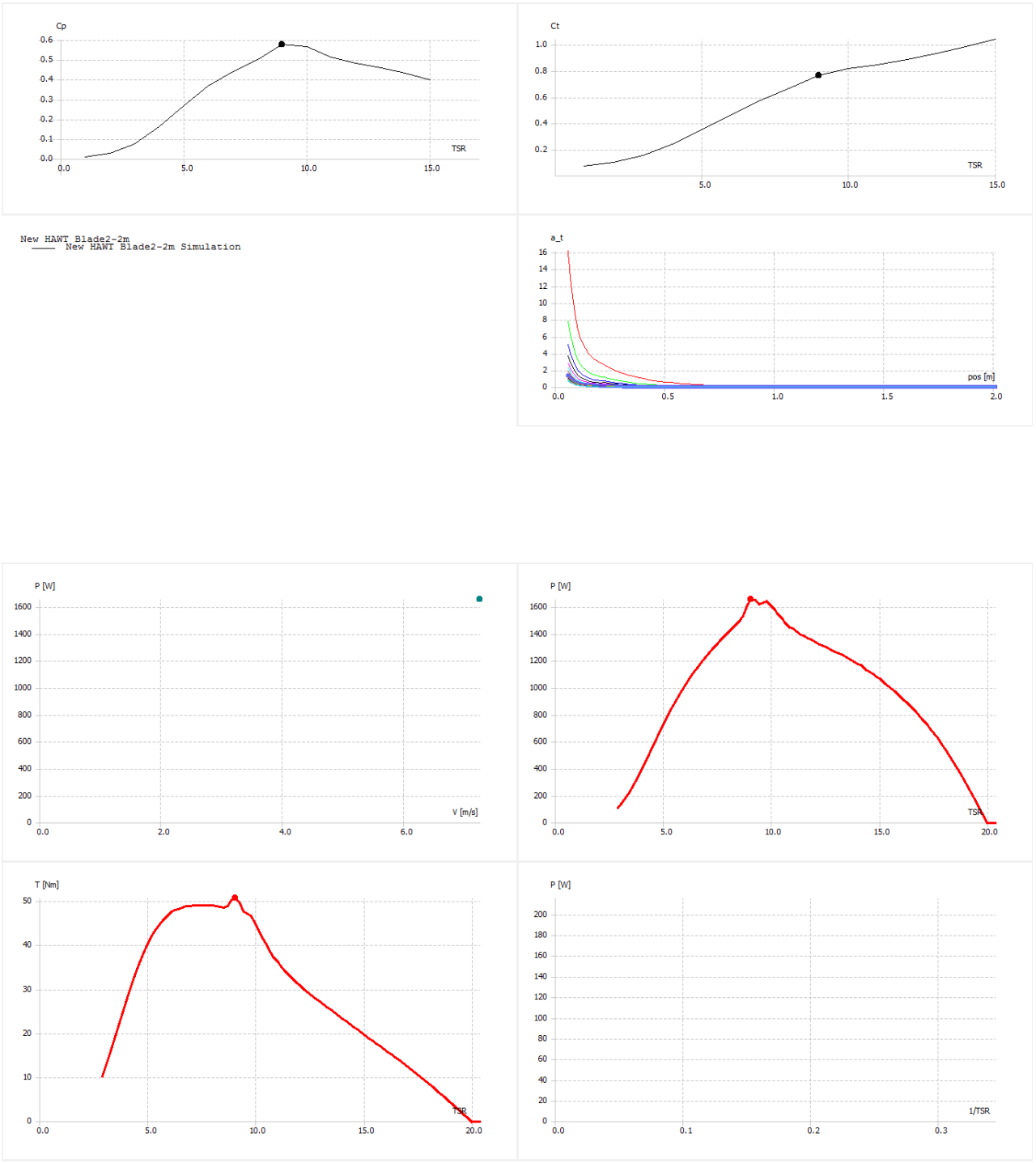

(Figure 4.4-4.5) Rotor Radius of 2m_Plots

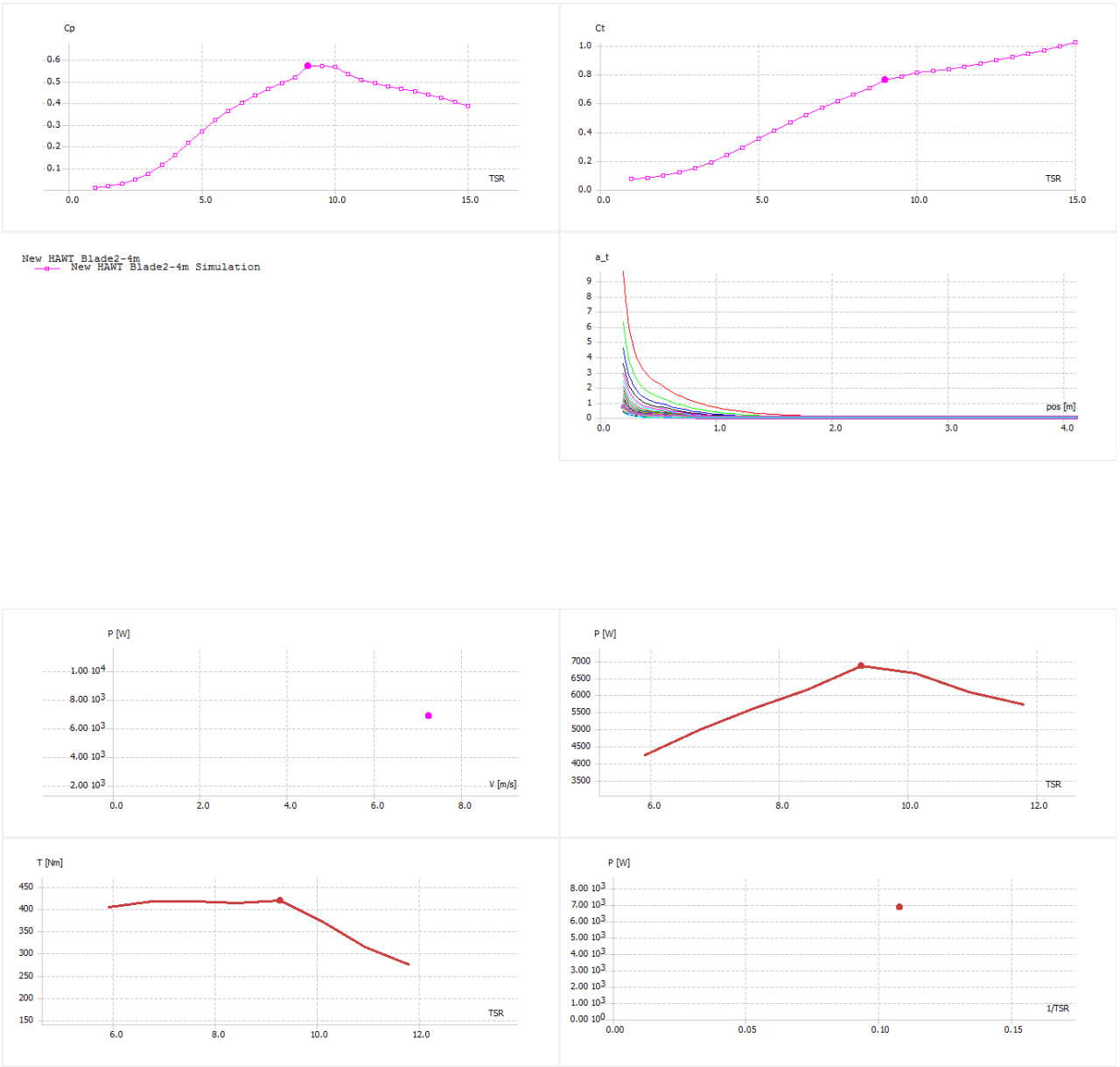

(Figure 4.6-4.7) Rotor Radius of 4m_Plots

(Figure 4.8-4.9) Rotor Radius of 8m_Plots

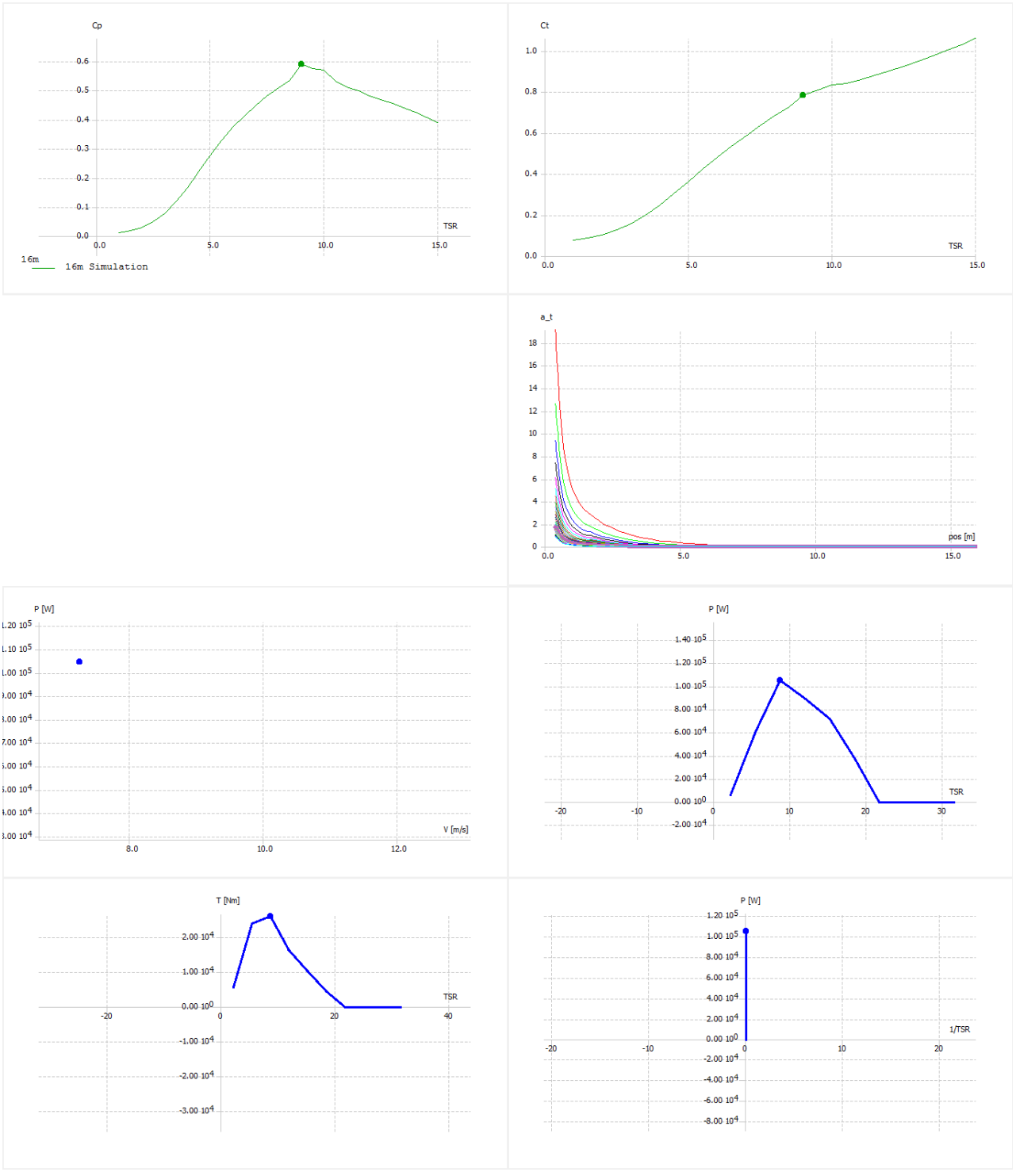

(Figure 4.10-11) Rotor Radius of 16m_Plots

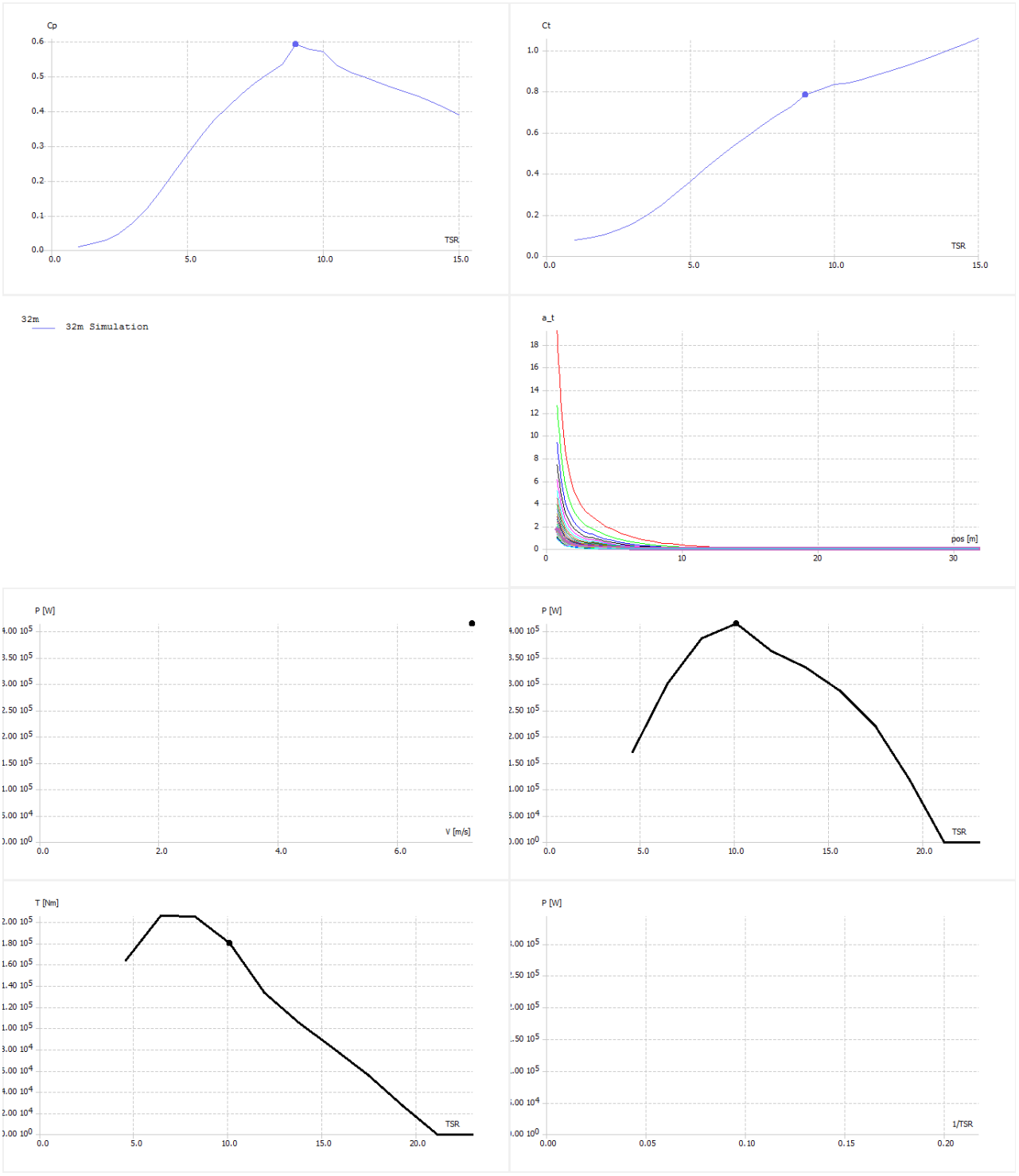

(Figure 4.12-13) Rotor Radius of 32m_Plots

(Figure 4.14-15) Rotor Radius of 64m_Plots

Figure 4.16 A 3D View of the Rotor

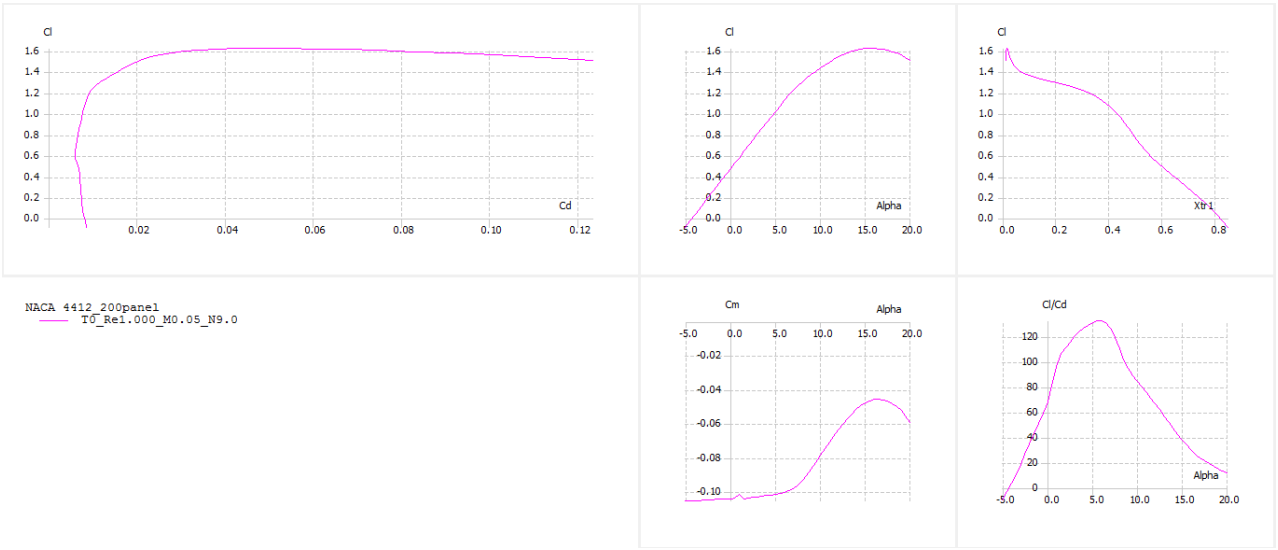

Figure 4.17 Polar of the Used Airfoil_NACA4412

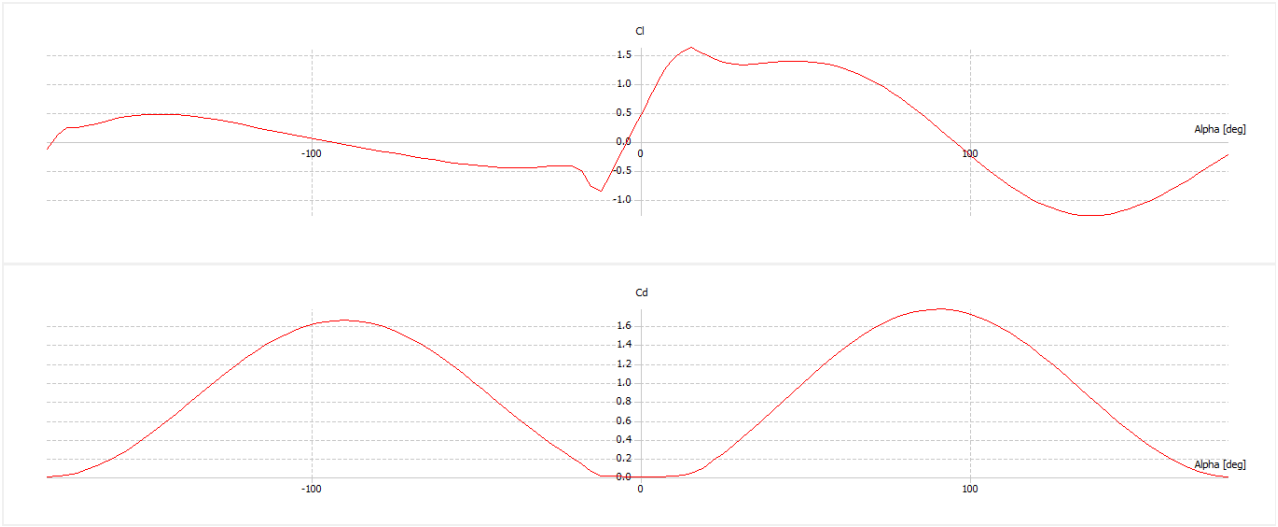

Figure 4.18 Extrapolated Polar of Airfoil_NACA4412

	Blade1		Blade2		Blade3		Blade4	
	Pos (m)	Chord (m)	Pos (m)	Chord (m)	Pos (m)	Chord (m)	Pos (m)	Chord (m)
1	0	0,07	0	0,142	0	0,28	0	0,56
2	0,025	0,071	0,05	0,14	0,1	0,28	0,2	0,56
3	0,08	0,108	0,15	0,206	0,3	0,432	0,64	0,88
4	0,13	0,0981818	0,25	0,194	0,5	0,388	1,04	0,8
5	0,18	0,08	0,35	0,16	0,7	0,32	1,44	0,64
6	0,23	0,0727273	0,45	0,136	0,9	0,28	1,84	0,56
7	0,28	0,06	0,55	0,116	1,1	0,24	2,24	0,48
8	0,33	0,0545455	0,65	0,1	1,3	0,2	2,64	0,4
9	0,38	0,044	0,75	0,088	1,5	0,196	3,04	0,32
10	0,418	0,04	0,85	0,078	1,7	0,156	3,344	0,31
11	0,48	0,035	0,95	0,07	1,9	0,14	3,84	0,28
12	0,528	0,0318182	1,05	0,064	2,1	0,128	4,224	0,256
13	0,5808	0,0289256	1,15	0,06	2,3	0,12	4,6464	0,23
14	0,63	0,026296	1,25	0,054	2,5	0,108	5,04	0,22
15	0,68	0,025	1,35	0,05	2,7	0,1	5,44	0,2
16	0,73	0,0217322	1,45	0,048	2,9	0,096	5,84	0,192
17	0,78	0,0197566	1,55	0,044	3,1	0,088	6,24	0,18
18	0,83	0,0179605	1,65	0,042	3,3	0,084	6,64	0,17
19	0,88	0,0163278	1,75	0,038	3,5	0,076	7,04	0,16
20	0,93	0,02	1,85	0,032	3,7	0,064	7,44	0,13
21	0,97	0,013494	1,95	0,022	3,9	0,044	7,76	0,09

	Blade5		Blade6		Blade7		Polar Data Source	
	Pos (m)	Chord (m)	Pos (m)	Chord (m)	Pos (m)	Chord (m)	Foil	Polar
1	0	1,12	0	2,24	0	4,48	Circular Foil	Circular Foil 360 Po
2	0,4	1,12	0,8	2,24	1,6	4,48	Circular Foil	Circular Foil 360 Po
3	1,28	1,76	2,56	3,52	5,12	7,04	NACA 4412	NACA 4412 360 Pol
4	2,08	1,6	4,16	3,2	8,32	6,4	NACA 4412	NACA 4412 360 Pol
5	2,88	1,28	5,76	2,56	11,52	5,12	NACA 4412	NACA 4412 360 Pol
6	3,68	1,12	7,36	2,24	14,72	4,48	NACA 4412	NACA 4412 360 Pol
7	4,48	0,96	8,96	1,92	17,92	3,84	NACA 4412	NACA 4412 360 Pol
8	5,28	0,8	10,56	1,6	21,12	3,2	NACA 4412	NACA 4412 360 Pol
9	6,08	0,64	12,16	1,28	24,32	2,56	NACA 4412	NACA 4412 360 Pol
10	6,688	0,62	13,376	1,24	26,752	2,48	NACA 4412	NACA 4412 360 Pol
11	7,68	0,56	15,36	1,12	30,72	2,24	NACA 4412	NACA 4412 360 Pol
12	8,448	0,52	16,896	1,04	33,792	2,08	NACA 4412	NACA 4412 360 Pol
13	9,2928	0,46	18,5856	0,92	37,1712	1,84	NACA 4412	NACA 4412 360 Pol
14	10,08	0,44	20,16	0,88	40,32	1,76	NACA 4412	NACA 4412 360 Pol
15	10,88	0,4	21,76	0,8	43,52	1,6	NACA 4412	NACA 4412 360 Pol
16	11,68	0,38	23,36	0,76	46,72	1,54	NACA 4412	NACA 4412 360 Pol
17	12,48	0,36	24,96	0,72	49,92	1,44	NACA 4412	NACA 4412 360 Pol
18	13,28	0,34	26,56	0,68	53,12	1,36	NACA 4412	NACA 4412 360 Pol
19	14,08	0,32	28,16	0,64	56,32	1,28	NACA 4412	NACA 4412 360 Pol
20	14,88	0,26	29,76	0,52	59,52	1,04	NACA 4412	NACA 4412 360 Pol
21	15,52	0,18	31,04	0,36	62,08	0,72	NACA 4412	NACA 4412 360 Pol

Table 4.2 Gemetry Details Of the Blades

The blade geometry is created with Qblade program. First a polar of NACA4412 profile is created by using XFOIL which is incorporated in Qblade. The polar angle range is between -5 and +20 degrees. Then, this polar is extrapolated to a full range of -180 to +180 degrees. In the Blade design sub-module the rotor is created. The blade consists of sections which are defined by their profile, position, chord and twist. Its length is selected as 2m and the hub radius 0,05m.

Then using advanced tools of the Qblade, the blade geometry is optimized for wind speed of 7.25 m/s. After creating the geometry in Qblade, it was exported as a txt file. This file was imported to CATIA, an advanced 3D modeler. By using the point cloud of the txt file, a 3D CAD data is created in CATIA which was exported to ANSYS CFX. But unfortunately, the CFX can not import a CAD model which has high order NURBS (Non-uniform rational B-spline). Thus, while creating the blade geometry in CATIA, instead of more accurate sweep function, again accurate but simpler blend function was used. The blade is connected to the hub by cylindrical profiles.

4.2 ANSYS CFX and SIMULATIONS

ANSYS CFX is a highly trusted and widely used commercial CFD package. In this dissertation CFX will be used. The Figure 4.19 describes the CFX steps.

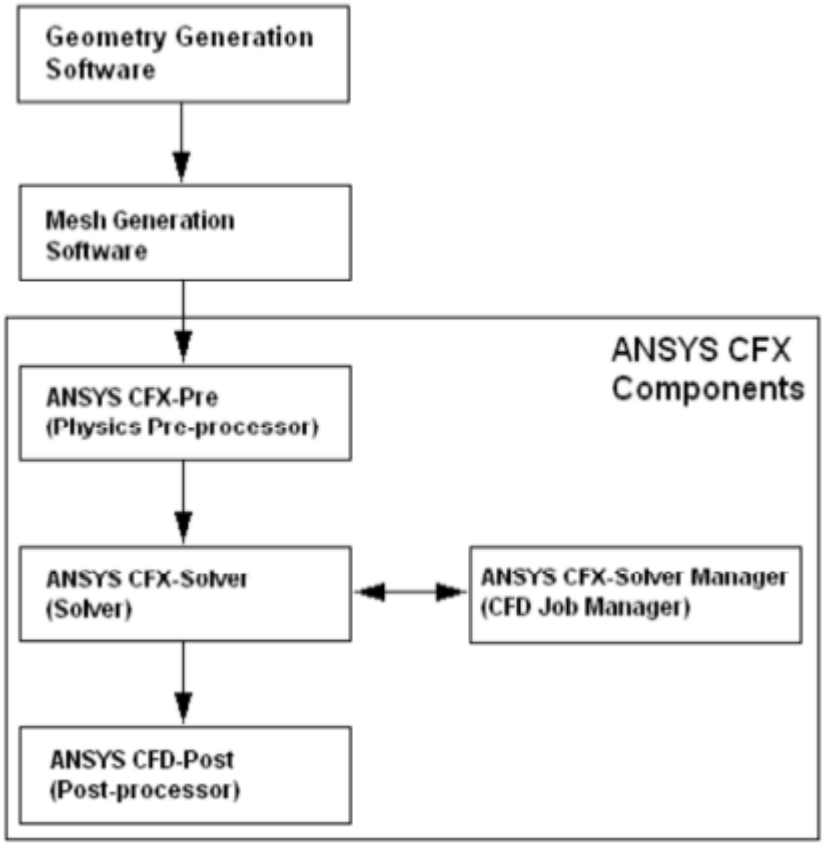

Figure 4.19 CFX Components

4.2.1 Validation of 2D model

At different angles of attack flow around NACA0012 profile is investigated and some CFX Post features are used to present the results.

As AoA increases Mach number also increases and the assumption of incompressible flow becomes no more valid. The simulation results deviate from experimental ones. But knowing that the stall starts around 16^0 and (37) CFX has good agreement with the test results up to 14^0 which is very close to stall angle, we can conclude that CFX is verified for 2D flow around airfoils.

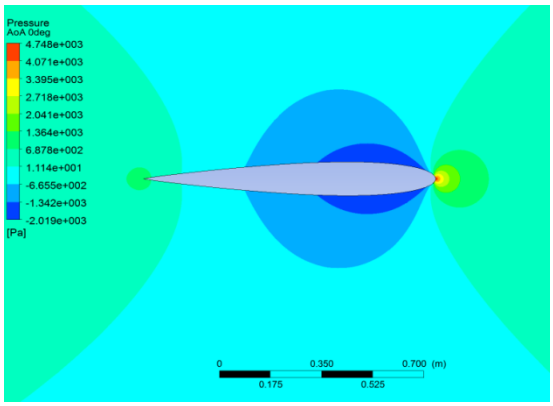

Figure 4.20 Pressure Contours at AoA= 0^0

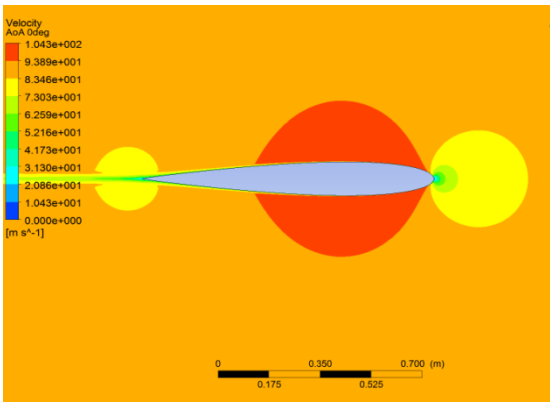

Figure 4.21 Velocity Contours at AoA= 0^0

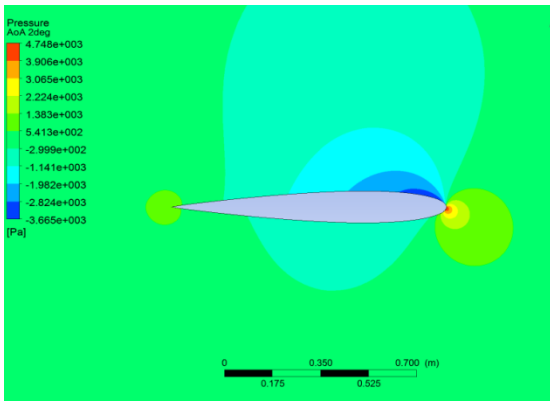

Figure 4.22 Pressure Contours at AoA= 2^0

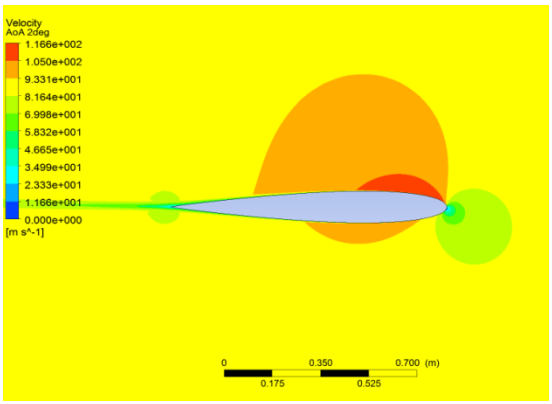

Figure 4.23 Velocity Contours at AoA= 2^0

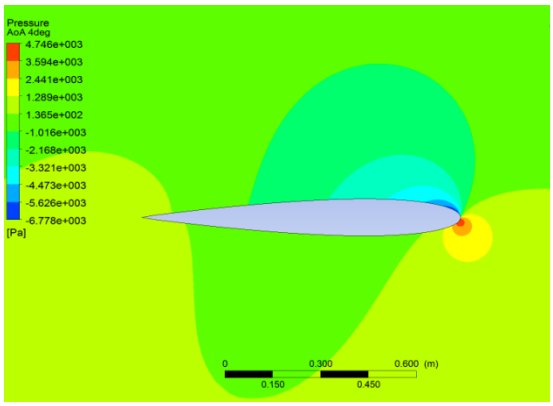

Figure 4.24 Pressure Contours at AoA= 4^0

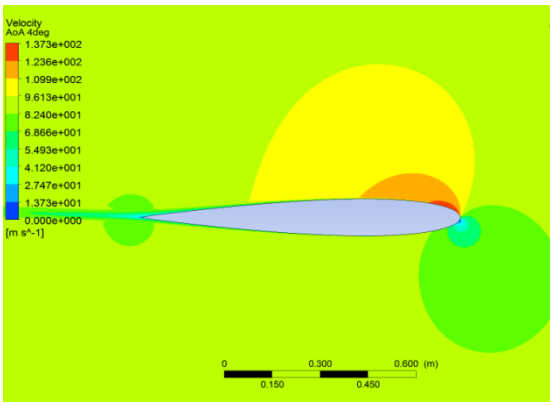

Figure 4.25 Velocity Contours at AoA= 4^0

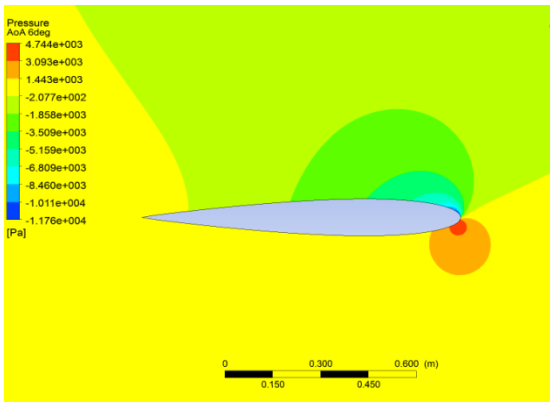

Figure 4.26 Pressure Contours at AoA= 6^0

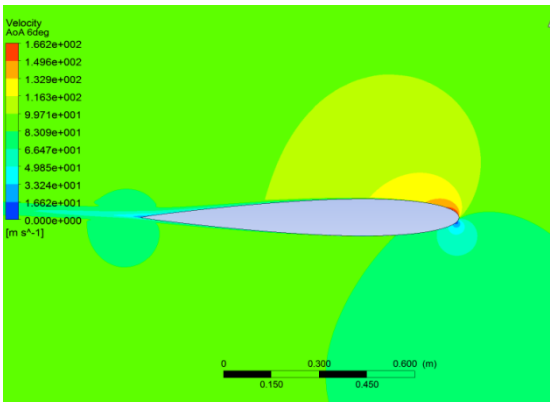

Figure 4.27 Velocity Contours at AoA= 6^0

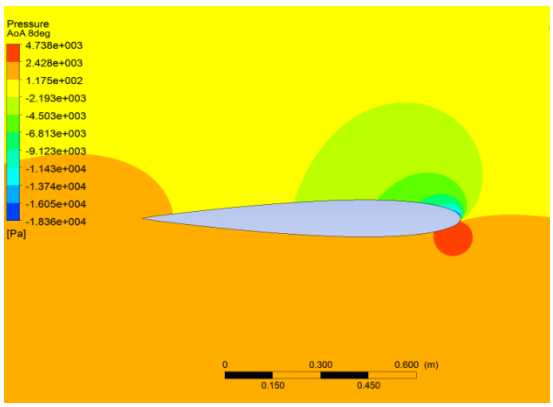

Figure 4.28 Pressure Contours at AoA= 8^0

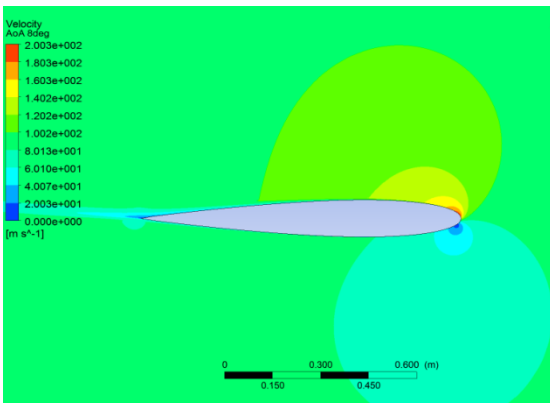

Figure 4.29 Velocity Contours at AoA= 8^0

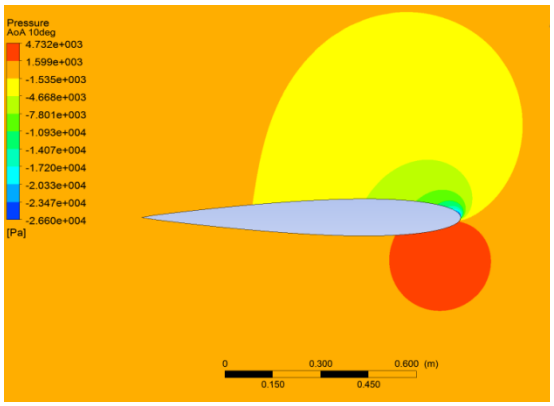

Figure 4.30 Pressure Contours at AoA= 10^0

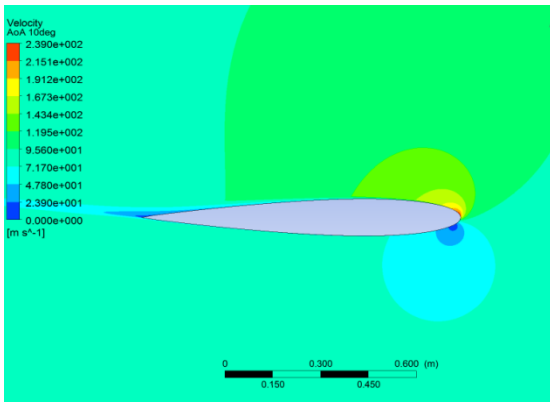

Figure 4.31 Velocity Contours at AoA= 10^0

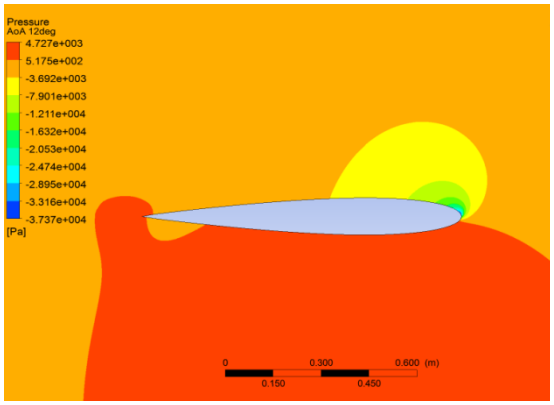

Figure 4.32 Pressure Contours at AoA= 12^0

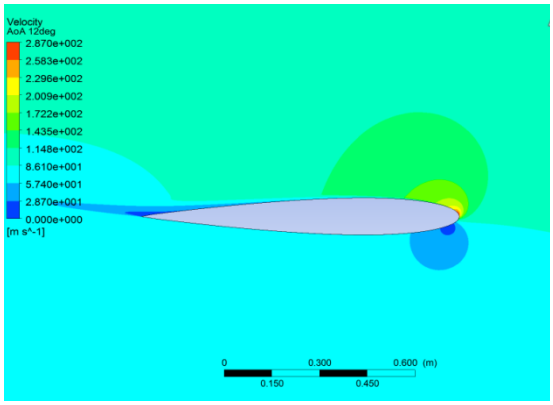

Figure 4.33 Velocity Contours at AoA= 12^0

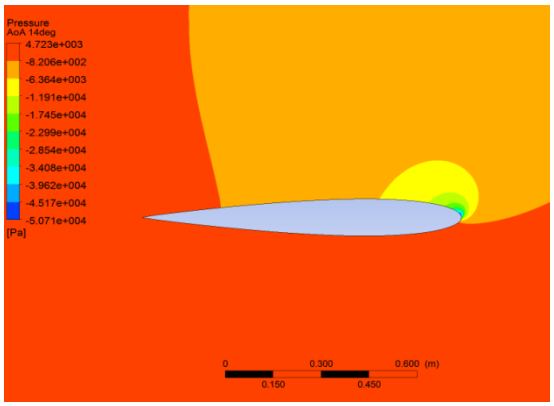

Figure 4.34 Pressure Contours at AoA= 14^0

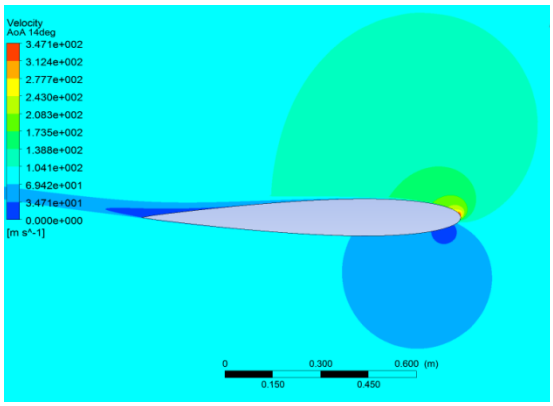

Figure 4.35 Velocity Contours at AoA= 14^0

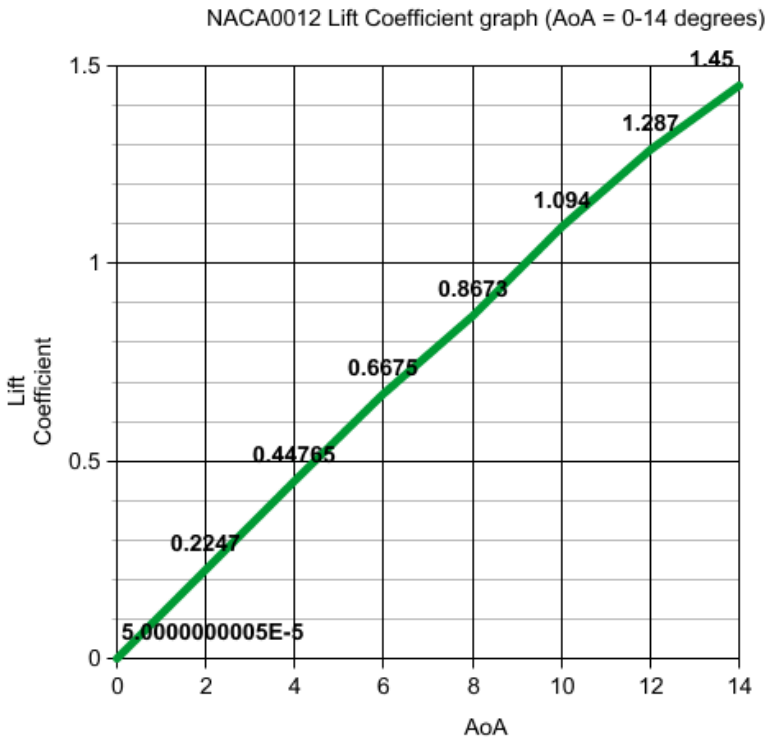

Figure 4.36 Lift Coefficient vs AoA for 2D Simulations

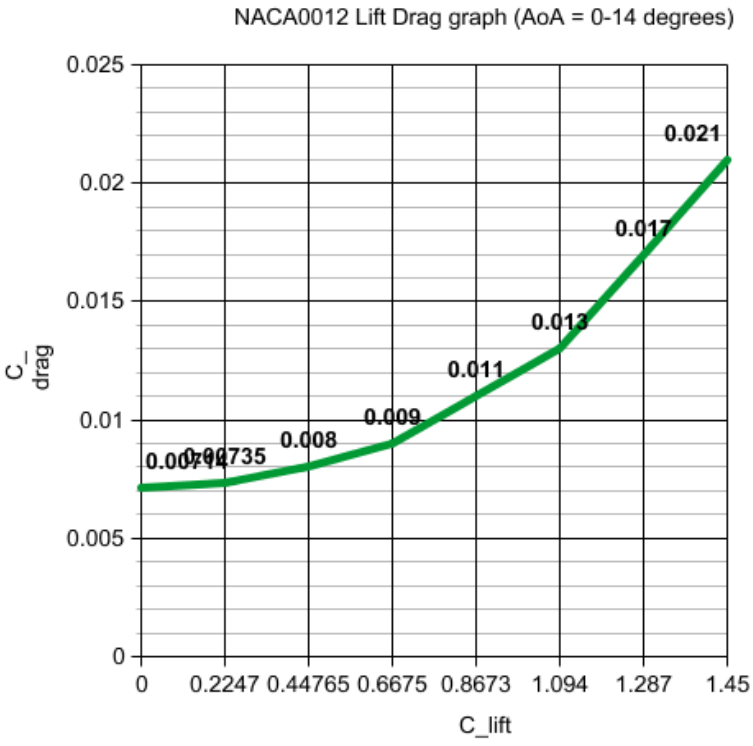

Figure 4.37 Drag Coefficient vs Lift Coefficient for 2D Simulations

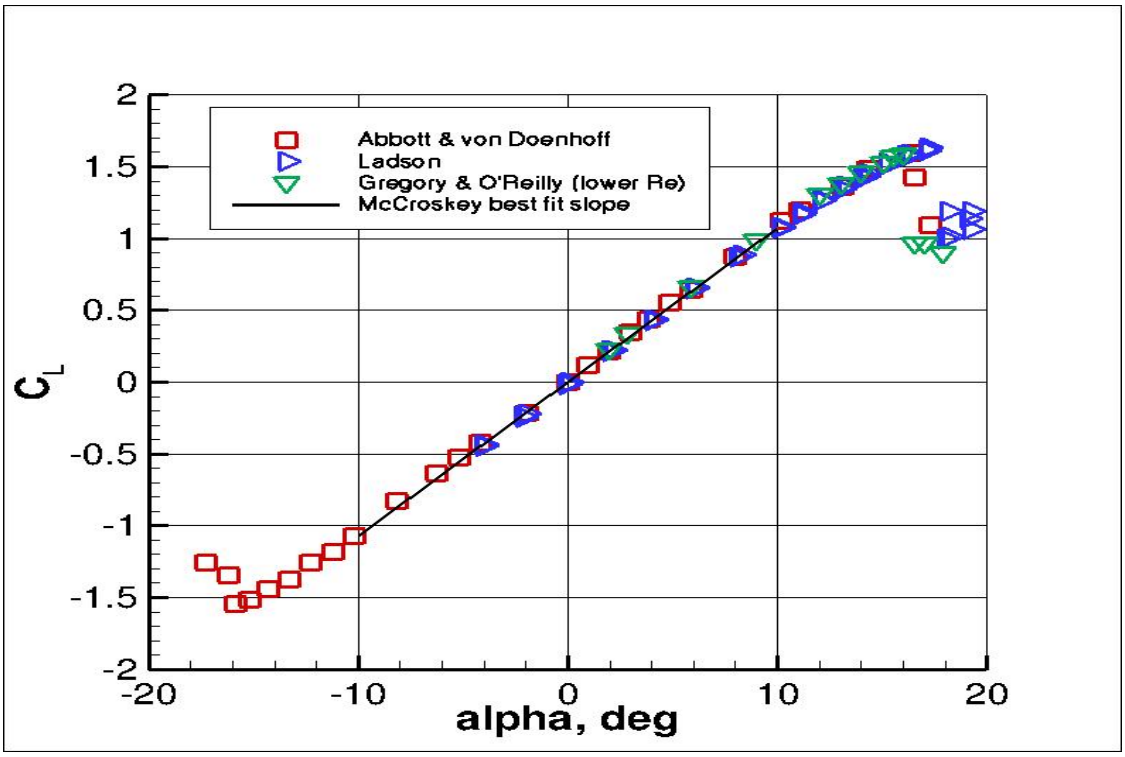

4.38 Lift Coefficient vs AoA for NACA0012 Experimental Results

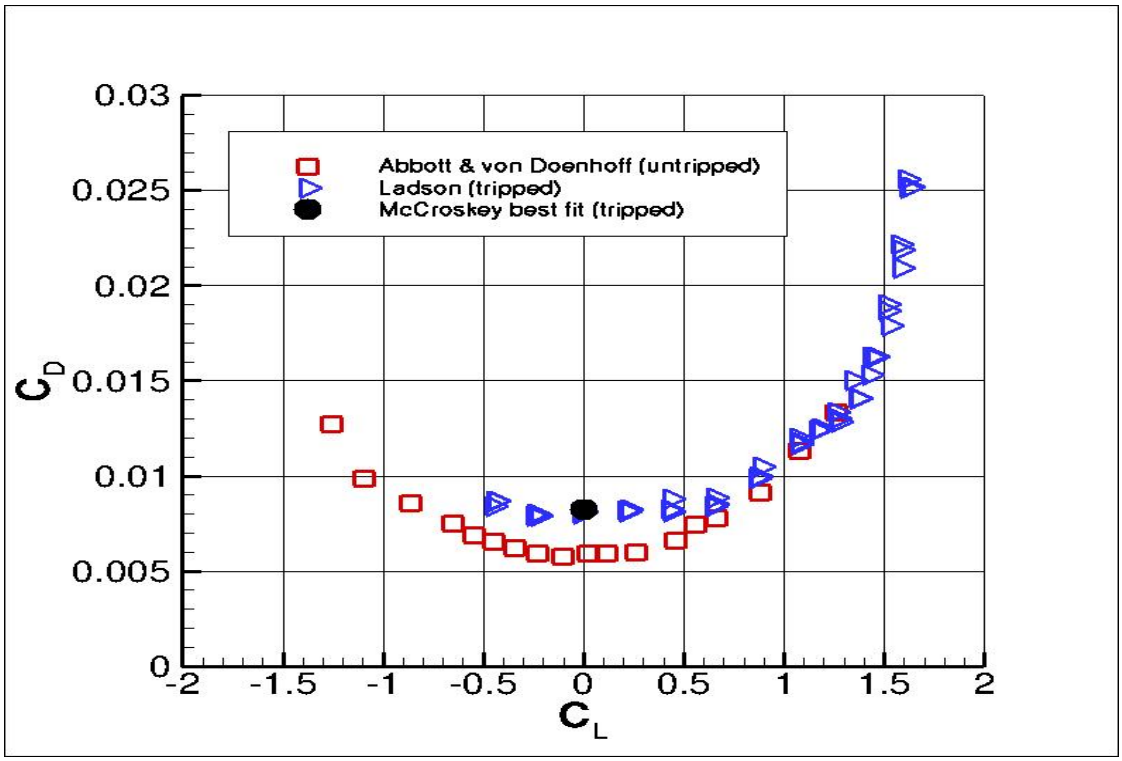

4.39 C_l vs C_d for NACA0012 Experimental Results

The results show that the C_L prediction of the 2D model is in very good agreement with test results up to 12^0 and good agreement up to 14^0. CFX has a tendency of over-prediction of C_L but the deviation is small and acceptable.

When we come to the C_L prediction of the CFX model, more or less the same conclusion is valid. That is, for small angles of attack, where the C_L is up to 1, the corresponding C_D values are in good agreement with the experimental ones. But the same problem occurs also here for higher angles where C_L values become more than about 1.1, the predicted values for C_D start to deviate from test results. CFX model over-predicts the C_D values.

4.2.2 Three-Dimensional Model

The model is created as a periodic one to save CPU time. As the analyzed turbine is a 3-blade one, a 120^0 part is simulated. The distance from the turbine to the inlet is 8 meters, while it is 12 meters to the outlet. Turbine is placed in an 8 meters diameter and 20 meters long cylinder.

The simulation is carried on in a rotating frame. The domain is discretized into 4.320.733 elements most of which are tetrahedrals creating 781.582 nodes. An extra inflation layer is put on turbine boundary and mesh density is higher in the vicinity of it.

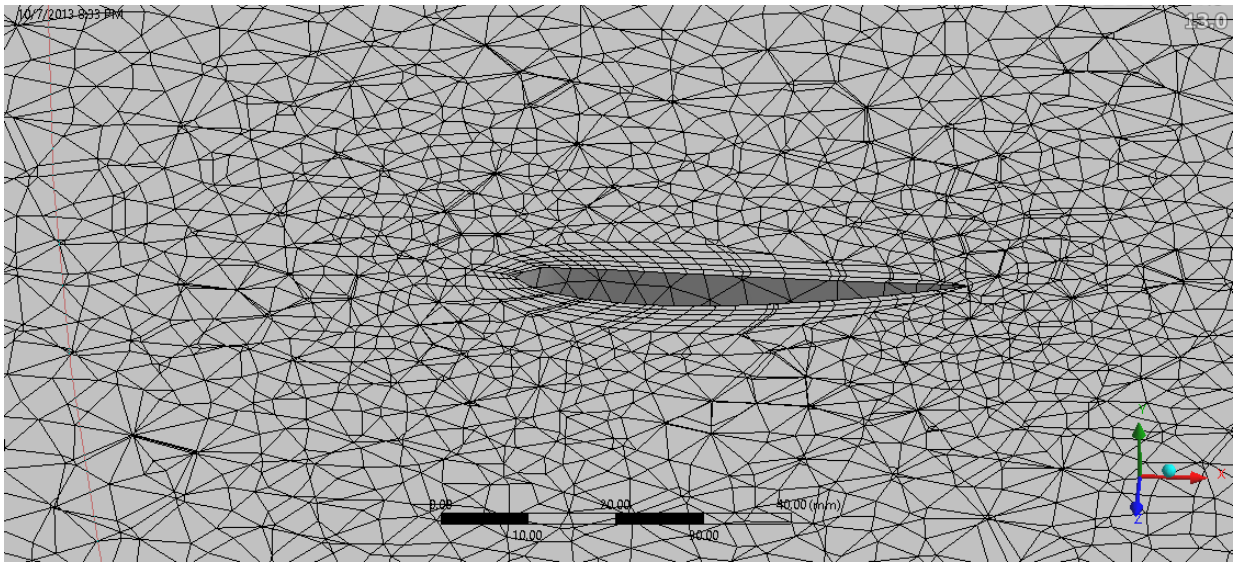

Figure 4.40 A section of meshing from 3D Simulation

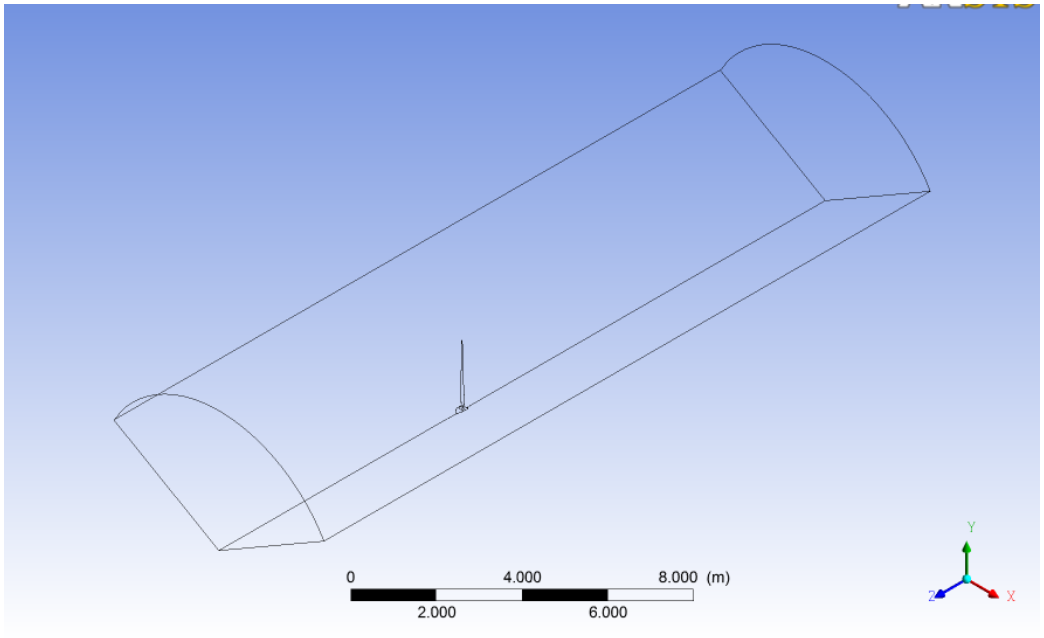

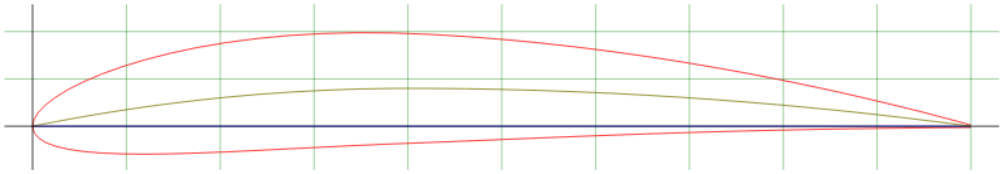

Figure 4.41 Turbine Simulation Domain(Iso View) and NACA4412 profile

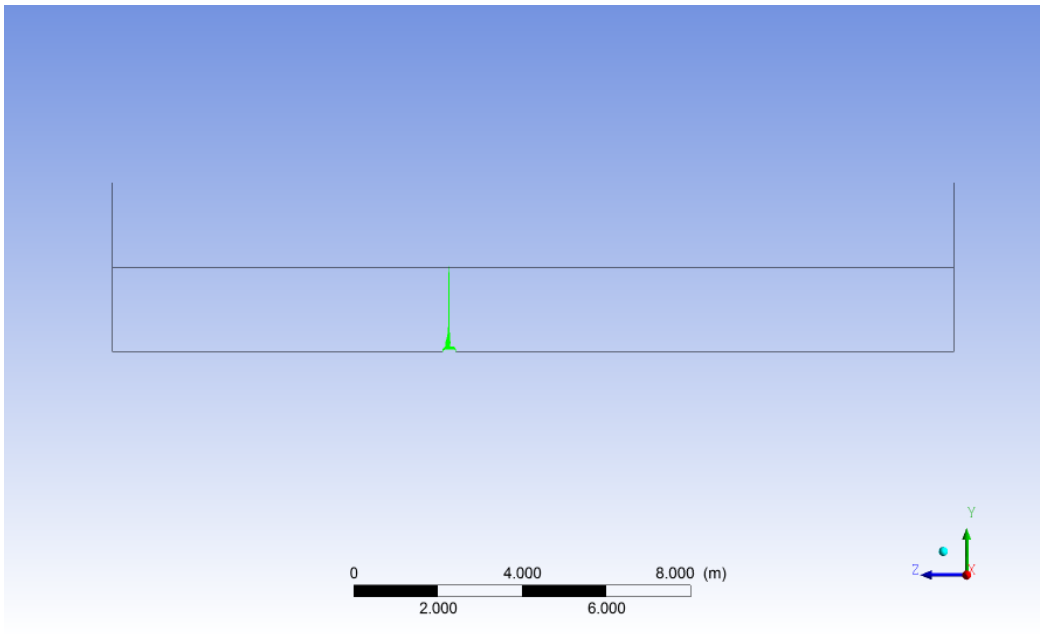

Figure 4.42 Turbine Simulation Domain (Right View)

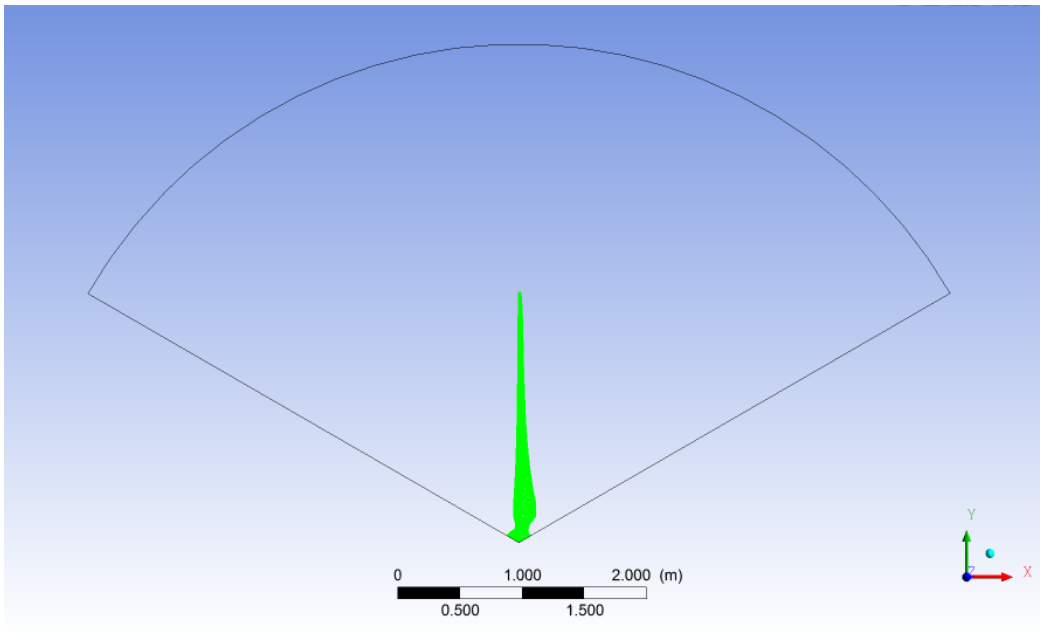

Figure 4.43 Turbine Simulation Domain(Front View)

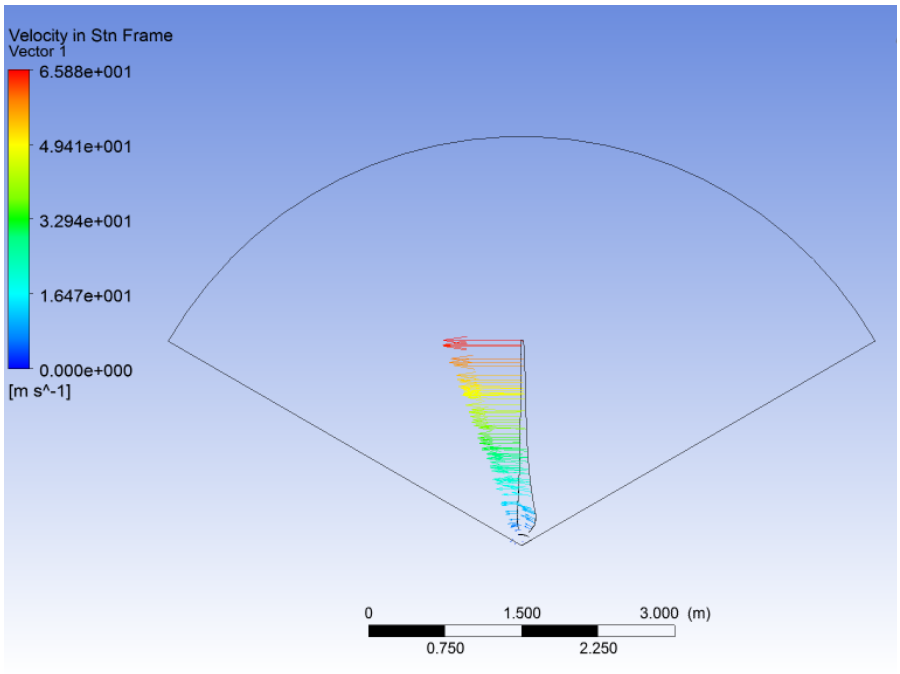

Figure 4.44 Rotational Velocity of a Blade

Power Calculations:

Power: T x ω

where ω is the rotational speed in rad/sec. In our case it is 2 x π x (313rev / 60sec)= 32.78

The torque of one blade is 12.6 Nm which means the torque of the turbine is 37.8 Nm

$P_{turbine}$ = 37.8Nm x 32.78(1/sec)

= 1239 Watt

The available power potential of the wind is;

$P_{available} = 0.5 \times \rho \times A \times U_{\infty}^3$

$= 0.5 \times 1.225 \times (\pi \times 2^2) \times 7.25^3$

= 2933 Watt

$P_{available(rotor\_not\_included)} = 0.5 \times 1.225 \times (\pi \times 1.8^2) \times 7.25^3$

= 2376 Watts

Efficiency of the Rotor including the hub area = 1239/2933

= % 42.2

Efficiency of the Rotor excluding the hub area = 1239/2376

= % 52.1

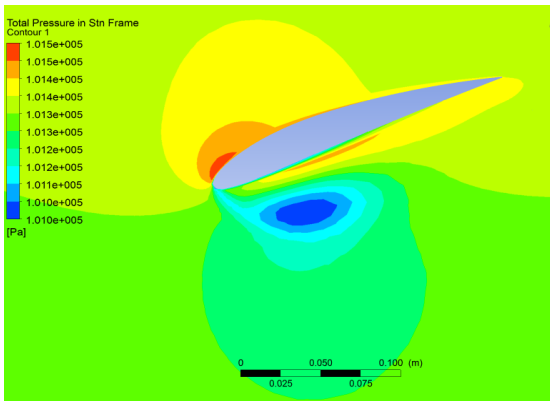

Figure 4.45 Slice at 0.3m from the hub (Pressure Distribution)

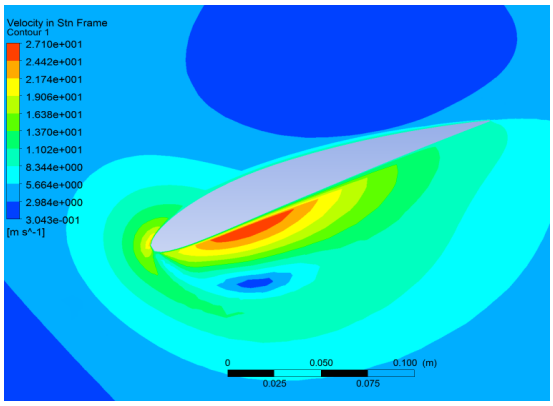

Figure 4.46 Slice at 0.3m from the hub (Velocity Distribution)

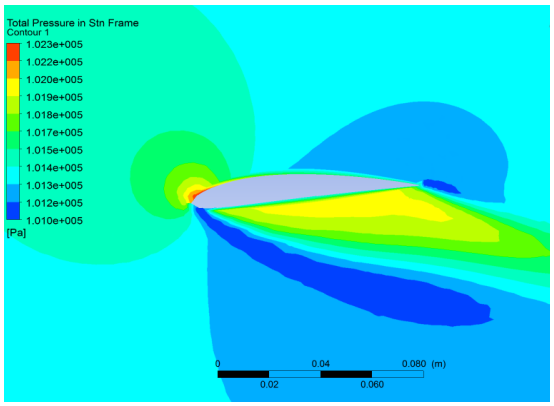

Figure 4.47 Slice at 0.8m from the hub (Pressure Distribution)

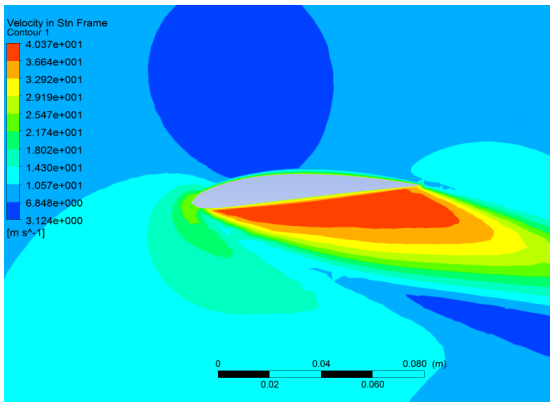

Figure 4.48 Slice at 0.8m from the hub (Velocity Distribution)

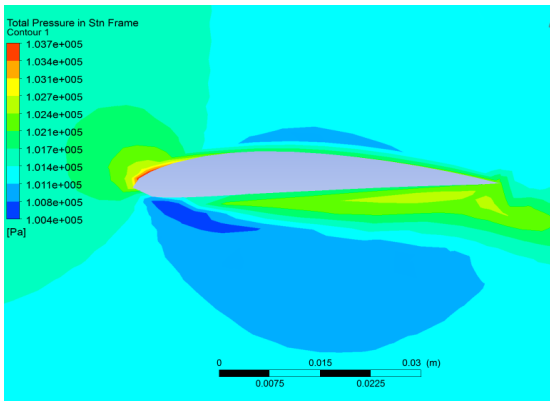

Figure 4.49 Slice at 1.3m from the hub (Pressure Distribution)

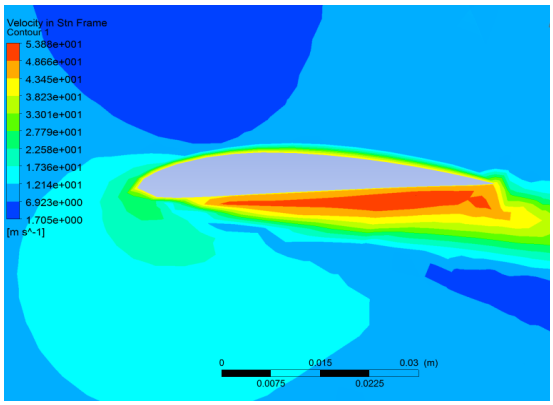

Figure 4.50 Slice at 1.3m from the hub (Velocity Distribution)

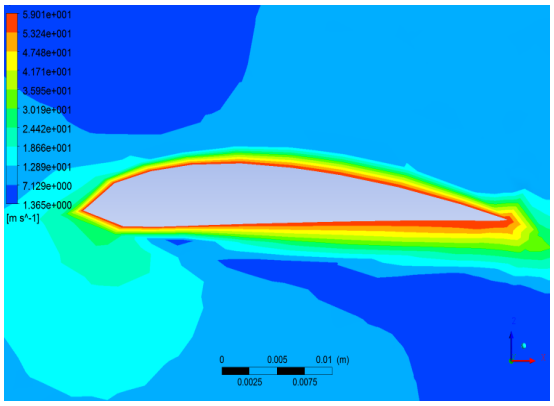

Figure 4.51 Slice at 1.8m from the hub (Pressure Distribution)

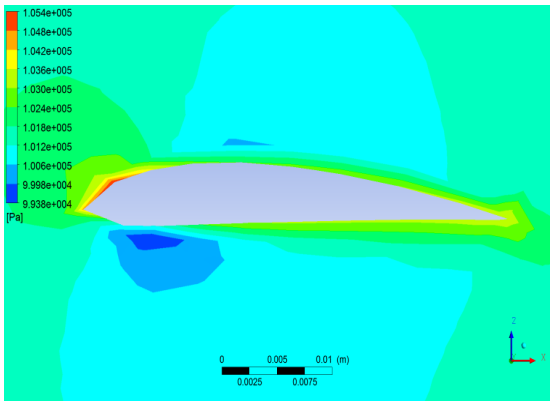

Figure 4.52 Slice at 1.8m from the hub (Velocity Distribution)

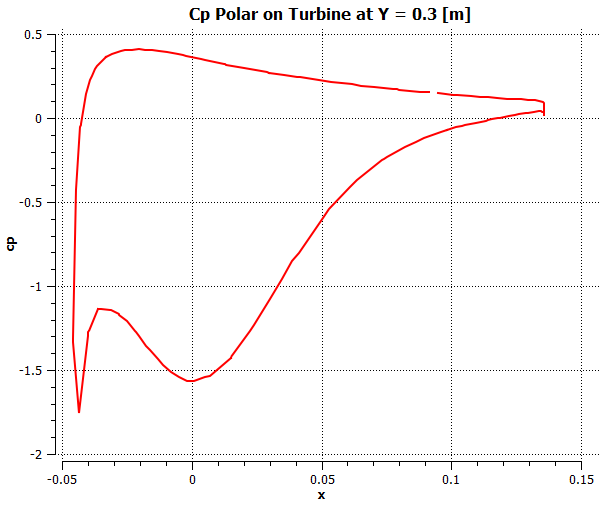

Figure 4.53 C_p vs X axis

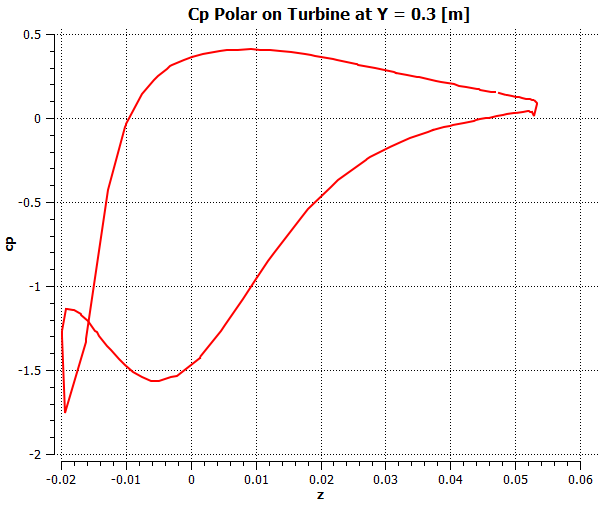

Figure 4.54 C_p vs Z axis

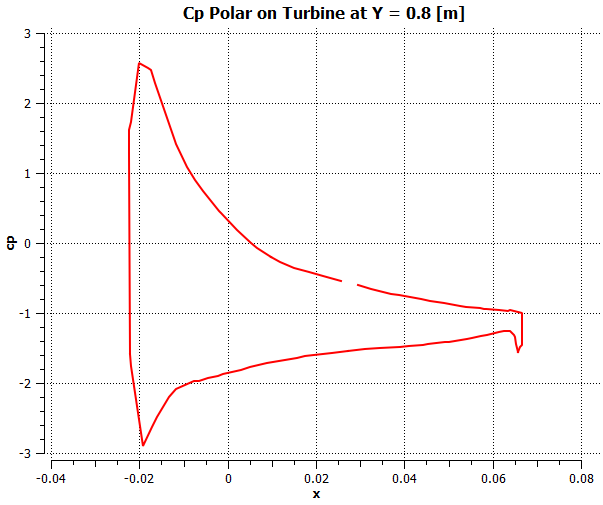

Figure 4.55 C_p vs X axis

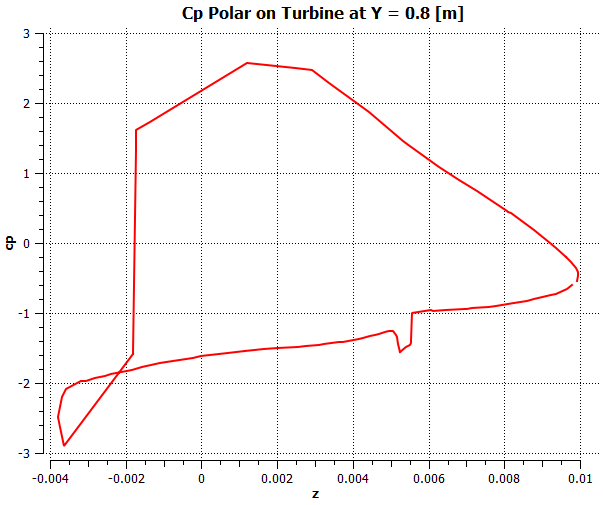

Figure 4.56 C_p vs Z axis

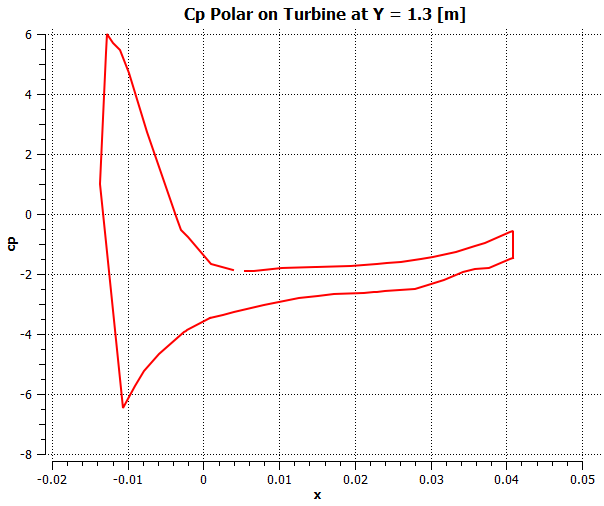

Figure 4.57 C_p vs X axis

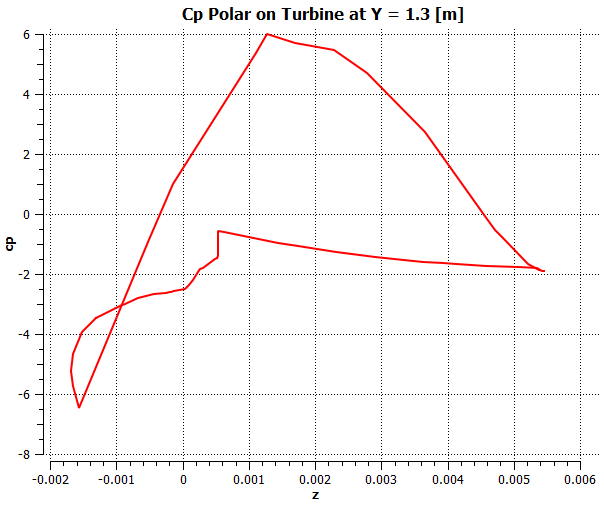

Figure 4.58 C_p vs Z axis

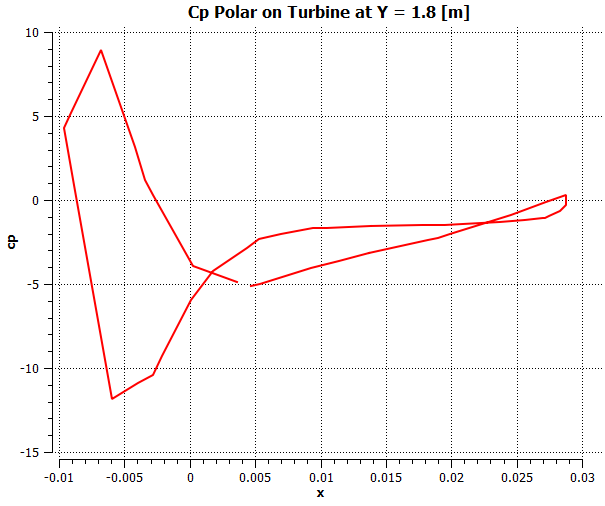

Figure 4.59 C_p vs X axis

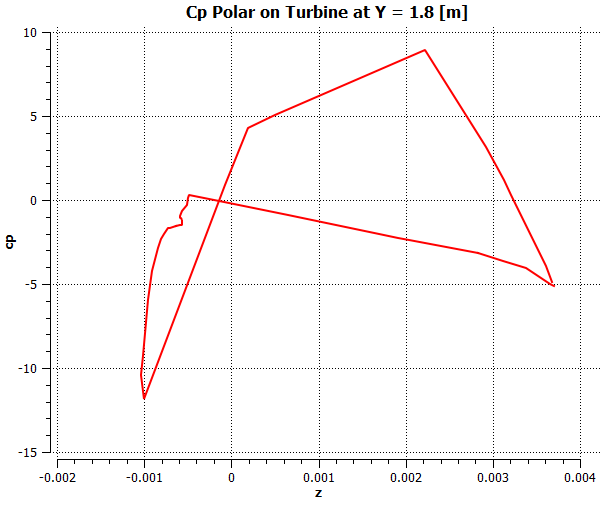

Figure 4.60 C_p vs Z axis

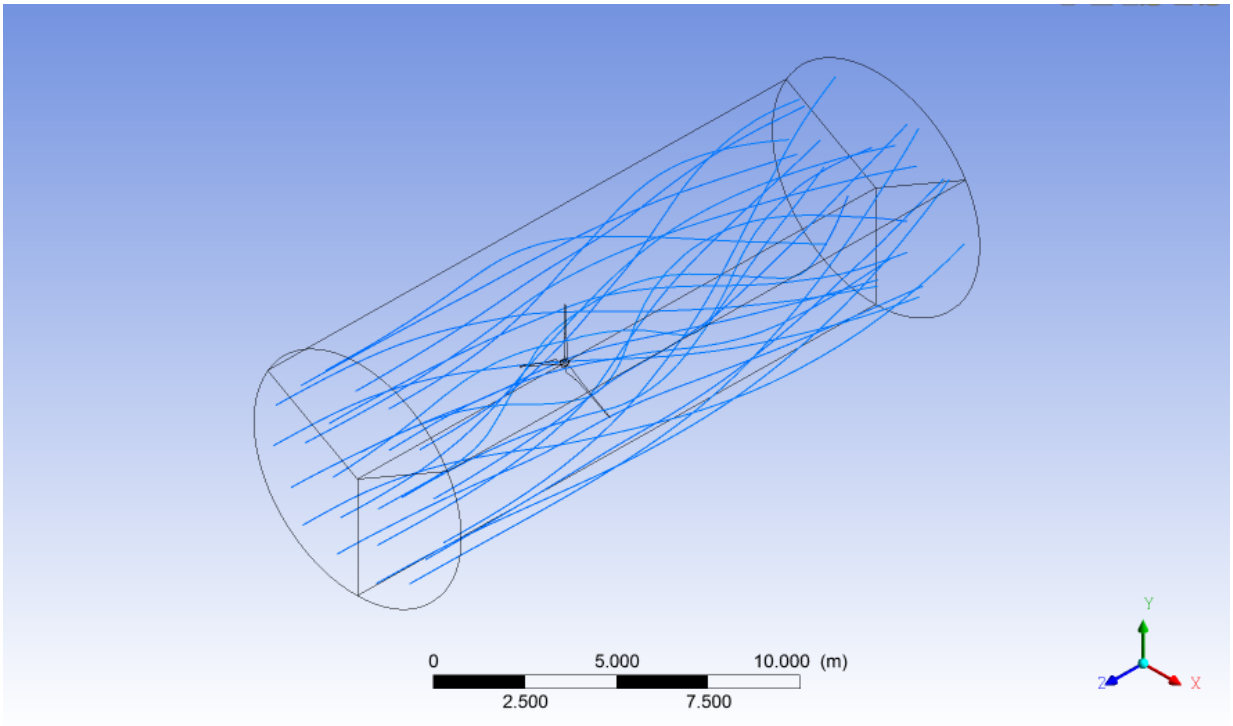

Figure 4.61 Deflection of streamlines in 3D domain

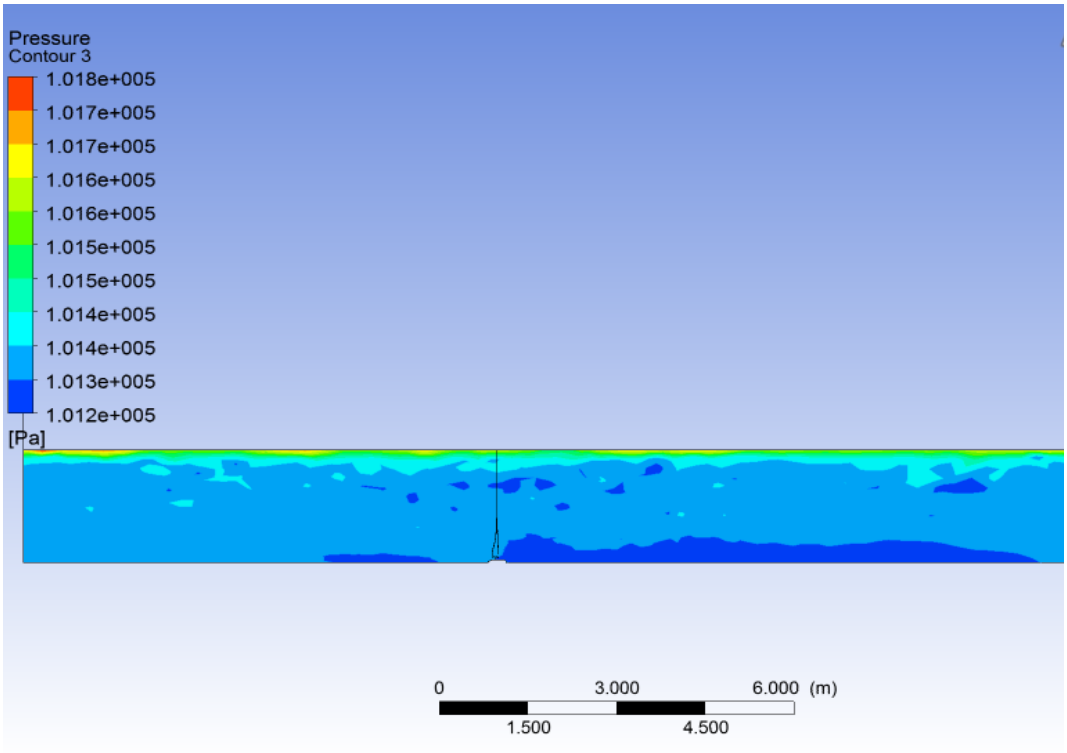

Figure 4.62 Pressure contours along wind direction

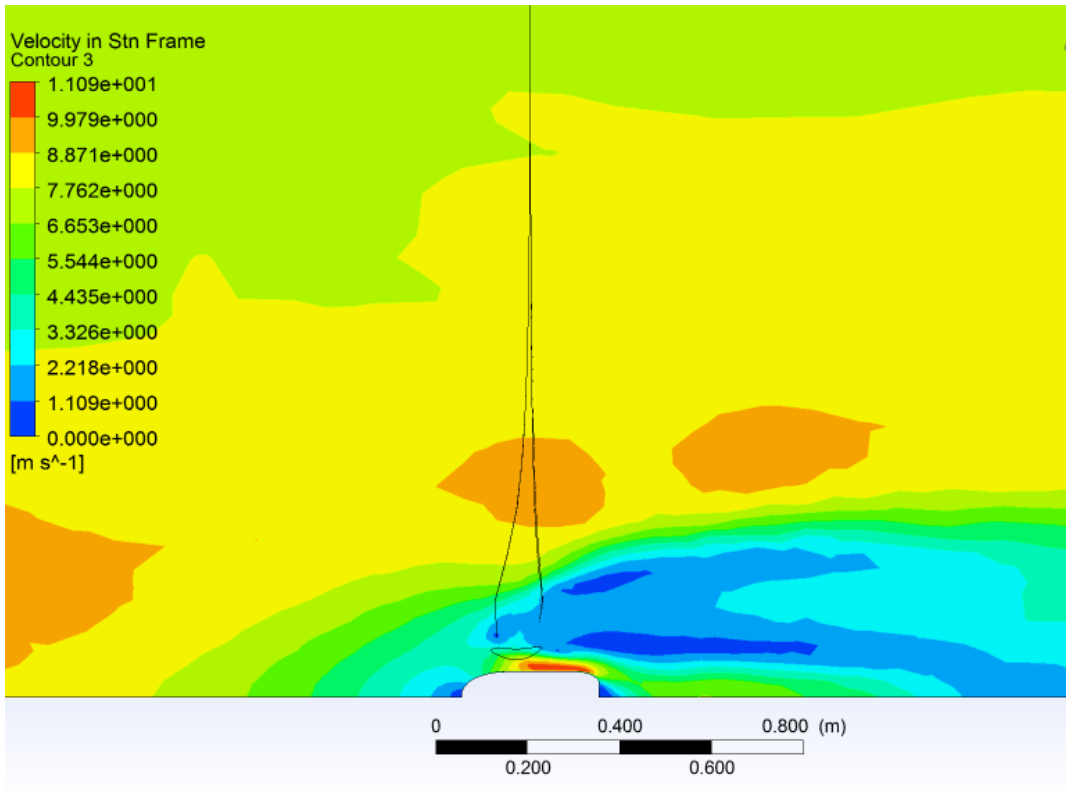

Figure 4.63 Velocity contours along wind direction

Chapter 5: CONCLUSIONS

The aim of this dissertation was to investigate the flow field around a wind turbine blade with the help of CFX and Qblade programs. Based on an extended review of literature and results of 2D simulations, SST turbulence model was selected for 3D simulation. The most important conclusions are as follows.

- The capability of SST model to simulate the flow around an airfoil in the pro stall region was verified. Also, the angle of attack at which stall begins can approximately be predicted using CFD.

- Pressure and velocity distribution around an airfoil was presented using pressure coefficient.

- An analysis of the flow field of a rotating blade was discussed. While doing so, periodicity concept was used to achieve information for the whole turbine. The distributions of pressure and velocity for four sections along the blade were illustrated.

- The power output was calculated. A comparison with the results of BEMT was done showing that the BEMT overestimates peak power for the given wind speed.

- The importance of choosing the right model is shown together with the role of correct meshing.

- The study proves that the 3D effects of actual flow around a turbine blade must be taken into account. BEM method can only be a first step in blade design process.

The above study forms a basis for a more comprehensive approach to the investigation of the flow field of a wind turbine blade using CFD simulation and its structure interaction. The study may be extended further at the following points:

- The 3D simulation can be done for a wide range of wind speeds in order to plot complete power curve of the blade using CFD.

- The study shows that an important loss occurs at blade-hub connection region. Better design of the above mentioned region considering structural issues can enhance the power output considerably. A Fluid Structure Interaction (FSI) study would be appropriate for this aim.

BIBLIOGRAPHY

1. BP World Energy Outlook Handbook,2013
2. EU Directive 2005/89/EC
3. www.ec.europa.eu/europe2020
4. Report of the World Commission on Environment and Development: Our Common Future. United Nations General Assembly (1987)
5. Bloomberg New Energy Finance, Summit April 2013
6. European Semester 2012
7. Tuncay Babali, Turkish Ministry of Foreign Affairs
8. Turkish Wind Energy Association, Turkish Wind Energy Statistics Report January 2013
9. Turkish Wind Energy Association, An Outlook for Investors
10. Dünyada ve Türkiye'de Enerji Görünümü, Ministry of Energy, Republic of Turkey
11. Turkey 2012 Progress Report
12. BP Statistical Review 2012
13. Rudolf Schilling, TU München.
14. White Frank, Fluid Mechanics
15. Douglas John, Fluid Mechanics, Pearson2010
16. Cengel Yunus, Fundementals of Fluid Mechanics
17. Fox Robert, Introduction to Fluid Mechanics
18. Munson, Fluid Dynamics 2008
19. Betz, A. (1926) Windenergie und Ihre Ausnutzung durch Windmüllen

20. Manwll, J.F. (2009) Wind Energy Explained:Theory, Design and Application

21. Eggleston and Stoddard(1987)

22. Burton, T, et al., et al. Wind energy handbook. s.l. : John Wiley and Sons, 2001,

23. Hansen M. O. L. (2008) Aerodynamics of Wind Turbines

24. Glauert,H (1935) Airplane Propellers

25. Lysen E. H. (1982) Introduction to Wind Energy

26. Manwll, J.F. (2010) Wind Energy Explained:Theory, Design and Application

27. www.nrel.gov

28. Chapra,Numerical Methods for Engineers,2007

29. Pope,S.B Turbulent Flows

30. Peterson et al (1989)

31. H. Tennekes and J. L. Lumley A First Course in Turbulence

32. http://www.cfd-online.com/Wiki/RANS-based_turbulence_models

33. E. Lutum and F. Cottier, Aerothermal predictions on a highly loaded turbine blade including effects of flow separation

34. ANSYS CFX, Solver Manual v13

35. ANSYS CFX, Theory Booklet

36. QBlade Guidelines

37. C. Ladson, U. S. N. Aeronautics

38. Robert Maier-Staude, Wind Turbine Modeling using ANSYS

39. Steve Connors, MIT

40. http://en.wikipedia.org/wiki/History_of_the_European_Union

41. http://www.grida.no/publications/vg/climate/page/3062.aspx

42. Dominik Rutz & Rainer Janssen 2008, Biofuel Technology Handbook

43. http://www.ehow.com/how_4842366_build-wind-turbine.html

ANNEX I: List of Figures and Tables

ANNEX II

Airfoil Theory

Wind turbine blades use airfoils to create mechanical power. That is why it is of utmost importance to realize how an airfoil develops mechanical power, or more precisely saying, to realize the forces which develop the power.

At this point, a short description of airfoil should be made. In the sketch below, a typical airfoil is shown with important parameters. More detailed info can easily be found but concerning the aim of this thesis it would be unnecessary.

The most important terms are leading edge, trailing edge, chord, chord line and angle of attack.

Leading edge is the point at which the flow (assuming it blows in x direction) first meets the airfoil shape and the trailing edge is the end point. An imaginary line connecting those two points is called chord line and its length as chord. The relative flow makes an angle with this chord line and this angle is called as angle of attack.

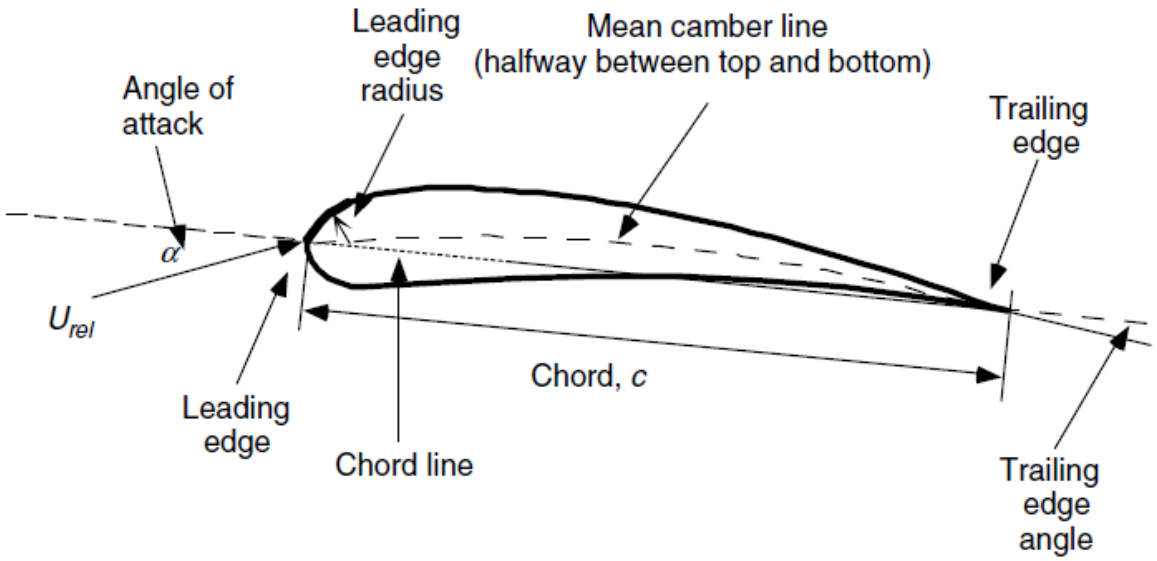

Airfoils have special geometry to separate the flow in a desired way to create special distribution of forces acting over it. They have two sides one lying above the mean chamber

line and one below. Those mentioned sides have different geometric characteristics. One of the sides is concave and the other convex. The concave side is called also as “pressure” side meaning there is higher pressure on this side. The convex side is named as “suction” side to emphasis that there is lower pressure on this side. By basic physics we can understand that the pressure difference causes uneven force distribution and finally this uneven force distribution gives rise to motion which turns a shaft attached to a generator. Another source of force on the airfoil, although not as predominant as the previous, is the frictional force developed on the surface of the airfoil due to the viscous air flow. Now we can carry on in more details of the underlying physics.

As mentioned previously, due to the uneven pressure distribution and friction a force distribution forms. For practical reasons, we can define a resultant force and a moment at a point. This point is chosen usually along the chord line at a distance chord length over four (c/4) from the leading edge.

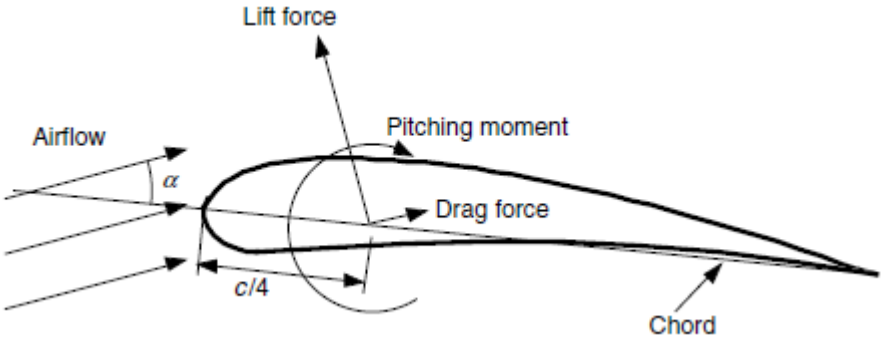

As seen above, we sum all forces and define them at a point with a resultant force and a moment. The reluctant force has two components, one perpendicular to the relative flow direction and the other parallel. The former force is called “Lift force” while the latter “Drag force”. The moment is “Pitching moment” and clockwise direction is chosen to be positive for this moment.

In fluid dynamics non dimensional forms of variables are used in great extend to ease the solution. There are also some non-dimensional variables used for airfoils. The most important of them are lift coefficient, drag coefficient and moment coefficient.

$$C_l = \frac{L/l}{\frac{1}{2}\rho U^2 c} \qquad C_d = \frac{D/l}{\frac{1}{2}\rho U^2 c} \qquad C_m = \frac{M}{\frac{1}{2}\rho U^2 c}$$

While the lift coefficient expresses the ratio of the lift force to the force produced by the dynamic pressure, the drag coefficient expresses the ratio of the drag force to the force

produced by the dynamic pressure. The moment coefficient is the ratio of the pitching moment over the dynamic moment.

After the long explanation, we are at a point to describe better the flow motion and its results. The lift, drag, and pitching moment coefficients of an airfoil are generated by the pressure variation over the airfoil surface and the friction between the air and the airfoil. The pressure variations are caused by changes in air velocity. If we look at Bernulli equation, it states that if a fluid's velocity increases so decreases its pressure and vice versa. (For more comprehensive info about Bernoulli equation, please see the related appendix) This explains why pressure differs along the surface of the airfoil. The velocity varies over the surface causing also pressure variations.

Pressure variations in return can change and in fact do change the flow pattern over the airfoil. We can distinguish here between two pressure gradient types, favorable and adverse. The firs of the mentioned two means the pressure is decreasing in the direction of the flow. This will make the flow keep going and even accelerating. The adverse pressure gradient slows down the flow in contradiction to the favorable gradient. There is one more phenomenon, surface friction, which slows down the flow too. Thus, if the adverse pressure gradient + surface friction is strong enough, it may cause the flow to stop completely. In more extreme cases, the adverse pressure gradient may even cause the flow reversal. If the flow reverses, the result is not after too long is the separation of flow over the surface of the airfoil. This is called stall and has dramatic effects on the lift of the airfoil. The lift decreases suddenly and to a large extent. An airfoil efficiently produces lift only if the surface pressure distributions can be supported by the boundary layer. Below the effect of different pressure gradients are shown in three different illustrations. The last one pictures the stall.

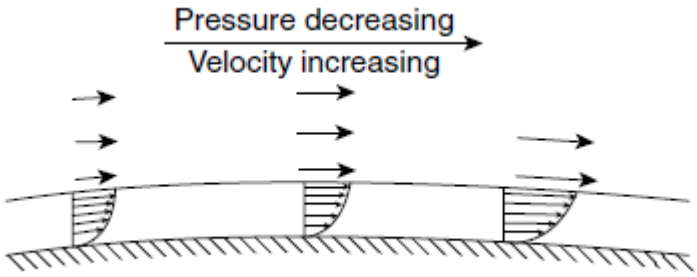

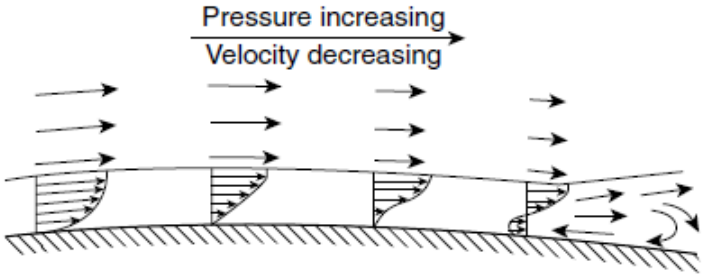

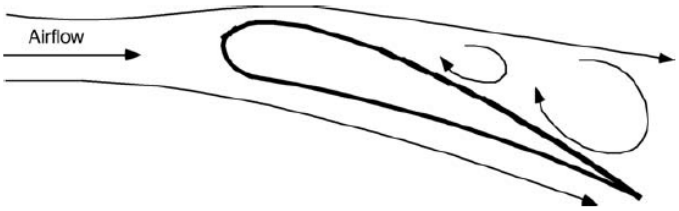

Mathematically expressing the lift:

The total lift force is the integral of vertical pressure forces over the entire wetted surface area of the wing. (Anderson, John D. (2004), *Introduction to Flight*, Section)

$L = \oint p\mathbf{n} \cdot \mathbf{k}\, dA$,

Here;

- L is the lift,
- A is the wing surface area
- p is the value of the pressure,
- $\mathbf{n}$ is the normal unit vector pointing into the wing, and
- $\mathbf{k}$ is the vertical unit vector, normal to the free stream direction.

Please note that the above equation is simplified by ignoring the contribution of skin friction.